BOTSWANA INTERNATIONAL UNIVERSITY
OF SCIENCE & TECHNOLOGY

DESIGN, MODELLING, AND SIMULATION OF A VISION-BASED AUTOMATIC GOLD PANNING SYSTEM

BY

BLESSING CHIPFURWE MAKONI
REG NO: 17100160

M.Eng. MECHATRONICS AND INDUSTRIAL INSTRUMENTATION

A THESIS SUBMITTED TO THE FACULTY OF ENGINEERING IN PARTIAL FULFILMENT OF THE REQUIREMENTS FOR THE AWARD OF THE DEGREE OF MASTER OF ENGINEERING IN MECHATRONICS AND INDUSTRIAL INSTRUMENTATION

JULY 2021

BOTSWANA INTERNATIONAL UNIVERSITY
OF SCIENCE & TECHNOLOGY

DESIGN, MODELLING, AND SIMULATION OF A VISION-BASED AUTOMATIC GOLD PANNING SYSTEM

By

BLESSING CHIPFURWE MAKONI

REG No: 17100160

B.Eng. Mechatronic Engineering (CUT, Zimbabwe)

Department of Mechanical, Energy and Industrial Engineering

College of Engineering and Technology

Botswana International University of Science and Technology

Student E-mail Address: blessing.makoni@studentmail.biust.ac.bw +26773047438

A Thesis Submitted to the College of Engineering and Technology in Partial Fulfilment of the Requirements for the Award of the Degree of Master of Engineering in Mechatronics and Industrial Instrumentation

Supervisor: Dr M. Namoshe

Co - supervisor: Dr O. Matsebe

Department of Mechanical, Energy and Industrial Engineering

College of Engineering and Technology, BIUST

namoshem@biust.ac.bw and matsebeo@biust.ac.bw

Signature: _____ Date: 23/07/2021

Signature: _____ Date: 23/07/2021

JULY 2021

BOTSWANA INTERNATIONAL UNIVERSITY OF SCIENCE & TECHNOLOGY

Declaration and Copyright

I, **BLESSING CHIPFURWE MAKONI**, declare that this thesis is my original work and that it has not been presented and will not be presented to any other university for a similar or any other degree award.

Signature..... .....Date.....1 JULY 2021.....

This dissertation/thesis is copyright material protected under the Berne Convention, the Copyright Act of 1999, and other international and national enactments, on that behalf, on intellectual property. It must not be reproduced by any means, in full or in part, except for short extracts in fair dealing; for researcher private study, critical scholarly review or discourse with an acknowledgment, without the written permission of the office of the Provost, on behalf of both the author and the BIUST

BOTSWANA INTERNATIONAL UNIVERSITY OF SCIENCE & TECHNOLOGY

Certification

The undersigned certifies that he has read and hereby recommends for acceptance by the faculty of a dissertation/thesis titled: Design, modelling, and simulation of a vision-based automatic gold panning system, in fulfilment of the requirements for the degree of Master of Engineering in (Mechatronics and Industrial Instrumentation) of BIUST.

Dr. M Namoshe

.....

(Supervisor)

Date 23/07/2021

Dr. O Matsebe

.....

(CO-Supervisor)

Date 23/07/2021

BOTSWANA INTERNATIONAL UNIVERSITY OF SCIENCE & TECHNOLOGY

Acknowledgments

My endless gratitude goes to the almighty God for His grace in my life and for keeping me in good health throughout the completion of this project.

My special thanks go to my academic supervisors Dr. M. Namoshe and Dr. O. Matsebe for their guidance, support, help, ideas, corrections, and mentorship during the execution of this project. It has been a great pleasure working with them.

I am much indebted to the Mechanical, Energy, and Industrial Engineering department and the members thereof who contributed immensely by providing a conducive environment for my learning and research and for the immense knowledge they had equipped me with through the course of this project.

Lastly, I take this opportunity to thank my wife, parents, siblings, and friends for their unwavering support.

ABSTRACT

To do away with the hazardous, tedious, repetitive, and export-dependent gold panning procedure currently practiced by artisanal and small-scale miners in developing countries an automated system for the gold panning procedure is presented in this thesis. Gold panning is one of the gravimetric separation processes which separate particles of greater specific gravity (particularly gold) from mineral waste. This separation method is prevalently used in low-tech areas and mercury is incorporated to make for effective and efficient gold recovery. The mercury used exposes the miners to hazardous health conditions and increases mercury pollutions. Little technical effort and knowledge are available to provide solutions adaptable to the African context. This study is devoted to the technical optimization of the gold washing process and hand-picking process involved in the current panning procedure through mechanization and automation. The design was achieved through the use of the V model for mechatronic system design (VDI 2206 guidelines). Morphological analysis was used to adapt and make use of the already existing concepts and designs to mechanize and automate the manual, expert-dependent, and tedious gold panning process. The design adopted was based on the usage of visual data to control the separation and picking process. In the automation of the gold panning process and robotic handling, it is important to identify and locate the gold particles in the images captured by the image sensor. Color image thresholding in the CIELAB color space was developed as a front-end technique to automate the visual feature identification and localization of gold particles in the pan. 3D CAD models of the designed system were developed in Solidworks. Finite element analysis of the designed washer concept was performed in ANSYS 2019 to precisely calculate material stress, strain, deformation, contact, and safety factor. This was done to predict the behaviour of the components and assembly under given boundary conditions and loading in a quasi-real scenario. Kinematic modeling of the handling system was performed using the Denavit Hartenberg convention and analytical methods. Physical modeling using MATLAB, Simulink, and SimScape was done to perform dynamic modeling and simulations of the handling system. Stateflow charts were developed to model state machines and flowcharts which were used in task planning to interface various components used in the vision-based control and picking process. Simulation and modeling results showed that the design is feasible, achievable, and efficient.

BOTSWANA INTERNATIONAL UNIVERSITY OF SCIENCE & TECHNOLOGY

Table of Contents

Declaration and Copyright i

Acknowledgments iii

ABSTRACT iv

List of Tables viii

List of Figures ix

List of Abbreviations xi

CHAPTER 1 1

1.0 Overview 1

1.1 Background 1

1.2 Introduction 4

1.3 Problem Statement 5

1.4 Main Objective (Aim) 5

1.5 Objectives 5

1.6 Significance of the study/ Socio-economic benefits 5

1.7 Contribution to the body of knowledge 6

1.8 Delimitation / Scope of research 6

1.9 Thesis organization 6

CHAPTER 2 7

Literature review 7

2.0 Overview 7

2.1 Current Gold recovery methods 7

2.2 Visual servoing 18

2.3 General hardware components for a visual servoing task (key hardware components for visual servoing) 19

2.3.1 Camera / visual sensing device 20

2.3.2 Artificial lighting System 21

2.3.3 Processor 22

2.3.4 Robotic manipulators 28

2.4.0 Camera Configurations in Visual Servoing 29

2.4.1 Eye-in-hand/Camera-in-hand (CiH) configuration 29

2.4.2 Eye-to-Hand / fixed camera configuration 30

2.4.3 Hybrid configurations 30

2.5 Visual Servoing Architectures (Basic approaches) 31

2.5.1 Position-Based Visual Servoing (PBVS)/ 3D Visual servoing 31

2.5.2 Image-Based Visual Servoing (IBVS)/ 2D visual servoing 33

2.5.3 Hybrid based visual servo Control 37
2.5.4 Enhanced visual servoing techniques 38
2.5.5 Machine learning techniques for visual servoing 42
2.6 Image features for visual servoing 43
2.6.1 Image moments as visual features 44
2.6.3 Part-aware key points as visual features 46
2.6.4 Eigenspaces of the image dataset as visual features 46
2.6.5 Luminance as image feature for visual servoing 46
2.6.6 Colour attributes as visual features 47
2.6.7 Image histograms as features 48
2.7 Image segmentation 49
2.7.1 Region-based image segmentation methods 50
2.8 Applications of visual servoing 52
2.8.1 Vision-based automation 53
2.8.2 Vision-based service robots 53
2.8.3 Visual servoing applications in the medical field 53
2.8.4 Visual servoing applications in industry 54
2.8.5 Visual servoing application in Aerial vehicles 54
2.9 Conclusion 55
CHAPTER 3 56
Methodology 56
3.0 Overview 56
3.1 The V model for mechatronics system design methodology (VDI 2206 Guidelines) 56
3.2 Work done using the V-model for mechatronics system design methodology 57
3.3 Conclusion 58
CHAPTER 4 59
Conceptualization, design, and modeling 59
4.0 Overview 59
4.1 Generating requirement list 59
4.1.1 The gold panning process 60
4.2 Design requirements 61
4.3 Concept generation 66
4.3.1 Functional Analysis system Technique for the automated system 66
4.3.2 Morphology Analysis 67
4.4 Domain-Specific Designs 75
4.4.1 Gold detection and localization framework (software domain) 75

4.4.1.3 Colour image thresholding-based segmentation of gold panning platform images (Algorithm 3) 82
4.5 Mechanical sub-system 85
4.6 Modelling, model analysis, and simulation of the mechanized gold-washing system. 88
4.6.1 Numerical modeling and analysis of the gold washer system 88
4.8 Conclusion 91
CHAPTER 5 92
Results, analysis, and evaluation 92
5.0 Overview 92
5.1 Results and comparative study of the image segmentation 92
5.2 Gold- washer finite element analysis results and discussion 94
5.3 Modelling and simulation of the handling system 99
5.3.1 kinematic modeling and analysis of the handling system 99
5.3.2 physical modeling and analysis of the handling system 104
5.3.2.1 Handling system controller design 105
5.3.2.2 Dynamic model study - Motion Planning for the handling system 107
5.4 Vision-based control of the handling system (Task planning) 112
5.4.1 Decision making and control logic of the designed system 113
5.5 Design evaluation 116
5.6 Conclusion 117
6.0 Overview 118
6.1 Conclusion 118
6.2 Future work 118
References 120
APPENDIX A 130

BOTSWANA INTERNATIONAL UNIVERSITY OF SCIENCE & TECHNOLOGY

List of Tables

Table 1. 1: Selected Sub-Saharan African countries ASM activities and main minerals mined by ASM 2
Table 2. 1: Gold pre-concentrating activities 9
Table 2. 2: Gravimetric gold recovery methods 11
Table 2. 3: Gold concentration processes 15
Table 2. 4: Vision sensing system nomenclature 21
Table 4. 1: Inputs, outputs, and processing in the gold panning process 61
Table 4. 2: Initial requirements for the vision-based automated gold panning system 62
Table 4. 3: Part of Pahl and Beitz requirement checklist 63
Table 4. 4: Incident matrix 64
Table 4. 5: Design specification table for the automated gold panning system 65
Table 4. 6: Morphological Chart 68
Table 4. 7: Design Questions Checklist 69
Table 4. 8: Selection of solution concepts from variants lists 71
Table 4. 9: Selected solution concepts 74
Table 4. 10: CIELAB Threshold values 85
Table 5. 1:D-H parameters for the handling system 101
Table 5. 2: Joint controller parameters and performance characteristics 106

BOTSWANA INTERNATIONAL UNIVERSITY OF SCIENCE & TECHNOLOGY

List of Figures

Figure 1. 1: Common scene of the panning procedure 3
Figure 1. 2: Amalgamation task which usually exposes miners to mercury droplets 3
Figure 2. 1: common gold recovery flowsheet in ASM operations 18
Figure 2. 2: Generic hardware components 20
Figure 2. 3: Segmentation techniques and their classification according to [121][123] 50
Figure 3. 1: Customized process model for the design of an automated vision-based gold panning system [153] 57
Figure 4. 1: Blackbox model of the gold panning process 59
Figure 4. 2: Function Analysis System Technique (FAST) diagram of the automated gold panning system 67
Figure 4. 3: Principle solution functional block diagram 75
Figure 4. 4: Otsu's thresholding segmentation flowchart and application example on a gold panning platform image 78
Figure 4. 5: Variable thresholding and application on grayscale images 81
Figure 4. 6: Histogram analysis of an image in 3 color space model 82
Figure 4. 7: 3D assembly drawing of the automated gold panning system 87
Figure 5. 1: Sample results of the segmentation process: (a) original image, (b) segmented mask for an algorithm I, (c) segmented mask for algorithm II, (d) segmented mask for algorithm III 93
Figure 5. 2: Feature extraction and localization of detected gold particles 94
Figure 5. 3: Stress distribution of the gold-washer 94
Figure 5. 4: Equivalent elastic strain of the gold-washer 95
Figure 5. 5: Total deformation for the gold-washer 95
Figure 5. 6 : Maximum total deformation {green}, average total deformation [blue], minimum total deformation [red] 96
Figure 5. 7: Total velocity of the components in motion 96
Figure 5. 8: Minimum total velocity(blue), Maximum total velocity (Green), and average total velocity (red) 96
Figure 5. 9: Total acceleration results of the gold-washer 97
Figure 5. 10: Contact status of the gold-washer assembly 97
Figure 5. 11: Penetration information of the gold washer 98
Figure 5. 12 : Maximum penetration{green}, average penetration [blue], minimum penetration[red] 98
Figure 5. 13 : Maximum sliding distance {green}, average sliding distance [blue], minimum sliding distance[red] 98
Figure 5. 14: Safety factor analysis of the washer concept 99
Figure 5. 15: kinematic chain for the handling system 100
Figure 5. 16: top left is the workspace, top right is the handling system configuration for end-effector point (800 500 400), bottom left configuration for end-effector point (200, 1000, 100), and bottom right (1000, 1000, 700). 103
Figure 5. 17: SimScape multibody physical model of the handling system 105
Figure 5. 18: SimScape multibody model of the handling system with joint controllers. 106
Figure 5. 19: Step plot for block response and tuned response for joint controllers 106
Figure 5. 20: Joint position and joint velocity under the controller effect 107
Figure 5. 21: simulation capture of the handling system executing (a) cubic trajectory (b) trapezoidal trajectory 108

Figure 5. 22:Dynamic modeling and simulation of the handling system 109
Figure 5. 23: Time sequences for trajectory following of the handling system..... 111
Figure 5. 24: Actuator force and Torque for trajectory following 112
Figure 5. 25: Part of the Stateflow chart for the handling system's control. 114
Figure 5. 26: Vision-based control block diagram 114
Figure 5. 27: Vision-based control simulation results 116

List of Abbreviations

2D	Two Dimensional
3D	Three Dimensional
ANN	Artificial Neural Networks
ASMs	Artisanal and Small-Scale Miners
CAD	Computer-Aided Design
CAE	Computer-Aided Engineering
CCD	Charge Coupled Device
CiH	Camera in Hand
CMOS	Complementary Metal Oxide Semiconductor
CNN	Convolutional Neural Network
DDTT	Differential-Drive Thunder Tumbler
DOF	Degrees of Freedom
DSPs	Digital Signal Processor
EKF	Extended Kalman Filtering
FAST	Functional Analysis System Technique
FEA	Finite Element Analysis
FEM	Finite Element Method
FOV	Field of View
GPU	Graphical Processing
GUI	Graphical User Interface
HIS	Hue Saturation Intensity
HOG	Histogram of Gradient
HSV	Hue Saturation, Value
IBVS	Image-Based Visual Servo control
IGES	Initial Graphics Exchange (file format)
KLT	Kanade – Lucas Tomasi
KSOM	Kohonen Self Organizing Map
LED	Light-Emitting Diode
LF	Light Field camera
LSMs	Large Scale Miners
MAC	Multiply-Accumulate
PBVS	Position-Based Visual servoing
PC	Personal Computer
PID	Proportional Integral Derivative

RGB	Red Green Blue
ROS	Robot Operating System
SCARA	Selective Compliance Assembly Robot Arm
SOC	System on Chip
SVM	Support Vector Machine
UAV	Unmanned Ariel Vehicle
USB	Universal Serial Bus

CHAPTER 1

1.0 Overview

This chapter seeks to introduce this research work which focuses on technical optimization of the gold panning processes through automation. The background information surrounding the area of study is laid out to expose the problems and issues of concern this work seeks to address. The main aim and the objectives which will lead to the achievement of the desired goal are also furnished in this chapter. Various justifications and benefits of the study together with the scope of the research are also outlined in this chapter.

1.1 Background

The mining industry has a significant impact and capacity on the economic growth of developing countries thereby reducing poverty in these regions. Gold mining has made a very profound contribution to the national economies and regional economies and this is particularly true for developing countries where gold makes up a major aspect of the economy like Ghana, Tanzania, Burkina Faso, Guinea, Suriname, Zimbabwe, etc.[1]. Gold is one of the main export earners for these developing countries. Due to high levels of unemployment and poverty in these countries, gold production is done by large-scale mines, small-scale miners, and artisanal gold miners.

In most of the developing countries, the artisanal and small-scale mining sector continues to grow in size and significance, contributing to the much-needed wealth, employment creation, and livelihood activities. As of 2012 ASM activities in Africa engaged about 8 million workers, who in turn supported 45 million dependents[2]. In Ghana in 2016, an estimate of one million people was employed in this sector and Zimbabwe records over 1,3 million both small-scale and artisanal gold miners [3]. Table 1.1 below shows an estimation of ASM activities in selected Sub-Saharan African countries and the corresponding minerals mined in those countries according to Hilson [4]. As witnessed in Table 1.1 ASM activities in gold production are prevalent in many Sub-Saharan African countries and it's one of the reasons this work focuses on gold production. The small-scale and artisanal gold miners are viewed as the new profitable economy drivers and employment creators as they employ cheaper methods to extract this precious mineral. This sector is often operating in remote, unregulated, and environmentally sensitive areas and is a low-tech, labor-intensive mineral processing and extraction sector. It is important to note that artisanal small-scale mining is formalized and legalized in various countries by way of granting of requisite licenses and

permits mandated by the law, to standardize and align to policies, regulations and good safety, health and management practices.

Table 1. 1: Selected Sub-Saharan African countries ASM activities and main minerals mined by ASM

Country	People directly working in ASM	Estimated number of dependents	Main minerals mined by ASM
Angola	150 000	900 000	Diamonds
Burkina Faso	200 000	1 000 000	Gold. Diamonds
Central African Republic	400 000	2 400 000	Gold, Diamonds
Chad	100 000	600 000	Gold
Cote DeVore	100 000	600 000	Gold, Diamonds
DRC	200 000	1 200 000	Diamonds, Gold, Colton
Eritrea	400 000	2 400 000	Gold
Ethiopia	500 000	3 000 000	Gold
Ghana	1 100 000	4 400 000	Gold, diamonds, sands
Guinea	300 000	1 500 000	Gold, Diamonds
Liberia	100 000	600 000	Gold, Diamonds
Madagascar	500 000	2 500 000	Coloured gemstones, Gold
Malawi	40 000	-	Coloured gemstones, Gold
Mali	400 000	2 400 000	Gold
Mozambique	100 000	1 200 000	Coloured gemstones, Gold
Niger	450 000	2 700 000	Gold
Nigeria	500 000	2 500 000	Gold
South Africa	20 000	-	Gold
Sierra Leone	300 000	1 800 000	Gold, Diamonds
South Sudan	200 000	1 200 000	Gold
Tanzania	1 500 000	9 000 000	Gold
Uganda	150 000	900 000	Gold
Zimbabwe	500 000	3 000 000	Gold, Diamonds, Coloured gemstones

The ASMs are faced with a lot of problems ranging from the acquisition of mining equipment, machinery, and materials that can enhance their work. The ASMs use outdated methods and techniques in the extraction and purification of gold which exposes them to hazardous conditions. The ASMs suffer exploitation from the milling companies who perform the comminution at a cost. The miners pay for the usage of milling facilities and sometimes incur losses as the comminution process is not carried out properly and enough to recover amenable gold using the gold panning method. The gold panning process is done manually and is tedious and repetitive and needs expertise to be carried out effectively. The

washing process during the panning process is usually dirty, tiresome, and dangerous. Figure 1.1 shows the common scene and environment during the panning process. Even after thorough panning by the ASMs, the millers recover a lot of gold from the residual crushed ore panned by ASMs as they further extract the mineral thoroughly using chemical methods. Mercury extraction is popular in this sector and it exposes these workers to health risks, especially women and children who usually carry out the amalgamation task and roasting of the amalgam to recover the gold from mercury. Mercury inhaled in airborne droplets from the extraction process can cause potentially fatal damage to the lungs, kidneys, may cause seizures and permanent brain damages. Mercury poisoning in pregnant women can cause long-term cerebral damage to the fetus. The miners are also prone to heavy metal poisoning like lead poisoning which takes place as they pulverize the ore (especially heavy metal-laden rocks) in search of gold for example the Zamfara incident [5]. There has been little knowledge and effort on the automation of the gold panning procedure for small-scale gold production to empower the small-scale and artisanal gold miners and separating them from health hazards.



Figure 1. 1: Common scene of the panning procedure



Figure 1. 2: Amalgamation task which usually exposes miners to mercury droplets

1.2 Introduction

This research is in line and in response to the call for contribution by engineering and technological institutions to train and educate small-scale and artisanal miners concerning safe and hazard-free gold extraction methods, design and fabrication of appropriate mining and processing equipment that are affordable and adaptable to the African environment [6]. The research focuses on the challenge of providing a safe and healthy methodology in the extraction of gold by small-scale and artisanal miners while improving the efficiency of gold extraction. The research work is geared toward providing technical intervention to ASM challenges by promoting automation technology through technical optimization of the key procedures in the gold panning process. This will be done by identifying the areas which expose the miner and the environment to hazard and provide ways to separate the miner and the environment from the hazard. The research study will be performed on the identification of automation solutions on generic extraction activities where integration, mimicking, and miniaturization are required. The research will involve the design, modeling, and simulation of software architectures, control logic, along with the mechanical and mechatronic design of extraction equipment and subsystems. This will be done towards the development of an engineering or technological artifact that caters to the needs of artisanal and small-scale gold miners.

Since the current gold panning process by artisanal and small-scale miners (ASMs) involve washing of the ore by leveraging gravitational force and sorting/handpicking of the gold particles or amalgam from the pan through hand-eye coordination, the research will focus on vision-based robotic manipulation as an automation solution. This will take advantage of fast feature extraction, vast amounts of precise information, and fast processing capabilities offered by machine vision systems and robotic manipulators which are fit for the automation of the gold panning process. Robotic and automation solutions which use vision information will be used to optimize the ore washing procedure and hand picking/sorting process. Machine vision has been used in simplifying tedious, complex, and subjective industrial processes hence the adoption of this technology in this automation project. Vision-based automated systems may effectively and completely replace human judgment, input, and involvement in performing hazardous and complex tasks.

1.3 Problem Statement

The gold panning process done by artisanal and small-scale miners is tedious, repetitive, and requires expertise to extract considerable amounts of gold while exposing the miner to hazardous health conditions.

1.4 Main Objective (Aim)

Technical optimization of the gold panning procedure through design, modeling, and simulation of a vision-based automatic gold panning machine for safe and efficient gold extraction.

1.5 Objectives

1. To design an effective ore washing system that mimics the gold panning process adequately and consistently.
2. To design a handling system that transfers the washed liberated gold particles from the gold pan to the next process.
3. To build gold detection models and use machine vision principles to detect and localize the gold particles after the gold panning stage.
4. To develop the necessary algorithms for the control logic of the washing system, object detection system (image processing system), and the handling system.
5. Modeling and simulation of the designed system and the developed algorithms to validate their functionality.

1.6 Significance of the study/ Socio-economic benefits

The outcome of this research project will help in solving the following: -

i. The research work promotes mercury-free or cyanide-free gold recovery thereby mitigating mercury poisoning and mercury or cyanide pollution problems.
ii. The research work will provide a fail-safe procedure to protect the environment from pollution and miners from heavy metal poisoning and ensure efficient and safe practices.
iii. The introduction of automation will solve the problem of the need for expertise as the machine will be able to process and detect gold on its own.
iv. The tedious and repetitive processes in the gold panning stage will all be done autonomously.

v. The use of mechanisms will efficiently extract and process the mineral with reduced processing time which can increase the profits significantly.

1.7 Contribution to the body of knowledge

- Providing a healthy and safe methodology in the area of gold extraction
- The research will contribute by employing vision-based methods in gold recovery instead of the gravity or chemical recovery methods currently used.
- Proposal of vision-based object detection models, methods, algorithms suitable for the mineral identification/detection field.
- Improvement and integration of existing models, methods, and algorithms used in other fields but now applied to mineral (gold) detection.

1.8 Delimitation / Scope of research

- This research is confined to gold extraction and processing using gravity methods – especially the panning method, as it is the commonly used method by the ASMs.
- The research is confined to the use of computer vision algorithms in detecting visible gold and other related elements and will not focus on other methods of metal detection.
- The research focuses on the extraction of gold from the concentrated ore and the purification of the gold - after milling processes.
- The research deals extensively with the automation and mechanization of the after-milling processes.

1.9 Thesis organization

Chapter 1 of the thesis presented the background and introduction of this research work together with the justifications of the need to carry out the research. The problem statement, aims, objectives, and scope of the work were articulated in this chapter. Chapter 2 focused on the review of the literature and it sought to expose the existing gaps, current practices, and recent trends in the area of study. The methodology of the research and design work was presented in chapter 3. Chapter 4 embodied the conceptualization, design, and modeling aspects of the research work and Chapter 5 presented the results, analysis, and evaluations of the research work. Finally, the conclusions and future works of this research work were documented in chapter 6.

CHAPTER 2

Literature review

2.0 Overview

This chapter explores and acknowledges the work done by other researchers in the area of gold recovery, vision-based control, image segmentation, and other topics which are related directly or indirectly to the main aim and objectives of this work. A review of the literature on the subject of gold recovery, vision-based control, image segmentation, object detection was done as these form the backbone of the research and design work. Various applications where the above technologies and methodologies were used were also reviewed and analyzed in this chapter together with other technologies and methodologies that were used in the system being developed. Subsections covering novel topics in machine vision such as object detection, object recognition, localization, visual features, various comparisons, and analysis are also included in this chapter. The review sought to expose common problems, existing gaps, trends, methods, and various justifications for certain practices to equip the researcher with the needed information in undertaking the current research. A general overview of some topics will be given without rigorous mathematical details to avoid repetitions as detailed explanations will be found in the preceding chapters. The output of this review will form the basis of the choices of the methods, technologies, configurations, practices that will be used in technical optimization of the gold panning processes through automation either by emulation, mimicking, or integration.

2.1 Current Gold recovery methods

Gold is usually found embedded or encased in the other mineral matter or rock types, and to liberate it and end up with pure gold various processes are employed [7]. Gold recovery is usually dependent on the mineralization type, comminution, and concentration method used. Comminution refers to the milling operations which encompass all methods used to reduce the size of the gold-bearing rocks to particles easy to work with [8]. This research focuses on the separation methods employed to liberate the gold particles from the gangue material after the comminution process (ore-run mine). The processes involved in separation are usually categorized as preconcentration processes and concentration processes [9]. All the concentration techniques increase the percentage of gold in the ore or sediment by discarding lighter particles. These processes are effective when the products from the

comminution circuit have relatively consistent grain size. The pre-concentration stage discards a greater portion of the mineral waste to remain with pre-concentrates which undergo further processing since they cannot be marketed in that form [10]. Pre-concentration methods are either mechanical, electrical, or magnetic focusing on enriching the ore by discarding most of the waste material through the exploitation of ore properties. Pre-concentration majors on the rejection of as much of low specific gravity deleterious wastes without compromising recovery. Concentration processes recover the valuable marketable metal with maximum possible quality and grade (90-99% gold by weight). Pre-concentration, when performed to reject harder non-metallic, ferrous, and other denser non-gold substances, lowers the energy cost of the recovery process and increases the concentration ratio of the ore thereby increasing the efficiency of the concentration processes [10].

The table 2.1 presents some of the pre-concentration methods.

Table 2. 1: Gold pre-concentrating activities

Method	Type of separation	Steps	Equipment	Reagents	Comments /Analysis
1. ***Magnetic Separation***[11][12]	magnetic	Sorting based on magnetic properties of the material.	Magnetic separator	n/a	Used for ores with much magnetic matter. It is an ore-depended and separate magnetic material. Used in conjunction with other methods. Not utilized in small-scale operations. Is of minor importance and not utilized small-scale operations.
2. ***Electrostatic separation***[13][14]	electrical		Esta-separator		Not widely utilized. More theoretical as it is practical. Is of minor importance and not utilized small-scale operations.
3. **Flotation (direct/indirect)**[15][16]	Surface mechanical	Conditioning Sorting washing	Conditioning tank and flotation cell	Frothing agents, collectors, depressants, activators, p-H reagents	Commonly used in large-scale mining operations. Works well for complex ores. Huge capital cost and operational cost hinder

					utilization by small scale and artisanal operations
4. **Gravimetric separation (gravity recovery)**[16]	Mechanical (hydro-mechanical) separation	Sorting and washing	Gold pan and manual labor [17]	Water	Commonly used, handy, require expertise and skill. No capital or operating cost. Can expose the miner to heavy metal poisoning. Low through-put
			Jigs [17]	water	Mainly used in large-scale operations. Complex operation
			Sluices (5°-15° inclined tables), carpets [17]	water	Uses more water. More effort in washing carpet to liberate the gold particles trapped in carpets. ASM does it along river banks. Set up is bulky
			Centrifugal classifiers [17]	water	Mechanized separation, haven't gained currency in ASM operations
			Spiral concentrators [17]	water	Mechanized separation with the gold pan with spirals has not gained currency in ASM operations.

			Cyclone separator [17]	water	Mechanized separation, creates an artificial cyclone to discard lighter materials. More theoretical and haven't gained currency in ASM operations.
6. **Dense medium separation** [18]	Mechanical separation	Float and settling separation	Glass flask sink Float separator	Dihydrogen dodecawolframate 3.1 g/cm^3	Laboratory experimented, not used in current ASM operations. Yield excellent concentration though it is slightly experimental.

From the above table, it can be noticed that the gravity recovery methods do not require reagents and some of them require no expensive machinery to be done but either skill, electricity, or water are used to leverage the force of gravity and density properties of the materials being separated. Gravity concentration when effectively employed can ease further downstream activities and reduce the usage of toxic chemicals in extraction. The following table presents the gravimetric recovery methods in detail and their analysis as they afford the opportunity to safely recover gold without huge capital expenditure for ASMs.

Table 2. 2: Gravimetric gold recovery methods

Method	Equipment	Process	Advantages	Disadvantages	Comments/ analysis
Shaking tables[19]	Shaking table with grooves raised on one side and tilted on the	Mineral feed and water released on the elevated side of the shaking table, gold, and	Concentrate a huge amount of mineral feed at a time.	Relatively expensive setup.	Usage mainly in large-scale operations

	other side. Motor to continuously shake and agitate the table	other heavy materials are trapped in grooves and directed to collecting points while the lighter matter is washed away	Can provide high grade concentrates and liberated gold	Require experience to operate. Require continuous supply of water	due to huge amounts of ore and capital. Rarely employed in scale operations.
Sluices [19]	5°-15° inclined platforms, carpets covering the surface of the platform as capturing device, buckets for washing the carpets or capturing materials, water sources	Ore or alluvium is washed by letting the ore and water travel down the sluice. Gold particles are captured by the carpets as water carries lighter materials away. Carpets or capturing rags are later washed to liberate the gold	Concentrate a large amount of ore in a short time	Low-quality pre-concentrates. Need consistent water supply. More work to be done in washing the carpets repetitively. Can be costly and require more downstream operations	Mostly used in ASMs operations along river banks as the process require much water. Lower quality pre-concentrates. The use of carpets increases the work of recovery. Can be modified by changing angels and adding more sluices.
Panning [19]	Medium-sized pan and water	Pan moved in a series of movements designed to eject lighter materials. Gold particles recovered at the bottom of the pan. Works well for ores with the course and well-liberated gold.	high quality concentrates and can produce liberated gold. Can lead to direct recovery. Can be done after the above processes.	Need expertise Concentrate small amounts therefore can be used as a final concentrating effort. Tedious if more ore is to be worked on.	The most applied method in ASMs and developing countries. Can be used in large scale operation to recover course and well-liberated gold.

			Cheap and less equipment.		Can be automated to increase speed.
Spiral concentrator [19]	Motorized pan with spiral grooves leading to the center hole which lead to the collector	Mineral ore and water are fed into a rotating tilted spiral pan. Water washes the denser particles to the center hole while lighter material is ejected	Yield high-grade concentrate ratios	Doesn't differentiate between non-gold dense materials. The setup is a bit complex. Lower throughputs, therefore, demand multiple units for great yield.	It can collect any denser material feed into it. Needs control to filter high-density materials. Haven't gained currency in ASMs in developing countries.
Vortex concentrator[19]	Vortex concentrator (circular tube with water input at the bottom side and drainage hole raised at the center)	Water filled in the vortex to the drainage hole level. The concentrate is introduced in the vortex in a thin layer to the bottom of the vortex. The process is initiated by introducing water through the bottom side tube to create a vortex that lifts less dense materials and discards them via	Capable of recovering high-quality concentrates even fine gold when operated correctly. Easy to operate. Requires knowledge of the appearance of gold.	The process has to be observed to control the flow rate on the inlet water. Fewer amounts of concentrates can be processed per time. Careful introduction of the ore has to be exercised.	Separation is based on the density of the materials. Used more in the laboratory and has not gained traction in the industry. Needs careful control of flowrate and a method to separate other denser materials from gold.

		the drainage hole. The vortex enhances gravity difference.			
Jigs (gold jig concentrator)[10][19]	Jig concentrator, electricity supply, water supply	Jig action is by jig motion which produces pulsating water velocities. The vertical water pulses suspend particles on the upward pulse and the free downward pulse expands the mineral bed and settles the particles in strata with denser particles at the bottom and the lighter at the top. Some of the gangue is rejected via the top of the jig on the upward pulse	Most suited for coarse gold recovery and roughing procedure. Process higher tonnage of ore in one cycle. Able to cope with variable grades and different flowrates	High-frequency cleaning and maintenance to avoid clogging and minimize losses. Lower recovery rates of finer gold. High capital cost and not suitable for lower tonnage as found in small-scale operations. Poor quality concentrate.	Used for large-scale operation for roughing and concentrating huge tonnage. Complex drive mechanism and sophisticated control due to varying hydro-dynamics. Accurate feed proportions to avoid dead spots and clogging. Require more downstream operations like panning. More of an art than a science because of its complexity.
Centrifuges (a vessel that rotates about the central point to	Motorized vessel (centrifuge) Water supply	Concentrate-slurry of 60-75% water is fed into the centrifuge over the top. The material	Usually employed together with the comminution	Generally expensive and mostly integrated with the	Huge capital cost is hence not commonly used in small-scale

separate mixtures by density) [19]	collects at the center of the vessel and high-speed rotation creates a centrifugal force that moves material to the vessel walls. Less dense material pushed out and denser material caught between ridges.	circuit to discard lighter particles. Very effective in gangue rejection.	comminution circuit in a large-scale operation. Separation is mostly by density.	operations. The setting of the separation parameters needs expertise because it is depended on the mixture being separated.

Efficient and effective gravimetric gold recovery is a function of the specific density difference and particle size of the mineral matter. Gravity gold recovery methods are mainly used for pre-concentration and ore enrichment. The products of the above pre-concentration processes do not yield market-ready products so they require further processing (concentration) to have a pure product. The table below presents the concentration processes.

Table 2. 3 : Gold concentration processes

Method	Type of separation	Steps	Equipment	Reagents	Comments and analysis
Amalgamation with mercury [17][19]	chemical	Alloying Amalgam pressing Distillation/vaporisation	Gold pan, amalgam press(hands), retort, amalgam barrel, gold traps	Mercury, nitric acid, caustic soda, sodium amalgam, ammonium nitrate	This is commonly used in ASM operations with mercury only as it is handy and fast. Amalgamation is viewed as the most vital process in gold production in ASM operations

					in developing countries because of its simplicity. In ASM operations there are usually no retorts and distillation equipment and direct vaporization is done. Healthy hazardous due to heavy metal poisoning and environmental pollution
Optical sorting and hand picking (manual separation)[17][19]	Manual	Eye detection (observation) Sorting and hand-picking	n/a	n/a	Common in ASM operation where mercury is not available. Sometimes gold grains are too small to handle. Tedious in terms of fine gold. The picking process is rarely completed
Cyanide leaching (heap leaching, vat leaching, agitation leaching, zinc precipitation, CIP, CIL, etc)[20][21]	Chemical	Chemical solution preparation. dissolution Spraying Adsorption Stripping	Leaching tanks absorbers	Sodium cyanide, calcium oxide for adjusting p-H, zinc, lead nitrate, activated carbon	Mainly used in large-scale operations. Used for low-grade ores or on mineral waste from ASM operations. It's a complex process with huge capital and operating costs for ASM operations. Pollution of water bodies.
Thiourea leaching[21]	Chemical	Chemical solution preparation. dissolution	Leaching tanks Absorbers	Thiourea, p-H reagents, aluminium powder	Not common compared to Cyanide leaching. Complex, capital

		Spraying Adsorption Stripping			expenditure on huge amounts of reagents
Chlorination bio leaching process[21][22]	Chemical	Halogen complexes formation, chlorine bromine complex	Reaction tanks, leaching tanks	Chlorine gas, organic Bromo dimethyl hydrate	Not common compared to Cyanide leaching. Complex, capital expenditure on huge amounts of reagents.
Bacterial leaching[22]	Bio-chemical	-	-	Bacteria, air as an oxidizing agent	Not commonly used, slightly experimental.
Separation by smelting[9], [19]	thermal	Smelting, separation of gold	Furnace, crucible	Borax, soda, potash	Not commonly used in ASM operations. Medium capital cost in acquiring furnace. Energy-intensive

Gravimetric gold recovery methods afford yields of high-quality pre-concentrates which will require less work in the concentration process and mitigate the use of toxic chemicals in the concentration stage. Optical sorting, handpicking, and thermal separation averts chemical separation and lowers disposal costs. Hence this work focuses on technical optimization of the gold panning method, optical sorting, and hand-picking procedure by the way of automation. Figure 2.1 below presents the common flowsheet employed by many artisanal and small-scale (ASMs) operations.

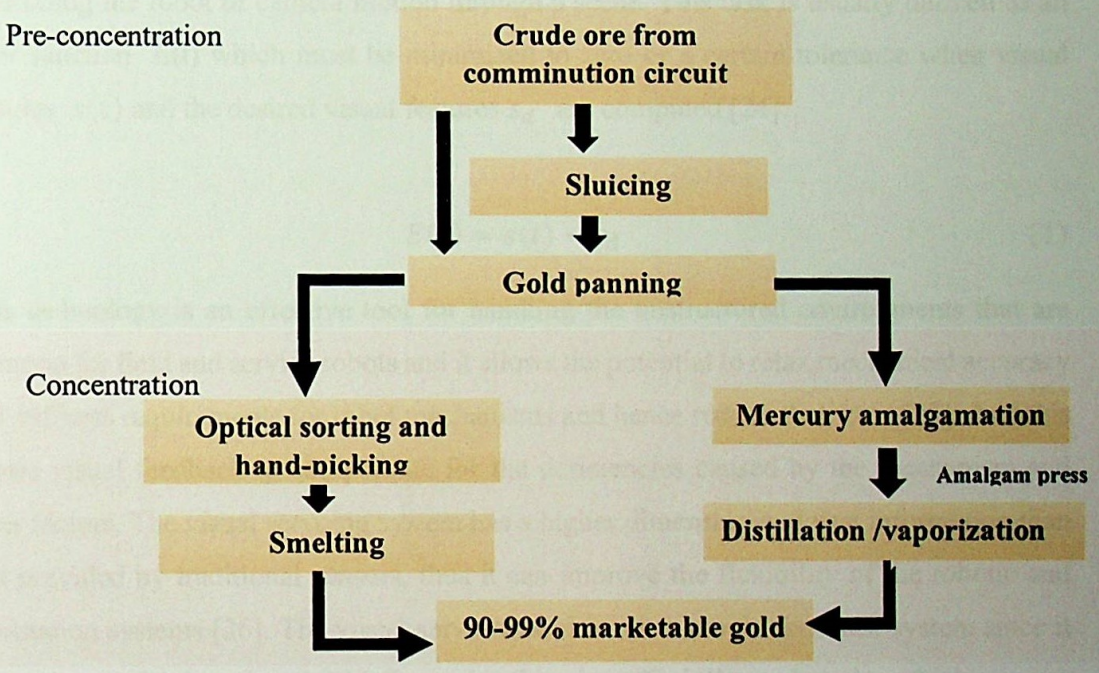


Figure 2. 1 : common gold recovery flowsheet in ASM operations

As seen on the flowsheet figure 2.1 most ASMs operations and other medium scale operations in developing nations employ sluices and gold pans for pre-concentration and amalgamation mostly for concentration. Hand-picking is employed in circumstances where no mercury is available or when the concentrate consists of much-liberated gold.

2.2 Visual servoing

Visual servoing (Vision-based control) has revolutionized the robotics industry and has gained recognition from the industry to become a standard solution for robotic automation tasks since it has simplified many of the industrial tasks [23]. This technique allows robotic systems to imitate humans in positioning tasks by exploiting artificial vision. In simple

terms, visual servoing is a control system that uses visual feedback. Meaning visual feedback is utilized in the closed-loop control method to realize real-time closed-loop control of the manipulator's pose by extraction of visual information. Through extensive research, it has been established that a visual feedback loop can be used to correct the position of the robot to increase task accuracy[24]. The basic visual servoing task is to guide the motion of a robot to a target object based on the aforementioned visual feedback. Classically visual servoing has been applied to position the robot's end effector in line with the target object before performing the desired task. In robotics, the visual servoing task is specified in terms of image features extracted from a target object and their use in controlling the robot or camera motion through a scene. This task is usually defined as an error function E(t) which must be minimized to zero or a certain tolerance when visual features $s(t)$ and the desired visual features s_d are computed [24]:

$$E(t) = s(t) - s_d \tag{1}$$

This technology is an effective tool for handling the unstructured environments that are common for field and service robots and it allows the potential to relax mechanical accuracy and stiffness requirements for robot mechanisms and hence reduce their cost [25]. And this allows visual feedback to compensate for the deficiencies caused by the mechanism and other factors. The visual servoing system has a higher dimension and vast information than that provided by traditional sensors, thus it can improve the flexibility of the robotic and automation systems [26]. The visual servo control is not a simple feedback system since it is based on multi-domain mixed information from interdisciplinary domains which consists of robotics, kinematics, high-speed image processing, control theory, machine vision, system analysis, and other fields [27].

2.3 General hardware components for a visual servoing task (key hardware components for visual servoing)

This section has been included because hardware requirements and technology have been one of the bottlenecks of visual servoing implementation since the inception of this control approach. Whether it is a service robot or vision-based automation task where visual servoing is being utilized there are key hardware components that are always connected to perform it. Figure 2.2 below shows generic hardware components involved in nearly all visual servoing tasks.

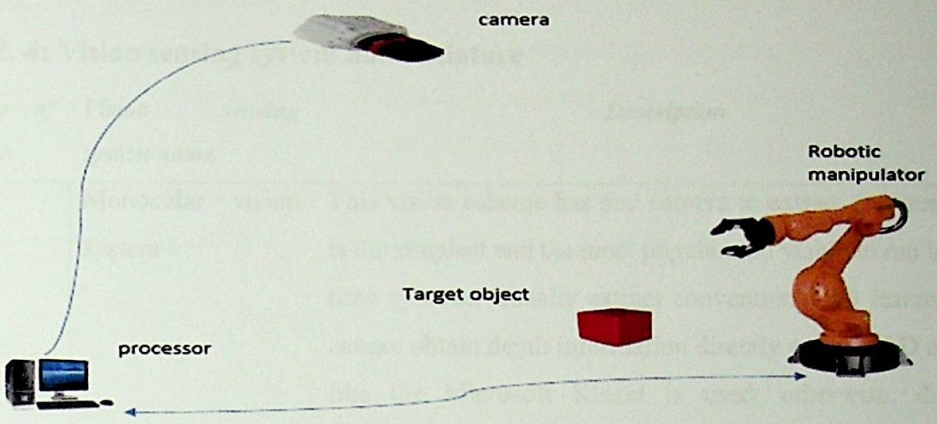


Figure 2. 2: Common hardware components for visual servoing

2.3.1 Camera / visual sensing device

The camera/vision sensor is at the center of visual servoing as it provides the visual data needed for the visual feedback control of the manipulator. The vision sensor has been used widely since it mimics the human sense of vision and allows for contactless measurements. This sensor extracts a large spectrum of potential visual features from the environment and provides them to the processor to work on the data and perform the necessary action. In vision-based control, the vision sensor is used to extract features from the target object or the pose of the robot, or both. From the variety of sensing devices available it is only necessary to select the model that best suits the needs of the application. The selection of the sensing device usually depends on the speed of sensing (retrieval interphase/frames per seconds), image format, resolution, noise-pixel ratio requirements among other things. Besides direct vision sensors which use light to create images, various imaging modalities have been used to perform visual servoing especially in the medical field and these include microscopic imaging, endoscopic imaging, computed tomography fluoroscopy, magnetic resonance imaging, x-ray fluoroscopy. The visual sensors used for object detection and recognition are broadly classified into two-dimensional (2D) cameras and three-dimensional (3D) visual imaging sensors. The 2D sensors acquire images that only represent morphological features of the target such as color, shape, and texture whereas 3D sensors provide the spatial location of the object in a 3D coordinate map. Omni-directional cameras are finding popularity because they increase visibility and the field of view of the system. The number of cameras is sometimes used to classify the vision sensing system:

Table 2. 4: Vision sensing system nomenclature

Number of cameras	*Vision sensing system name*	*Description*
1	Monocular vision system	This vision scheme has one camera to extract features. This is the simplest and the most popular and viable to run in real-time systems. Usually extract conventional 2D features and cannot obtain depth information directly unless a 3D camera like the Microsoft Kinect is used, otherwise, distance information is obtained by measuring the distance moved by the camera or robot. This system has a narrow field of view, accuracy, and precise 3D localization compared to other schemes [28].
2	Binocular /stereo vision system	This consists of two cameras arranged at an angle as it tries to mimic human vision. It is mainly used for depth-related applications[29]. It has a greater field of view compared to monocular [30]. Though stereo vision solves the depth problem it comes with complexity in algorithm processing.
3 and more	Multi-vision system (redundant system)	This consists of multi-cameras used to extract features from the scene. This scheme can be used to extract depth information and can achieve multi-angle observation objectives to access more comprehensive information. The distributed vision is usually used to improve estimation accuracy in 3D positioning and orientation tasks and when there is enough time and resources for processing [31][32].

2.3.2 Artificial lighting System

Along with the vision-sensor is the lighting system. A lighting system is usually provided to enhance the quality of images or features extracted and to remove unnecessary noises and disturbances on the scene. The lighting system must be spectrally uniform, and stable over time, and provide uniform radiation across the scene, and remove shadows, to extract quality features thereby reducing pre-processing efforts and time for analysis [33]. A cautiously selected lighting system can overcome common problems such as reflection, shadowing, and noise. Image clarity, repeatability, and reliability of the machine vision system are a function of the light source, power of light, method of illumination, the shape of the light beam, and light color. The configuration of the light sources for the sample on which features are to be extracted is important. These arrangements include Frontal

lighting (for applications requiring surface extraction), backlighting (to facilitate edge dimensioning and subsurface extractions), and structured lighting (depending on application)[34]. The commonly used light sources include incandescent lamps, fluorescent lamps, quartz halogen, lasers, light-emitting diodes, X-ray tubes, infrared lamps, etc. and their selection depends on the power rating and application requirements. Artificial lighting is needed when feature extraction is done in places void of enough light especially in enclosed platforms and in tasks where low-level image processing is done.

2.3.3 Processor

The processor is responsible for processing the visual data extracted by the image sensor (image processing) and compute this data to control the manipulator. It is the brain for visual servoing tasks, it connects perception and action components of the system. The processor computes the object detection algorithms and visual servoing algorithms to perform the intended robotic manipulation task. Computational efficiency has been one of the bottlenecks in the progression and adoption of vision-based control. These technical limitations for a duration of time prevented the important developments in visual servoing [35]. The processor has to be able to provide fast image processing to provide for reactive control of the robot or automated system. The rapid progression of image progressing hardware technology and computer processing capability has caused a lot of research to be conducted on visual servoing technology. The selection of these processors depends on various factors including, speed requirements, power requirements, ease of system integration, etc.

Real-time image data acquisition and processing is a vital issue in visual servoing applications. A high frame rate and low processing latency are essential since the visual servoing system must make quick decisions based on the information extracted from a scene. To meet real-time constraints, the development of visual servoing systems usually requires high-cost specialized hardware and software [36]. The quality of the digital image is enhanced before image analysis using methods such as image resizing, image enhancement, noise removal, edge detection, filtering, etc. Other operations of processing can be done to separate the wanted object from the whole image and these fall under image segmentation operation (for example threshold-based, region-based, gradient-based or classification-based method)[34]. The processor can come in the form of a specialized Digital Signal Processor (DSPs), Graphical Processing Unit (GPUs), single board computers (CPUs), embedded processors (System on a Chip), Field Programmable Gate Array (FPGA), or hybrid systems.

2.3.3.1 CPU (Central Processing Unit)

The usage of conventional computers in the form of laptops, desktops, and industrial computers for machine vision applications is more common since they are almost found everywhere and can do various operations as long as the specific package for the operation is installed. The usage of computers usually ends up increasing the price of implementation in some cases. In [37] authors used a general computer to perform vision-based automatic grading of fresh fruit bunches. [38] Implemented vision-based control of a robotic manipulator for citrus harvesting. A PC was used for the visual servoing for low-cost SCARA robots using an RGB-D camera as the only sensor [39].

2.3.3.2 Graphics Processing Unit (GPUs)

These are computer chips for rapid mathematical computations to render images. They work separately from the Central processing unit (CPU) to avoid straining the CPU when processing graphics-intensive applications. GPUs may be integrated with a CPU on the same circuit, on a graphics card, or in the motherboard of a computer. GPUs can render images more quickly than a CPU because of their parallel processing architecture which allows them to perform multiple calculations at the same time. Usually, vision-based projects take advantage and harness the massively parallel computational power of modern GPUs for simulation (3D model rendering) and evaluation (segmentation, feature extraction, and weight calculation) [40]. The authors in [40] accelerated particle evaluation up to 49 times over a comparable CPU-only implementation, providing increased particle count while maintaining real-time frame rates using a GPU (Nvidia CUDA). A GPU was used to receive the images from the scanner and process them to send commands to the robot in real-time needle detection and tracking using a visually servoed 3D ultrasound probe [41]. K2200 GPU (2Go memory) was used to train a deep neural network-based method to perform high-precision, robust and real-time 6DOF positioning tasks using visual servoing and it took two hours which might have taken more had they used a general CPU [42]. GPUs are frequently used to improve system performance, get better efficiency, accuracy, and stability in visual servoing systems as witnessed in [43][44][45].

2.3.3.3 Digital Signal Processors (DSPs)

These are efficient processors/microprocessors for applying algorithms for image processing as well as other signals like video, audio, etc. These processors are suitable for a wide variety of computationally intensive real-time applications. They provide high computing power by employing high-level on-chip parallelism, integrated hardware

multipliers, carefully tailored instruction sets, memory organization schemes, hardware support for loop execution. These features have made them be used in control applications such as robotics, high-precision servo control, Artificial Intelligence applications such as machine vision, neural network simulation, pattern recognition, object detection, etc. [46]. A TMS320C6711 IDK Digital signal processor (DSP) was used to implement visual servoing of an under-actuated system (inverted pendulum: 2DOF and one actuator) using Discrete Wavelet Transform [47]. The DSPs are normally used to handle complex mathematical calculations and control laws. This kind of processor is used as a robot controller to compute the torque control, low-level control of robot motion, and process dynamic compensation from measured poses and velocity [48]. TMS320C40 DSP was used to perform image processing and visual servoing control for micro-positioning of a probe of a micro-assembly of hybrid MEMs (microelectromechanical system) to numerous holes on a machined template [49]. While doing a comparative study between DSP systems and ANN ensembles for motion detection and filtering authors in[50] pointed that the high cost of DSPs at high bandwidths and high power consumption and size can make them unsuitable for simple very low-power or small applications. With the upward steep demand curve in the processing requirements for imaging and other industrial vision processing applications, increased complexity of vision processing algorithms, need for higher resolutions, faster frames per second rates, and image and video analytics, the manufacturers of DSPs have responded with a range of processors that can fill any level of application to curb the demands [51].

2.3.3.4 Embedded systems, System on Chip (SOC), and FPGA

The issue of cost, miniaturization, availability, and shorter prototyping times have been the driving factors towards designing robotic and automated systems. The cost of the processor is one of the driving forces in the development of a visual servoing system. Embedded platforms allow keeping the size and cost as low as possible. Research works have been conducted to optimize the computationally intensive image processing and visual servoing algorithm so that they can run smoothly on embedded platforms.

2.3.3.4.1 Field-programmable Gate Arrays (FPGAs)

FPGAs have allowed the application of re-programmable hardware technology specific for the implementation of visual controllers. The implementation of a direct visual control system embedded in an FPGA allows improving these systems by reducing processing

delays, obtaining stable delays in the feedback and it allows the implementation of a dedicated parallel architecture that can be adapted in runtime to the plant needs [52]. Real-time and low-power hardware implementations of classification and detection algorithms have been realized in both FPGAs and custom ASICs, with FPGA implementations becoming popular due to the lower cost, availability, and shorter prototyping times. Kyrkou C in [53], [54] investigated three popular object detection algorithms (Neural networks, Support Vector Machines, and the Viola-Jones detection framework) and their hardware implementation using the FPGA platform for Viola-Jones detection framework and tested the proposed architecture on an ASIC implementation. The proposed architectures were experimentally evaluated on FPGAs computing platforms demonstrating real-time performance (over 30 frames-per-second) which enables them to be used in real-time object detection applications and maintain detection accuracy comparable to software implementations. Field Programmable Gate Arrays (FPGA) promise flexibility and sufficient computing performance at affordable design costs [55]. Open embedded architecture for direct visual servoing of industrial robots which is easily extensible to control any multi-joint robot manipulator based on FPGA was presented [52]. The open architectures for robot control [52], [56] using these embedded systems are being created to avoid continuous dependency of the end-user on the particular vendor when maintenance, update, or incorporation of new functionality to a working system is required. An image processing system for robot vision applications was prototyped on an FPGA for real-time servoing [36].

2.3.3.4.2 Single-board Computers

These provide all the features of a normal computer on a single card, that is, the processor, memory, input/output(I/O), and other units are integrated on a single card. They are designed to be simple, low cost, and low powered devices, and they are preferred to develop systems and prototypes for educational studies but are finding a way for menial industrial tasks [57]. Many types of single-board embedded computers can be used for vision-based projects but the Raspberry Pi seems to have many works performed on it and many support packages from other developers like MATLAB from MathWorks. Few works on raspberry pi will be discussed briefly in the preceding section.

A Raspberry Pi embedded computer was used for vision processing on a robotic label applicator using visual servoing[58]. The work in [59] used a raspberry Pi controller to

compute a complex vision algorithm that recognizes specified objects and transmits signals to an Arduino controller which generates signals to grip the specified object using a grasping 6DOF robotic arm using Pi-camera. The Raspberry Pi and an Arduino microcontroller board were used to implementing vision-based trajectory control for autonomous vehicles [32], the Raspberry Pi was used as the embedded computer and was responsible for calculating the desired steering angle from the computer vision system and make correctional actions based on the differences between the desired and measured steering wheel angles. A real-time implementation of a visual servoing algorithm (Position-based visual servoing) and fusion of data from a proximity sensor was implemented on an embedded platform (Raspberry Pi) for a wheelchair mounter robotic arm using parallel tracking and mapping of task objects[60]. The Raspberry Pi II embedded computer board was used for vision-based cruise-position-directional control of Differential-Drive Thunder Tumbler (DDTT) mobile robot when the author of [61] presented work on image processing based control of mobile robotics. The Arduino and Raspberry Pi permitted the performances of the complicated task at a low cost. Position-Based Visual Servoing (PBVS), Image-Based Visual Servoing (IBVS), and the encoder–camera-based speed –directional outer loop were implemented on the Raspberry Pi II. Real-time object tracking using Kanade-Lucas-Tomasi Feature Tracker algorithm (KLT) and Continuous Adaptive Mean Shift (CAMSHIFT) using color histogram for features was implemented in C++ with OpenCV on a Raspberry Pi II [62]. The Raspberry Pi was used as an on-board controller of an Unmanned Ariel Vehicle (UAV) to run the detection and navigation algorithm running an Ubuntu and ROS platforms. The embedded computer ran all the ROS nodes: the main control loop of the system to run the whole system, the mavros mode that provide communication between the systems, target detection node and image capture node for capturing images from the Raspberry Pi camera [63].

The authors in [64] presented object detection and Keep on a mobile robot by using a low-cost embedded color vision system. A CCD camera with an embedded system to perform small tasks with high flexibility, low cost, ease of construction, and energy saving. Their mobile robot could detect a ball and its diameter in different positions. The embedded camera would send the coordinates of the position of the ball to the STM32F103RBT6 Microcontroller to control the movement of the mobile robot.

Performance studies of the processors for machine vision have been conducted to guide the developers, hobbyists, researchers, academies, and other interested parties. In [65] a

comparative study of the processor technologies and solution approach to various image processing algorithms in the real-time embedded systems were presented for the GPU, FPGA, DSP, and general-purpose CPU. The authors brought up issues of accuracy, computational efforts, and power requirements as the main issues pointing to the fact that technology selection for various applications is a critical task. The general trade-offs were given which pointed to the fact that: Application-specific systems deliver high performance with little flexibility while general-purpose processors provide flexibility with average performance. Analysis and discussion of the processors were done focusing on the issues of power consumption, developmental time, parallelism, code translation effort, integration, and physical space [65]. The results of power consumption and execution time profiling for the software components that can be allocated on different computing platforms were presented in [66]. With measurements and analysis being done on power consumption and execution time based on various components such as image filtering and object detection the overall best choice between GPU, CPU, and FPGA could not be established as one platform performed better in other areas.

2.3.3.4 Distributed Control (Multi-processor-based solutions)

Due to some problems faced in visual servoing tasks, the use of multiple processors (distributed control) is common, where a processor is completely devoted to its task at hand. For instance, one processor dealing with visual data processing, while a separate processor takes care of the scheduling of tasks and the global control law [23][67]. The cost of a multi-processor-based solution is considerably higher compared to a single processor.

In [56] an industrial robot for welding processes was controlled using a standard PC and an FPGA –based interface, the FPGA was used to decode the feedback position data (computing the control output and communication signals, and transmitting such data to the actuators) and the PC interpolated movements, computed kinematics solution and transmitted the position reference for each joint while it receives its current position. Robust real-time visual servoing control of an inverted pendulum was implemented using DSP and FPGA[36]. The FPGA computed the image processing algorithms to meet real-time constraints and the control law was implemented on the digital signal processor to enforce robustness to model uncertainty and to attenuate the disturbances. A distributed parallel image processing for the visual servo control of two 1DOF linear motor modules over a network was presented in [68] to overcome the low sampling rate problem in vision-based

control systems. The captured image was sent to different nodes for processing to overcome the various delays in the process. The authors of [68] presented again a cloud-based networked visual servo control in [69]. The framework integrated networked computational resources for cloud image processing using real-time transport protocol for transmitting large-volume image data on a cloud computing platform which enables high sampling rate visual feedback. The performance of the networked visual servo control system was then validated on a 14DOF dual-arm robot with superior performance. In [70] a host computer was used to monitor the robot on a Graphical User Interface (GUI), a real-time controller (NI-compact RIO) was used to run the actual control loop, which is the core of the control system (open-loop and vision-based control algorithms, the inverse kinematics, and the motion generator) and an FPGA was used for vision-based real-time position control of a semi-automated system for robot-assisted joint fracture surgery. A PC and Arduino –based microcontroller were used to control a VICRA robot to perform visual servoing and grasp planning[39]. The PC computed the visual servoing algorithms and the Arduino microcontroller was responsible for robot control based on the information from the PC. The work in [67] used the concept of distributed control to implement an uncalibrated visual servo control with a neural network. Two nodes were used, the robot controller DSpace DS1102 motion controller board executed joint servo-control algorithms and the image processing node acquired the images from the camera, extracts the image features, and executes the visual control algorithms. The concept of distributed control mimics the function of the human brain where each part of the brain is responsible for certain processes and can be used to ease computational requirements from the single processor by adding different processors for dedicated processes.

2.3.4 Robotic manipulators

In the context of this discussion and subject matter, the robotic manipulator is that device where the visual servoing algorithm will be applied on, either an industrial manipulator, autonomous vehicle, vision-based automated system, unmanned aerial vehicle (UAV), etc. In general, a robotic manipulator is an electronically controlled mechanism, consisting of multiple segments that perform tasks by interacting with the environment. These manipulators are composed of rigid links, connected in series by joints, having one end fixed(base) and another free to move and perform useful tasks when properly tooled (end-effector)[71]. The design of these autonomous systems perform tasks that are dull, dirty,

dangerous, repetitive, or require skill, speed, strength, or dexterity beyond the capability of humans such as manufacturing, excavation, construction, undersea, and planetary exploration, toxic waste clean-up, robotic-assisted surgery, etc. [72]. The end-effector at the end of the manipulator could be a gripper, a welding torch, an electromagnet, or any other tool/device that is required to perform the intended task. The fundamental functional requirement of the manipulator is to be able to locate its end-effector in the robot's working space. The robot manipulators are multi-degree-of-freedom position devices[72]. The number of degrees of freedom (DOF) of a machine is defined as the number of independent variables that are required to completely identify its configuration in space. The robot manipulators are classified by motion characteristics, kinematic structure, and the number of Degrees of Freedom. There are five types of robotic arms commonly used and these are Cartesian, cylindrical, polar, SCARA, and articulated.

2.4.0 Camera Configurations in Visual Servoing

For visual servoing, there are two general camera placements for the end-effector that end up with two camera configurations. These configurations have their advantages and disadvantages in terms of precision and field of view limit that oppose each other. The camera configurations are the eye-in-hand system and the eye-and-hand system.

2.4.1 Eye-in-hand/Camera-in-hand (CiH) configuration

In this configuration, the camera is mounted on the end-effector of the manipulator. This is done to measure the target object's information in the workspace and move the robot's end-effector accurately to obtain the position of the target in the work space thereby realizing robot control. This arrangement can decrease the payload of the system since the camera is attached to the end-effector. In this configuration, there is a constant relationship between the pose of the camera and the pose of the end-effector[24][67]. The fact that the camera is located on the end-effector creates a dynamic measurement system and the constant relationship between the camera pose and end-effector pose gives a kinematic relationship between the target object and camera directly resulting in a more robust and accurate system [23]. The eye-in-hand configuration allows the target object or scene to be kept in the field of view once the target is captured by the camera but if not captured it can take longer to control the robot. Since the camera moves frequently in this configuration active vision ability and precise manipulation must be guaranteed.

2.4.2 Eye-to-Hand / fixed camera configuration

This configuration has the camera fixed in the workspace and does not move with the movement of the robot during the working process of the robot. The target in this image is independent of the robot's motion unless the camera is connected to the second robot[24][67]. In this configuration, the camera weight does not affect the payload of the system since it is not attached to the robot end-effector. The camera is related to the base coordinate system of the robot and the target object[24]. This configuration allows the servo system to be designed as an endpoint closed-loop system where both the target and the end-effector are observed during the execution of the task thereby solving the problem of image features escaping the field of view [73] [74]. This configuration was used in [67] with a fixed camera within the workspace to provide positional information of the robot's end-effector and the target in the robot's workspace. The camera observes the target and the robot from a distance, creating the extra difficulty that the error to be minimized is dependent on the calibration and visual processing to have robust positioning accuracy[23]. The transformation between the camera frame and the robot end-effector frame is computed at each iteration using the transformations between different frames[25]. The robot is controlled by observing the relative positional relationship between the target and the end-effector. One of the advantages of this configuration is that the camera angle can be adjusted in advance (calibrated) to obtain a wide range of field of view (FOV) [27]. Usually, when using this configuration, the robot cannot be collinear with the image sensor and the target object since this will result in object occlusion.

2.4.3 Hybrid configurations

These can be constructed where both eye-in-hand and eye-and-hand systems complement each other. In multi-arm robotic cells, visual systems are usually equipped with a hybrid camera configuration with two or more cameras in which some are in eye-in-hand and others are eye-to-hand configurations, with the eye-in-hand configuration guarantying good accuracy and ability to explore the target although with limited sight while the eye-to-hand configuration ensures a panoramic sight of the workspace but with lower accuracy[75]. The use of both configurations at the same time makes visual servoing tasks easier and offers flexibility in dynamic scenes. Hybrid configuration is used to solve occlusion problems and to exploit all the potentials of the separate configurations. In [75] a hybrid configuration was

used for position-based visual servoing and a study comparing a hybrid configuration to eye-to-hand configuration was done, proving the hybrid configuration to have lower estimation error than the eye-to-hand alone. A multi-camera framework for visual servoing of a collaborative robot in industrial environments which can be generalized to any number of eye-to-hand and eye-in-hand cameras was presented, with 90% of picking success according to experimentation. An eye-to-hand approach on eye-in-hand configuration using markers was proposed for real-time visual servoing [76] using a robotic manipulator. This configuration managed to resolve the drawbacks in separate camera configurations.

Camera calibration and the determination of the intrinsic camera parameters such as focal length, pixel, pitch, and the principal point are nearly important for both configurations before the visual servoing task is initiated [24][25].

2.5 Visual Servoing Architectures (Basic approaches)

The visual servoing architectures are focused on positioning the end-effector or maintaining a constant relationship between the robot and the moving target (tracking) and in both cases, visual cues are used to measure the error between the current location of the target object and its reference and desired location. The visual cues are used to perform the task in a two-dimensional plane which is expressed as image coordinates or to perform tasks in the three-dimensional plane which is expressed in the retrieval of pose information of a camera/object model about the camera/world/robot coordinate system. The definition of the task function in either 2D or 3D plane brings about the visual servoing classification approaches. The classification addresses the domain in which the error function will be computed from either pose space or image space. The approaches are Image-based Visual Servoing (IBVS)/ 2D Visual Servoing and Position-Based Visual Servoing (PBVS)/ 3D Visual Servoing. The combination of these two basic approaches gave rise to the hybrid approach/ 2 ½ D visual servoing.

2.5.1 Position-Based Visual Servoing (PBVS)/ 3D Visual servoing

Position-based Visual servoing involves features being extracted from the image during an iteration of the control loop and evolving an estimate of the target's pose to the image sensor, meaning it uses the image features to estimate the current pose of the target[26]. This is indirect control since pose estimation (image interpretation) is done before robot control which results in longer processing times. The 3D information about the scene and the

geometric model of the target is retrieved and used to estimate the position and orientation (pose) of the target about the camera/world/robot coordinate system [77]. The error function is treated as the difference between the current and the desired poses[78] in 3D pose space. This approach approximates quantities to parameterize the feedback and is closely related to the problem of recovering scene geometry from the camera. The pose of the object is estimated relative to the image sensor and this requires the transformation between the robot and the camera to be known so that the required motion of the manipulator will be generated [77]. The position and orientation of the target object is estimated from the object image and the prior knowledge it has of the object. Usually objects with well-defined geometric shape are usually represented as a wire-frame model in the pose estimation stage and servoing task is completed when wire frame model coincide with object model [79]. PBVS feedback has no control over the trajectories in the image space [23]. The accuracy of this approach depends on the target pose estimation, which depends on the 3D spatial model of the object and it is difficult to ensure accuracy in this system if the target is out of the visual field [26]. PBVS demands that the camera be finely calibrated (the camera parameters must be expressly known) so that the current and desired camera poses will be accurately estimated leading to excellent performance and accuracy and avert failure of the visual servoing task. The transposition of data from the 2D image plane to 3D Cartesian space demands high computational effort which limits the applicability of the algorithm in real time systems [79]. 3D visual servoing feedback and estimation are more time consuming than 2D visual servoing as the relative pose must be estimated online. PBVS has better response to large rotational and translational camera motions than IBVS and does not suffer image singularity, local minima and camera retreat which are problems specific to IBVS. This approach has no way of regulating features in the image space and is more sensitive to camera and object model errors compared to IBVS [80].

The application of 3D visual servoing and its accuracy is dependent on the pose estimation problem. Research work on pose estimation has been carried out and solutions which are broadly grouped as analytical and least-squares solutions have evolved as witnessed by different solutions for coplanar scenes (analytic solution) which do not apply for collinear feature points (least square solution). Iterative solutions to refine pose estimation problems based on real-time observation have evolved since the least-squares solution to pose estimation is a nonlinear optimization problem with no known closed-form solution. For

example, Extended Kalman filtering (EKF) provides an excellent iterative solution to pose estimation problems [81]-[83]. A fast, robust and accurate approach for pose estimation problems for robot motion was given which combined the Extended Kalman filter (EKF) and the use of multiple cameras [84]. Pose induction and pose alignment are used for position-based visual servoing control of a quadcopter [85]. Pose induction inferred the desired orientation to the target from the desired pose given about the source, while pose alignment approximated the present orientation for the target and control the robot to the desired pose. Pose induction did the job of pose estimation by using the deep neural network to compute a reconstruction in the camera frame and servoing of the target instance in the feedback loop. The induced desired poses through pose alignment generated the velocity commands for the robot through the PBVS controller. Pose induction and pose alignment are iteratively executed until the PBVS control error reaches the desired tolerance. The particle-filter approach was used to estimate the relative camera pose between different camera frames [86]. This was made possible by using a Bayesian tracking-based pose estimation algorithm which predicted the current pose using velocity control signals which were known prior. The approach enabled model-free position-based vision-based control through online estimation of 3D pose information needed in the control law design.

The advantage of PBVS is that it is possible to describe tasks in terms of the pose as cartesian coordinates and that the camera/robot trajectory is controlled directly in 3D space which allows easier trajectory planning and obstacle avoidance. One of the disadvantages of this approach is that it is highly calibration-dependent [67].

2.5.2 Image-Based Visual Servoing (IBVS)/ 2D visual servoing

This approach performs control objectives directly from the image without pose estimation of the target object meaning visual information is directly used to control robot motion. The task function is based on the image characteristics. The error signal in the image plane is used to control the end-effector movement to the target position. The feedback is computed from the image plane and the error function is treated as the difference between the desired feature vector and the current feature vector. For this approach, pose estimation is omitted and the control law is directly expressed in the image space [87]. This control architecture has reduced processing times for the algorithm and increased sample rates since the 3D reconstruction of the target are omitted. The task in this approach is defined in the image space (2D) rather than world space [67]. The error function is defined as the difference

between the current and the desired feature position:

$$e = f^c - f^x \quad (2)$$

f^c *and* f^x are the current and desired feature vector in the image plane. And these image features are used in the estimation of the robot's joint parameters such as position, velocity, acceleration, meaning the error signal in the image space is directly mapped to motion commands (actuator commands). The result of the error function in the image space is used to generate the control signal for the robot in Cartesian space or joint space. IBVS control involves the computation of the image Jacobian or the interaction matrix which represents the differential relationship between the scene frame and camera frame [78]. The Jacobian encodes and decodes the relationship between the velocities in the robot's workspace and image space velocities [88]. The interaction matrix / Jacobian contains the coordinates of the end-effector in some parameterized task space and image feature vectors. The image Jacobian connects the image parameters 'f' with the velocity of the end effector 'q' by the relationship:

$$\dot{f} = Jq' \quad (3)$$

The estimation of the image Jacobian requires the knowledge of the camera's intrinsic and extrinsic parameters as these might present a mapping between the scene and the camera frame. Usually, if a monocular vision system is used and the camera used does not provide depth information which is used to update the image Jacobian, the Jacobian is lost and this has caused many existing systems to rely on a constant Jacobian which is computed for the desired camera/end-effector pose[77]. There are three cases in which the image Jacobian is used in IBVS to ensure the global asymptotic stability of visual servoing system[78] and these are:

i) Estimation/learning of the image Jacobian during camera/robot motion without considering the analytical form. Artificial Neural Networks (ANNs) have been used in the estimation of the image Jacobian. In [67] a Kohonen's self-organizing Map (KSOM) image-based visual servoing scheme using neural networks was shown to approximate an estimate of the inverse kinematic Jacobian from the image space to the joint space. The learned map by ANNs ensured global stability and computational efficiency in real-time. Estimation of a composite Jacobian using a dynamic recursive least squares algorithm was performed

during the development and demonstration of an un-calibrated vision-guided tracking control [74].

ii) Up-dating the image Jacobian iteratively on the execution of the control law. The accuracy of this method is dependent on the knowledge of the depth information and is susceptible to inadequate camera motion which might lead to possible local minima and singularity problems. The method of updating the interaction matrix performed better than the preceding method of using a constant interaction matrix [89]. In [79] the image Jacobian was computed based on the real values of the image pixels and depth value at each iteration. Though this provides the most efficient Jacobian computation updating the Jacobian iteratively requires huge computational effort.

iii) Offline determination of a constant image Jacobian obtained using estimation of the depth of the point at the desired pose and using the desired value of the image features. This approach usually ensures stability in the neighborhood of the desired position [78].

The image Jacobian and its computation for the IBVS approach depends on the type of features used. The image Jacobian has to be decoupled properly otherwise the steady-state errors will increase with large commanded relative motion [80]. Pixel coordinates of the set of image points are not the only possible choice since they are nothing but the camera intrinsic parameters to go from image measurements expressed in pixels to the features [73]. IBVS approach does not need geometric modeling of the target and camera calibration since the closed-loop is defined in the image space and is robustly satisfactory in the presence of calibration error. Despite its robustness, the issues of stability and convergence associated with IBVS stem from the image Jacobian (singularity error, lost Jacobian, etc.) leading to unstable behavior and local minima and local convergences issues [78]. IBVS may reduce computational delay, eliminate the necessity for image interpretation and errors due to sensor modeling and camera calibration[24]. IBVS feedback lacks the design of motion in Cartesian space as it is executed directly in the image space [23]. Since this approach does not have direct control over robot trajectories induced by the servoing loop in the physical space, the possibility of trajectories that might go beyond joint limits or physical constraints is abundant[26]. Theoretically, IBVS is suitable only for small displacements but less than optimal in terms of 3D motion because of the non-linearity in the relationship between

the image space and the workspace and the coupling between the degrees of freedom[90] [91]. A minimum of three nonlinear points is necessary to compute the control law for image-based visual servoing and increasing the number of points increases its robustness.

IBVS popularity and usage over PBVS are mainly because of its shortcomings in terms of calibration, 3D reconstruction, and errors in task execution. The main advantage of IBVS over PBVS is that no camera calibration is needed[67] and it is considered to be more robust for camera and robot calibration. Because of the nature of IBVS, which limits its application to several features less than the number of degrees of freedom, its systems are often attracted to the local minimum far away from the desired configuration, thus in terms of stability, only local asymptotic stability is obtained for IBVS [73]. The computation of the image Jacobian seems to cause many drawbacks in the use of IBVS, especially the use of constant Jacobian in monocular systems have been one of the major drawbacks of IBVS since convergence is ensured only around the desired position [77] and adaptive depth estimation, use of the stereo system, concatenation of two monocular image Jacobians have been used to cater for this problem. A majority of IBVS algorithms employ conventional monocular vision systems which are heavily plagued by lack of depth information, a constrained field of view, occluded view, and specular highlights [92]. Plenoptic cameras/light field cameras have provided potential solutions to some of these issues since these cameras provide depth and multiple view information. The application of Light Field cameras in [92] displayed superior performances compared to conventional monocular and stereo IBVS though they come with a cost of complex calibration procedures compared to other cameras. The LF cameras are robust in handling occlusions and specular reflections which can make them useful in mineral processing, jewellery identification, and precious stone processing. Recent work in [93] proposed a simplified methodology for IBVS without computation of the interaction matrix. The method is based on parallelogram features (point error and area error of 4 feature points). The parallelogram model was used in the 6-DOF IBVS control since it captures the most important features of interest. The method employed parallelism invariance and decoupling of the proportional control principles to perform the orientation tasks. One drawback of the method is that it does not apply to arbitrarily shaped objects as it is limited to objects with 4 interiors/exterior vertices or which have parts that can be defined with 4 vertices. The method proved excellent results for pick and place tasks. Correspondence-free Image-based visual servoing which can perform control tasks without

rigorous feature matching with stable camera motion was recently presented in [94]. In this method, a stabilizing control technique that solves the correspondence of features and visual servoing together was utilized, doing away with feature tracking and image processing requirements. The approach is robust for symmetrical and asymmetrical target objects and in applications where image feature arrangement is of less importance.

2.5.3 Hybrid based visual servo Control

Combining both methods image-based and position-based visual servoing can result in an improved performance as seen by hybrid or portioned approaches. The hybrid control scheme avoids the respective drawbacks of 2D and 3D visual control. This approach is 'halfway' between classical PBVS and IBVS approaches which is why it is termed 2 ½ D visual servoing and was originally proposed for the eye-in-hand configuration. The error function in hybrid visual servoing is computed partly in 2D image space and partly in 3D space[95]. This approach allows the decoupling of rotational and translational control loops thereby allowing convergence in the entire task space. 2 ½ D visual servoing is made possible by estimating the homography of feature points between the current and desired camera poses. And the use of homography does not rely on the 3D geometric model of the target as compared to the PBVS alone. Iterative estimation of homography in conjunction with the control law makes 2 ½ D visual servoing independent of precise camera calibration. The hybrid approach guarantees the convergence of the control law in the whole task space as compared to IBVS. The hybrid visual servoing approach affords the capability of utilizing both global and local vision to independently determine the pose of the target by allowing the controller to automatically switch from either global vision or local vision when either fails to recognize the marker[77]. In [96] the visibility constraint problem was solved by combining the image-based visual servoing (IBVS) and Pose-based visual servoing (PBVS), and a classical balance between these two approaches were established. Only 2D features which were vital in keeping the object in a constant field of view (FOV) were used to produce a control law with local stability and a global minimum at the PBVS intended pose. A hybrid architecture that uses a switching scheme between the traditional image-based visual servoing control and neural network reinforcement learning was presented in [97], which provided a decoupled control process for the vision-based control task. The error between the current image features and the desired image features is calculated and a correction in the robot pose for alignment with the desired object is performed using a neural

network reinforcement learning controller. The image-based control scheme is activated when the second desired area is within the area of interest as the first and it included estimation of the image Jacobian and error vector. This hybrid switching approach managed to solve the visibility constraint issue while maintaining the preferred path of the robot for the entire servoing task and it was robust to the changing environmental conditions. The main benefits of PBVS and IBVS were harvested using a task composition algorithm for a hybrid visual servoing with a dynamic and hierarchical task-priority control framework that controlled an aerial vehicle with a robot arm [98].

2.5.4 Enhanced visual servoing techniques

In visual servoing literature, other methods do not fall directly into the categories mentioned above. These methods were mainly an improvement or sought to solve some of the drawbacks of the original method. These methods include techniques like:

2.5.4.1 Shortest path visual servoing

This was presented by Kyrki and Kragic [99] when they were addressing the problem of the target leaving the camera's field of view and the problem of joints working too close to their limits. This approach solved the issue of the uncertainty of the trajectory which occurs in several methods. The shortest path approach to position-based visual servoing (PBVS) allowed for the shortest cartesian trajectory and guaranteed object visibility was demonstrated together with a homograph-based partial pose estimation visual servoing. The shortest path visual servoing is viable on 3D visual servoing and hybrid method. This improved technique had better performance than PBVS in terms of execution time and maximum features excursion [79].

2.5.4.2 Partitioned approach to IBVS control (Corke & Hutchinson Visual servoing) [88]

This addressed the contorted robot trajectories which may be undesirable in the cartesian space and the camera retreat problem in IBVS which is experienced for pure rotations around the optical axis of the camera. Their methodology separates the control of translational and rotational motion over the z-axis from the other degrees of freedom and it only focuses on the z-axis since camera retreat and IBVS failure are Z-axis translation and Z-axis rotation phenomenon respectively. The performance of this method is depended on the relative position of the features in the image to ensure that all the features remain in the field of view throughout the robot trajectory. This method performs well for generic motions

than the original IBVS and performed excellently for pure rotations around the optical axis. This method does not require much computational effort and has improved task execution for tasks that require large z-axis rotations [88].

2.5.4.3 Photometric Visual servoing [100]

This approach is based on IBVS but it uses the luminance of all pixels instead of geometric features or homographs to remove the tracking or matching process. The basis of this approach was the analytic computation of the interaction matrix which relates the time variation of the luminance to the camera motions. This method is robust in approximating depths, low textured objects, and partial occlusions.

2.5.4.4 Deguchi Visual servoing [101]

This is an appearance-based visual servoing approach that does not need image processing for feature extraction and correspondence search as it removed the assumptions that the object images are expressed with simple primitive features (points, lines, conics, etc.) and the assumption that the correspondence of the primitive features is always maintained in the sequence. This approach sought to apply visual servoing to more complex situations since the above assumptions do not always hold. In this technique, the relationship between dynamic images and camera motion was presented and its application to visual servoing was shown.

2.5.4.5 Marker aided visual servoing:

In an attempt to simplify detection and tracking using visual servoing, artificial points (markers) which are easy to detect and localize are common in usage. This approach applies to both IBVS and PBVS. Various libraries to track the markers are already in use. AR marker which provided 2D image features of four corner points was mounted on a robot, the markers were used in the computation of the visual Jacobian of a 6D Image-based Visual servoing using a stereo camera [102]. Markers were used to estimate the complete pose of the five degrees of freedom manipulator and to provide angular information of the robot's joints and the position coordinates of the system in real-time [103]. The fiducial markers (index or point marks used for referencing) were stuck on the links of the manipulator so that through visual extraction by an eye-to-hand camera complete spatial configuration and the control laws for the manipulator can be computed. The ARTooKit module was used to read the markers and estimate the angles of the robot and provide inputs for the computation

of the Jacobian matrix. 3D markers were used as a passive target to robustify a real-time pose detection scheme for a visually servoed underwater vehicle [104]. The markers which consist of geometric and symbolic features provided by the ARTag toolkit made it easy to perform visual servoing as they allow the robot to communicate visually thereby controlling its behavior easily [105]. Mainly the use of markers is a bridge to pose estimation problems and an easy fail-proof strategy to visual servoing since some markers are embedded with error-correcting mechanisms to improve robustness. Marker-less visual servoing solutions are guaranteed as long as the pose estimation challenge is solved and precise knowledge of both the end effector and the target object is known. This was demonstrated in [106] where an IBVS control was used to maneuver the robot's end-effector to the desired pose. The least-square minimization was formulated to find the volume of the target object using stereo vision, 6D pose estimation of the end effector without markers was done by a recursive Bayesian filtering technique and nonlinear constrained optimization was formulated to compute the desired graspable pose, all this was done to fulfill the pose estimation challenge.

2.5.4.6 Structured light assisted visual servoing

The success of a visual servoing task is dependent on the extraction of visual measurements and all the visual servoing approaches assume that extraction of visual features is possible but it is not so for non-textured objects and in cases where feature extraction is nearly impossible and time-consuming [107]. The dynamics of a visual servoing task must be in real-time hence time should not be wasted on feature extraction otherwise the effectiveness of the servoing task will be compromised. Structured light is a result of controlled illumination and it falls under active stereo vision which is aimed at simplifying computer vision tasks. Casting structured light on non-textured and complex objects is a viable proven solution to the aforementioned challenge. The advantage of using structured light is that there are a lot of patterns that can be produced and some of the patterns are robust to the object's appearance. This approach was first experimentally validated in [108] on an IBVS technique and it showed good results for positioning a robot to a planar object though it was limited to static objects as it showed some problems on moving objects. T. Heitzmann et al [109] addressed the use of visual servoing in an unknown environment with un-textured objects using structured light on a Position-Based Visual Servoing scheme. As opposed to

the work in [107], [108] the target object's surfaces were assumed to be piecewise and were free to move and were subjected to some deformations. The focus was for the method to be able to navigate inside the human body with an articulated endoscope and it was designed to be robust to partial occlusion. The decoupled nature, performance characteristics, and stability properties of structured light-assisted visual servoing were analyzed in [110] and better visual features that improve the properties and global asymptotic stability were presented. However, the visual features from the projected patterns are not inherent features of the object at any given moment and their usefulness can be questionable. The use of structured light and structured environments in visual servoing is a way of controlling the environment to make it conducive for the application of the technology but it can be one of the drawbacks of its utilization as this increases the cost and removes the flexibility that visual servoing seeks to bring.

2.5.4.7 Particle filter-based vision-based control[111]

Many techniques are evolving and are being employed to solve the problems encountered in visual servoing. The particle filter method sought to solve the convergence issues faced in servoing techniques as it treats the servoing task as an optimization task. With this approach, the task function is solved statistically rather than analytically as done in common approaches. The method is based on the statistical estimation of the 2D or 3D relative pose parameters of the robot or camera between the current pose and target pose depending on the observations or measurements. The approach can be applied independently of the type of visual features selected either global or local features. The particle filtering-based method is capable of averting the local minima and divergence issues robustly. Depending on the chosen parameters (especially the number of particles) the method can be restricted in terms of real-time performance due to huge computational effort. Experimental validation of this approach on a 6 DOF manipulator showed how this method solved the camera retreat problem and how it can curve out suitable trajectories notwithstanding limited precision and noisy trajectory near the desired targets when using point features [111]. According to the author's statistical analysis, the Particle filter-based visual servoing performed excellently compared to direct visual servoing in terms of the convergence area. Increased perfected performance is expected with more particles which entail increased computational power. Particle filtering was used in a PBVS scheme for grasping purposes [112], to solve some of the problems faced in an industrial environment. The particle filter was incorporated to cater

to different noises found in uncontrolled unstructured industrial settings. This approach enabled the system to reach a 99-100% success rate in overcoming different kinds of noises introduced to the system.

2.5.5 Machine learning techniques for visual servoing

The complexity that comes with the visual servoing schemes, the relationship between the image features and the required robot/camera motion, and the computation of certain visual servoing parameters have inspired researchers to investigate the application of various machine learning techniques on vision-based control. Machine learning techniques automates interpretation and prediction processes from the given datasets. Various machine learning techniques are being applied in the field of computer vision and robotics and object detection. Localization and robot position or end effector positioning for the desired object can be learned. Various works in literature embody the application of machine learning techniques in visual servoing applications. A model-free self-learning robot controller which performs positioning tasks without prior knowledge of the camera/robot system geometry based on artificial neural networks was presented by Yan-Xi Yang et al [113]. In their, work ANNs were used to directly translate input from the monocular eye-in-hand vision sensor to joint velocities of a 3DOF robot arm. Simulation results expressed fast stable robust results with adaptability. An adaptive artificial neural network was constructed to cater to the output nonlinearities and unmodeled dynamics associated with a vision-based control of robotic systems [114]. A recurrent artificial neural network was used for the kinematic control of a robotic manipulator with a camera in hand system[115] for static point targets. With the neural network, visual cues were used directly to control the robotic manipulator with increased flexibility. This method handled the joint limits easily guaranteeing the safety of the manipulator. Simulation results and theoretical analysis validated the performance of the proposed technique. An artificial neural network (PDP network) which was able to learn the mapping of coordinates of the four visual features (input patterns) to joint angle changes of a manipulator (output patterns) was presented [116]. The neural network was trained to learn the link between the visual information and the needed robot joint angles required for the positioning and orientation of the end-effector to the target object. The advantage of this technique is that the visual data is integrated directly into the control system without splitting the process into object detection, localization, and robot control. Computer simulations on a 6DOF robotic manipulator

established the effectiveness and validity of this approach. Deep learning techniques (Convolutional Neural Networks) are in a recent application to perform visual servoing under occlusions, varying lighting conditions, unstructured environments, varying view angles, identifying and executing robotic grasping, and performing camera-end-effector coordination [117]-[121].

Various libraries, tools, datasets, machine learning frameworks that can train and construct learning systems have been developed to fuel research and application of machine learning techniques. The main drawback in terms of the application of these techniques is long training times, large datasets for training and validation purposes, and the computational resources needed.

Generally, from comparison, IBVS is better in terms of camera calibration, hand-eye calibration, robot modeling, scene, and target modeling, and also with issues regarding the processing time required to compute the sensor signal [87] and it seems to be the most versatile method since it requires less information to compute the control law and most of its drawbacks and limitations are solved by the partitioned and hybrid approaches. As revealed with the developments, research, improvements; more effort and work are being done on the IBVS scheme than the PBVS scheme. A comparison of IBVS and PBVS servoing techniques running under the same conditions was done and the main advantages and disadvantages were pointed in [87]. Another comparison measuring the influence of image noise in the performance of the several visual servoing techniques (IBVS, PBVS, Hybrid, Shortest path visual servoing, Corke & Hutchinson) and the comparison of generic motions around the optical axis, translation along the optical axis, rotation around an axis coplanar with target plane was done in [79]. In the comparison of 2D, 2 ½ D, and 3D Visual Servoing in [80], it was noted that IBVS and PBVS had nearly the same response speed and Hybrid Visual Servoing had a little faster response probably due to the faster estimation algorithm.

2.6 Image features for visual servoing

The selection of image features has an impact on the performance of the visual servoing closed-loop system and its ability to analyze the system's dynamics [90]. An image feature is any structural feature that can be extracted from an image corresponding to a projection of a physical feature of the object onto the camera's image plane. These are usually

characterized by a set of parameters that can be calculated from the image such as coordinates of points, the distance between two points, the orientation of line connecting points, area of projected surfaces, parameters of lines in the image plane[75]. The image features are usually classified as global or local features/region-based features. Global features are usually exploited in the context of visual servoing to avoid complex image processing steps such as feature extraction, matching, and tracking. The use of geometric features such as shape descriptors is generally ranked as region-based or contour-based descriptors. Contour based descriptors only capture the contour information while region based descriptors captures the interior content of the shape thus capturing more information [122].

The choice of features used should not suffer control coupling and non-linearity between the image space and the 3D space[123] as this can cause unpredictable behavior in the task space like divergence or convergence to local minima in some situations. In most cases for IBVS image point coordinates are considered but other geometric primitives which can solve the decoupling and linearization issues can be used [73]. The image features for pose estimation using camera-in-hand configuration usually escapes the Field of View (FOV). This is due to the narrow view provided by that configuration and the fact that the control law does not incorporate any constraints when it comes to image plane feature coordinates [77], this is why the choice of features and ways to keep the features in the field of view is important.

According to Burlacu. A et al [124], image features for the design of vision-based control law are generally categorized as point features (centroids or corners), lines/ellipse features, and generic descriptors (image moments which are statistical descriptors of the object in the image plane). The usage of general coordinates of points, straight lines, ellipses, or parameters describing the configuration of image segments as input to the visual servoing control scheme is usually limited because the kinds of objects defined by these will require feature matching between initial and desired images as a prerequisite[122], [125].

2.6.1 Image moments as visual features

From a binary or segmented image or a set of extracted points, it is easy to compute image moments which are generic visual features. These features can characterize any shape complexity irrespective of the geometric entity. Usage of generic visual features (image

moments) in frame sequences guarantees stability and robust computational process compared to the usage of point features since the high-level global matching of the object is required and not a precise match of each object point [124]. The use of point features or lines in image-based visual servoing applications presents problems due to the extensive coupled nature of the interaction matrix but the inclusion of image moments in the feedback loop can help to decouple the interaction matrix. The image moments have been employed in visual servoing schemes due to their ability to represent object regions and to represent objects defined by contours or a set of discrete points [90]. Image moments have provided the platform of choosing a minimal number of features to control the whole degrees of freedom while achieving control decoupling properties.

In [90] low order "shifted moments invariants" were proposed as new visual features for visual servoing as they allowed the definition of a unique combination of visual features to control a robotic system independently from the object shape while significantly enlarging the convergence domain of the closed-loop system. Low order classical moments include using coordinates, area properties, the center of gravity, etc. And these usually minimize the impact of measurement noise on the control performance and enable visual servoing task on complex object shapes and tasks which are independent of object symmetry.

The use of image moments in IBVS requires the analytical form of the interaction matrix for it [125]. Due to their invariant properties image moments can be utilized for pose estimation and task sequencing. In using image moments determination of features that will not lead to local minima or coupling which leads to unplanned robot trajectory is an important aspect as witnessed in [122][90]. Both simulation and experimental work presented correct, desired, and stable behavior of the visual servoing system either using simple symmetrical objects or planar objects with complex and unknown shapes [90], [122], [125]. Image moments have solved the problem of the determination of the set of features to use in the IBVS control scheme as they offer optimal behavior of the system. An advantageous property of the image moments is that a combination of moments that are invariant to some transformations such as scale, 2D rotation, and 2D translation is possible [126]. In [127], perspective image moments were computed from coplanar landmarks on the level ground to dynamically control an Unmanned Aerial Vehicle (UAV) with a fixed downward camera to control its vertical motion and rotation around the roll axis for positioning and orientation purposes.

2.6.3 Part-aware key points as visual features

Part-aware key points were used as visual features to extract only the important needed information for instance PBVS control from the global perspective of the image. This was done to avoid the usage of low-level geometric features which are insufficient in generalizing matching of scenes or objects [85]. The convolutional neural network (ConvNet) using the hourglass architecture was used to learn the part-aware key points on annotated images of cars. The resulting predicted features were used for reconstruction and pose estimation to perform excellent position-based visual servoing. The part-aware key-points computed by the deep neural network match descriptors of the instances/scenes accurately and were robust to illumination and textural variations.

2.6.4 Eigenspaces of the image dataset as visual features

In a bid to avert the problems that come with local features and the image processing tasks K Deguchi and T. Noguchi [89] performed image-based visual servoing tasks without image feature extraction and correspondence. They presented a general scheme that related dynamic image and camera motion and its application to visual servoing. Principal Component Analysis (PCA) algorithm and eigenspaces were used to reduce image dimension and a dynamic estimation of the interaction matrix from these eigenspaces was done to achieve a simple and effective robot control without complex image processing procedures. The method experimentally showed better performance though the pose errors did not decrease effectively to the desired tolerance level. An upgrade method using the reduced image form (eigenspaces) with the reconstruction of the eigenspace was done in [101] to enable a more effective robot control. Improved usage of eigenspaces was shown by rearranging each eigenspace by relating it to its image position where it was obtained around the goal. This improved method was experimentally proven to be useful for the control of vision-guided robots.

2.6.5 Luminance as image feature for visual servoing

A method that is not dependent on geometric features or homography but luminance of all pixels in the image was proposed in [100], [128]. Usage of luminance as visual features is superior to other features in that no feature tracking or feature matching is needed. Using luminance of pixels for 2D visual servoing is depended on the analytical computation of the

interaction matrix that relates the time variation of the luminance to the camera motion. This visual servoing method was converted into an optimization/minimization problem to coin a new control law known as photometric visual servoing which can handle convergence issues easily. Lambertian model or Phong model were incorporated into the control law to make it robust to complex illumination changes. The approach was experimentally validated for positioning and tracking tasks and it proved that only image intensity / pure luminance signal can be used to control robot motion with less sensitivity to partial occlusions and coarse approximations of the interaction matrix [129].

A direct approach independent of feature matching which represents the entire set of pixel intensities of the object where it appears instead of local features was presented in [130]. This method made use of all the information provided by the image and measured the similarities between the patches of intensities to realize the visual servoing task. Using the similarity measure between patches robot/camera movements that maximize the mutual information between the current and desired were performed. This made it easier for the visual servoing problem to be reduced to an optimization problem.

2.6.6 Colour attributes as visual features

Colour attributes were used in the visual servoing control loop in [131] in an approach similar to [100], [128], [129] since color contributes to luminance though the color is more discriminant. Colour enhanced the use of luminance in visual servoing tasks and it avoided complex problems associated with feature extraction and matching. In using color attributes, it is vital to select optimal features for the scene being observed since some color parameters influence the convergence of the control law and the trajectory of the camera/end-effector. Experimental validation of the approach was done and proved that the approach is insensitive to partial occlusions and coarse approximations of the depth information required to compute the interaction matrix.

In [132] usage of primary color space to perform visual servoing tasks was witnessed. MATLAB was the primary controller used for Image processing to perform object detection and localization based on primary color space. Pixel count calculated using the Euclidean distance was used to determine locations of the colored object from the robot, this pixel count is computed to regulate the motor movement of a three-wheeled robotic platform in the (x-axis) and (y-axis) to reach the target. Colour in HSV space, edges, and corner features were used to develop an object detection algorithm using MATLAB, to robustly extract the

correct target object and the color features were used in a Pose Based Visual Servoing (PBVS) scheme [133] to precisely detect objects and their positions and sizes to make possible the sorting and storage operation. RGB color intensity and an online color intensity threshold correction using the standard deviation of RGB color distribution were used for objection detection and pose estimation approach in PBVS [134]. The planes represented by 3 feature points were used to represent objects and scenes. The task was to align the object's current plane with the desired plane aiming at minimizing the accumulated error of transformation. With this approach, the requirement of prior knowledge about the objects and scene is minimized while effectively estimating object pose with different characteristics in different lighting conditions.

2.6.7 Image histograms as features

In an attempt to circumvent the bottlenecks that come with feature correspondence, tracking, use of geometric features, and rigorous image processing as was done with photometric features and image moments, a technique that utilizes histograms as visual features was presented [135][136]. A framework that accepts an estimate of the probability distribution of image variables such as color, gradient orientation, intensity, etc. as visual features for vision-based control was presented [135]. The proposed framework works for a wide range of histograms and permitted the formulation of efficient and robust control laws as witnessed in [135], [136]. An intensity histogram was used as a visual feature and robot control was achieved by minimizing the distance between two computed histograms [135]. The intensity histograms were plagued with global illumination variations when the method was implemented on 6 degrees of freedom robot. [136] Used histogram of gradient vectors to formulate a global feature that is robust against occlusion and photometric transformations. Minimization of the Bhattacharya distance of the gradient vectors was the basis of the control. The technique included a novel formulation of the interaction matrix for this kind of visual features leading to efficient control law and greater positional accuracy. Some of the work of Bateux Quentin in [111] analysed various kinds of histograms as visual features under different conditions and reached a conclusion that histograms are able to compare images and their performance is visual servoing task can surpass that of classical direct visual servoing with the benefit of multiple options to choose from.

2.7 Image segmentation

To satisfy the requirements of objective 2 and the demands of visual servoing it is needful to explore some of the techniques used in image processing for object detection and localization. To automate the identification and localization of gold particles in the gold pan and automate the sorting and picking process using a robot manipulator and visual data, image segmentation is a vital process. Image segmentation is the process of identifying and extracting homogeneous regions from the image domain satisfying a homogeneity criterion based on features formulated from spectral components of the image. Extracting and understanding information from vision data which can be used for various tasks such as object detection, image classification, detect detection, object recognition, etc. is a vital aspect of artificial intelligence. Segmentation entails dividing an image into regions of homogeneity and this division depends on the challenge at hand. Also, segmentation can be viewed as a pixel/region labeling process since homogenous regions/pixels are assigned the same label [89][137]. Mathematically the complete segmentation procedure partitions an image R into a finite number S of regions $R_1, \ldots, R_S$.

$$R = \bigcup_{i=1}^{S} R_i \text{ and } R_i \cap R_j = \emptyset \quad \text{where } i \neq j \ \#(1) \tag{4}$$

Segmentation is a psychophysical process and there are a lot of techniques/algorithms developed to carry out segmentation because there is no one solution that caters to all segmentation problems [138]. Segmentation helps to simplify an image or part of the image into something easy to understand, easy to analyze, and easy to work with. The two main segmentation domains which many segmentation techniques fall into are unsupervised segmentation (fully automatic) and supervised segmentation (manual /semi-automated). Techniques under the unsupervised segmentation class are geared towards developing algorithms/frameworks that are fully automated in partitioning the chosen image into several homogeneous regions based on a given criterion. The techniques in the supervised segmentation class depend on the user interaction to initiate or select regions to be partitioned. Image segmentation is based on various features in the image such as color features, pixel information, geometric features, edges, etc. The various segmentation techniques can be done on both color images or monochromatic images (Grayscale images). Colour image segmentation is viewed as an extension of monochromatic image segmentation though some of the monochromatic image segmentation methods do not apply

directly to color images [139]. All the segmentation techniques seek to partition the image based on similarity (region-based methods) or discontinuity (boundary/edge-based methods) or a hybrid of similarity and discontinuity. Edge/boundary-based methods locate discontinuities, abrupt changes in intensity values, or sharp contrasts in the image data whereas region-based methods are based on continuity and classifies adjacent pixels based on similarity or common patterns in intensity values[140], and partition the entire image into sub regions based . Fig 2.3 below shows some of the segmentation techniques and their classification. Region-based image segmentation methods such as thresholding, region growing, clustering, split and merge, and normalized cuts techniques are going to be discussed briefly due to their popularity in literature and bearing in this research work [141][142].

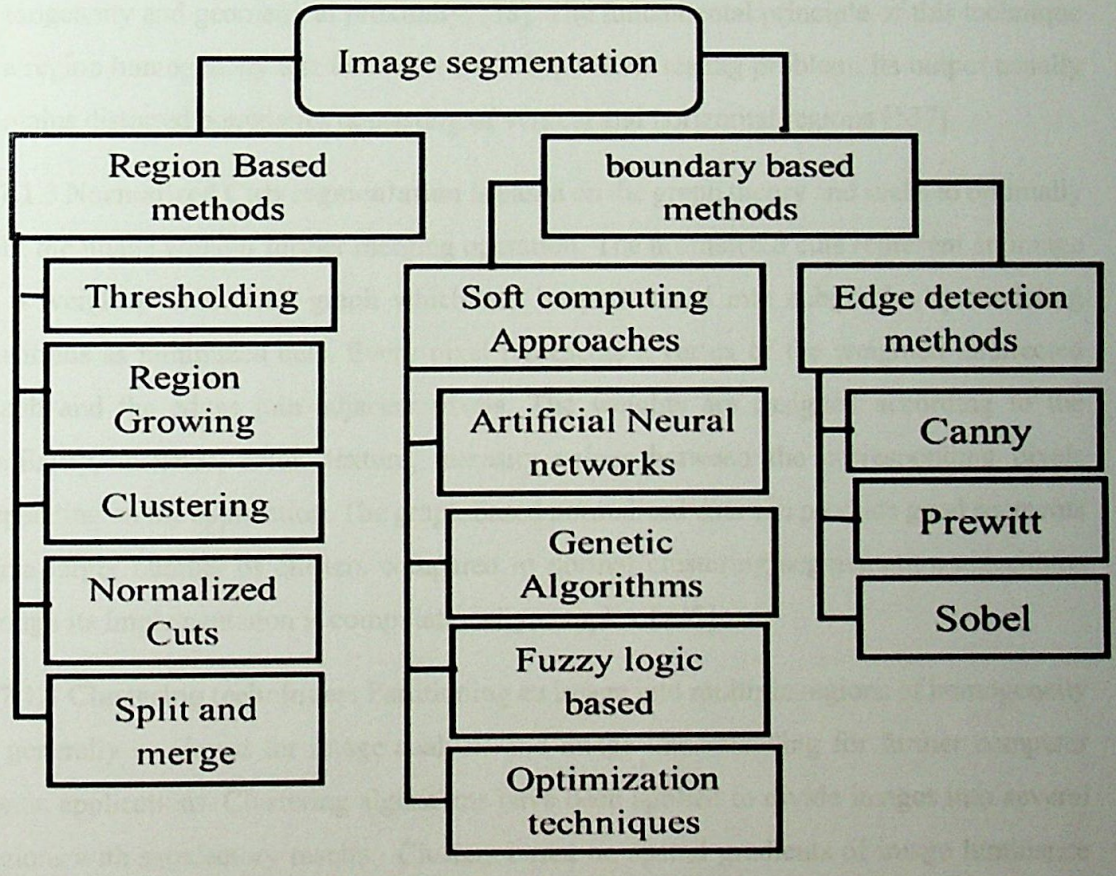


Figure 2. 3: Segmentation techniques and their classification according to [121][123]

2.7.1 Region-based image segmentation methods

2.7.1.1Thresholding segmentation techniques: This technique partition images by defining a range of pixel values in an image and assigning those pixel values as either object

or background (bi-level thresholding) [143]. Image regions are classified based on the chosen threshold value. Image segmentation by thresholding is simple and straightforward, allows rapid segmentation, smaller storage space with less computational efforts [144]. Techniques under thresholding segmentation can be bi-level or multi-level depending on the number of image segments wanted. Bi-level thresholding outputs the image with two parts which are background and foreground or target object and non-target object.

2.7.1.2 Split and merge segmentation techniques: The split technique divides the heterogeneous image into segments of homogeneous regions based on a global criterion. The split process is terminated when all segments are homogeneous. The merging technique iteratively merges similar neighboring regions based on the local criteria and the given fusion decision rule. The split and merge techniques partition images based on notions of homogeneity and geometrical proximity[138]. The fundamental principle of this technique is a region homogeneity test formulated as a hypothesis testing problem. Its output usually contains distorted boundaries consisting of vertical and horizontal regions [137]

2.7.1.3 Normalized Cuts segmentation is based on the graph theory and seeks to optimally split the image without further merging operation. The normalized cuts represent an image as a weighted undirected graph which can be partitioned into subgraphs by modeling partitions as minimized cuts. Every pixel represents a vertex of the weighted undirected graph and the edges join adjacent pixels. The weights are assigned according to the similarity, distance, color, texture, intensity values between the corresponding pixels depending on the application. The graph-based normalized cuts can produce good segments for a larger number of clusters compared to normal clustering segmentation algorithms though its implementation is computationally complex [145].

2.7.1.4 Clustering techniques: Partitioning an image into multiple regions of homogeneity is generally employed for image analysis and image understanding for further computer vision applications. Clustering algorithms have been applied to divide images into several regions with satisfactory results. Clusters based on spatial gradients of image luminance are produced using the watershed algorithm [137][146][147] and the clusters based on pixel distribution or chromatic information are produced by various clustering approaches such as K-means clustering, Fuzzy C clustering, mountain clustering, subtractive clustering, K-hyperline clustering, fuzzy local information C-means, etc[148] [149], [150]. Clustering-based segmentation algorithms can partition relatively close intensity/pixel values into one

segment even if they are not geometrically close [145]. A lot of clustering algorithms are not robust to illumination variations to an extent that identical pixels of the same color with different illumination can be clustered into different clusters. The other drawbacks with clustering techniques are usually over-segmentation or under-segmentation which rises due to the fact of not knowing the number of clusters or watersheds needed [146]. A lot of clustering methods are constantly being proposed, improved and some are being combined with other techniques to overcome the drawbacks experienced with pure clustering segmentation methods [151][149]

2.7.1.5 Region growing segmentation techniques: This is an iterative segmentation technique that is initiated by selecting a small desired region/pixel/(s) (seed) in an image that grows iteratively by assigning other non-selected pixels/regions that meet the required homogeneity criterion[152]. The seed can be manually or automatically selected. The growing/assigning process continues until no more pixels satisfy the given homogeneity criteria [139]. This technique is dependent on a careful determination of the seed pixel, the selected homogeneity criterion/ formula, and decision rules to terminate the growing process. Region growing segmentation methods can produce multiple regions with less noise but can be time-consuming. Poor selection of seed points and choice of homogeneity criterion often leads to sub-segmentation or over-segmentation [153]

2.8 Applications of visual servoing

Visual servoing is a relevant technology for nearly all robotic systems that use vision information to perform positioning, tracking, and manipulation tasks. This control technique can be used for a wide variety of applications and on different robotic platforms including industrial manipulators, mobile robots, medical robots, and humanoid robots [154]. The most general of applications is in the manipulation of objects which entails alignment, grasping, tracking, pick and place. A vast of vision-based control applications are done in laboratories, research stations, structured environments, and simulated scenarios mainly to check for feasibility but with Opto-mechatronics technological advancements, a lot has improved in terms of the technology and its utilization. Visual servoing is generally applied in vision-based automated systems or in vision-based service robots which can be found in almost every field be it agriculture, medical, manufacturing and processing industry, entertainment, security, and surveillance, etc.

2.8.1 Vision-based automation – these ensure certain accuracy and repeatability for a certain position or object. Visual servoing has allowed the execution of these tasks under variability of positions because of its robust object localization capabilities[23] compared to the traditional fixation systems. In vision-based automation visual servoing is used for such applications as lane tracking in autonomous driving and navigation systems, vision-based welding of thin plates, and manipulation of objects in an assembly line or manufacturing platforms.

2.8.2 Vision-based service robots– these assist humans in a wide range of tasks that are considered dull, dirty, and dangerous. These encapsulate navigation and motion control of dynamic systems such as mobile robots, robotic arms, cameras, and virtual systems (virtual cameras or virtual robots).

2.8.3 Visual servoing applications in the medical field

Usage of imaging techniques and visual feedback is utilized in the medical field both for the automation of medical procedures or by medical robots to either assist the medical personnel to increase the accuracy and ease of medical procedures. Due to the sensitiveness of the medical field sometimes the human operator is part of the feedback control loop [155] and this has made supervised automation of medical robotics receive much attention and its utilization be on the rise. There are a lot of imaging procedures in the medical field but visual servoing is defined if and only if the visual features are used in closed-loop control, for the operation of a robotic system in real-time. Medical robots demand fast real-time imaging to avert aliasing in image-based tracking. Various imaging techniques are used for visual servoing in the medical field and these include ultrasound imaging, x-ray fluoroscopy, magnetic resonance imaging, computed tomography, endoscopic imaging, and direct vision. Visual servoing has been used in laparoscopy to position the laparoscopic camera to continuously keep the tools or the section of the tissue/part in the field of view or to maneuver the movement of the laparoscopic tools. This was witnessed in [156] [157]where a reliable and practical image analysis and tracking were used to automate instrument localization and scope maneuvering in a robotically assisted laparoscopic surgery. Viky robotic scope holder was developed in [158] to assist the surgeon by holding the endoscope. The lightweight robot could automatically move the endoscope to the tip of the instrument using visual servoing. Visual servoing has been used to automate the alignment of needles with the insertion points or control the motion of the laparoscopic tools in a suturing

procedure [159]. Laser pointers were used to specify the stitching points and curved needles were aligned automatically using visual servoing and a hybrid visual servoing method was used for the stitching process. Stereo microscopes have enabled the visual servoing of micro-robots which are used by surgeons to perform micro-surgeries and delicate procedures with increased accuracy [160]–[162]. A thorough review of utilization, challenges, trends, and future works of visual servoing in medical robots was presented in [155]

2.8.4 Visual servoing applications in industry

Visual servoing has brought flexibility to path planning and motion planning of industrial robots and has found various applications in these manipulators. A Hybrid visual servoing scheme was used in robotic arc welding [163]. PBVS control was used to move the end-effector along the weld seam and the IBVS control was used for adjusting the seam tracking maneuver. A camera in hand configuration with a laser emitter was utilized to have a good real-time stable performance which was insensitive to illumination variation. For increased production and manufacturing rates industrial robotic pick and place (sorting and packaging) using visual servoing is popular because of its flexibility and increased profitability. Object pick and place visual servoing based manipulation system which achieved accurate real-time results was designed and tested [164]. An image-based visual servoing control scheme was employed and a structured edge detector was used for contour extraction and object detection. Visual servoing was used for slaughterhouse automation to provide a generic pick and place and object manipulation solution[165]

2.8.5 Visual servoing application in Aerial vehicles

Visual servoing has been used in the control of the highly complex and demanding flying, navigation, and landing operations of aerial vehicles. Both demonstrated and actual applications of aerial vehicle visual servoing for target tracking, odometry, obstacle avoidance, SLAM (Simultaneous Localisation and Mapping) when flying or landing in unknown conditions are well document in the literature. Simulation results with good performance of vision-based control of a helicopter ship landing on a moving ship deck were presented in [166]. Good stability and performance of the landing and descent approach maneuver on the moving helipad were guaranteed by an image-based visual servoing and Points of Interests (POIs) features were employed. A depth-independent

interaction matrix IBVS enabled linear parameterization in mapping image errors onto actuator space of a small-scale autonomous helicopter was presented [167]. An adaptive algorithm was developed to estimate the unknown parameters and coordinates based on the online minimization of the error function using the results of the linear parameterization.

Demonstrated application of visual servoing to collision avoidance for an aircraft was presented in [168]. IBVS control provided feedback control from the image space without range estimation to perform avoidance of point targets in the lateral or vertical plane. Simulation results validated the visual servoing controller's ability to avoid static and constant velocity targets. The actual design and implementation of vision-based control of an autonomous helicopter in urban areas were presented [168]. Position and velocity estimation of the features in the image plane using visual sensing was done to generate the velocity reference for the flight control.

2.9 Conclusion

A brief review of the gold extraction methods covering the various pre-concentration and concentration techniques and the analysis and critique of these techniques was presented. A generic overview of vision-based control in terms of tools, techniques, approaches, and applications was given. Image segmentation techniques and Image features for visual servoing were discussed as they form the basis of stable and robust traditional visual servoing performance. Various comparisons between the techniques, configurations, and tools were discussed. Recent contributions and techniques were reviewed and discussed as they sought to cover some of the gaps and problems suffered by the traditional methods. Finally demonstrated applications and implemented applications of the technology in various fields were reviewed as a way of showing how the technology is being utilized and has revolutionized various fields.

Chapter 3

Methodology

3.0 Overview

This chapter outlines the methodology used in the design of an automatic vision-based gold panning machine which focuses on technical optimization of the ore washing process and hand-picking process. The methodology set up will ensure that the main aim of this research project is realized. The approach used will ensure that all the objectives of this research project are fully met. The steps to meet each objective will be outlined individually. The work done using the selected methodology is outlined in this chapter

3.1 The V model for mechatronics system design methodology (VDI 2206 Guidelines)

The multidisciplinary nature of visually servoed systems and the complexity of mechatronic systems require a flexible systematic cross-domain methodology for the design and development of such systems. The multidisciplinary design approach VDI 2206 guidelines (V model for mechatronic systems) [169]was customized to formulate a process model for the design of the automated vision-based gold panning system. This approach handles the complexity that comes with the cross-linkage of different engineering disciplines with ease and supports the cross-domain design of a mechatronic system in a systematic way [169].

This methodology was chosen since its outcome is a reliable concept of a mechatronic system that is principally defined. The design approach allows both verification and validation to go in parallel, as test plans and test cases are created to verify and validate the product according to the requirements at every stage. This process model allows for; designing before building, inclusion of modeling, simulation and model analysis in the design process, and allows rapid prototyping. The nature of this methodology which split up the main functions of the future product into smaller sub-functions leaves no room for functions being neglected. Different active principles will be utilized by the sub-functions and the optimal solution will be an integration of the gathered solutions. The design methodology consists of a tripartite procedure based on three main elements:

a) The general problem-solving cycle on the micro-level
b) The V-model on the macro-level

c) Predefined process modules for repeated operation steps during the design of mechatronic systems.

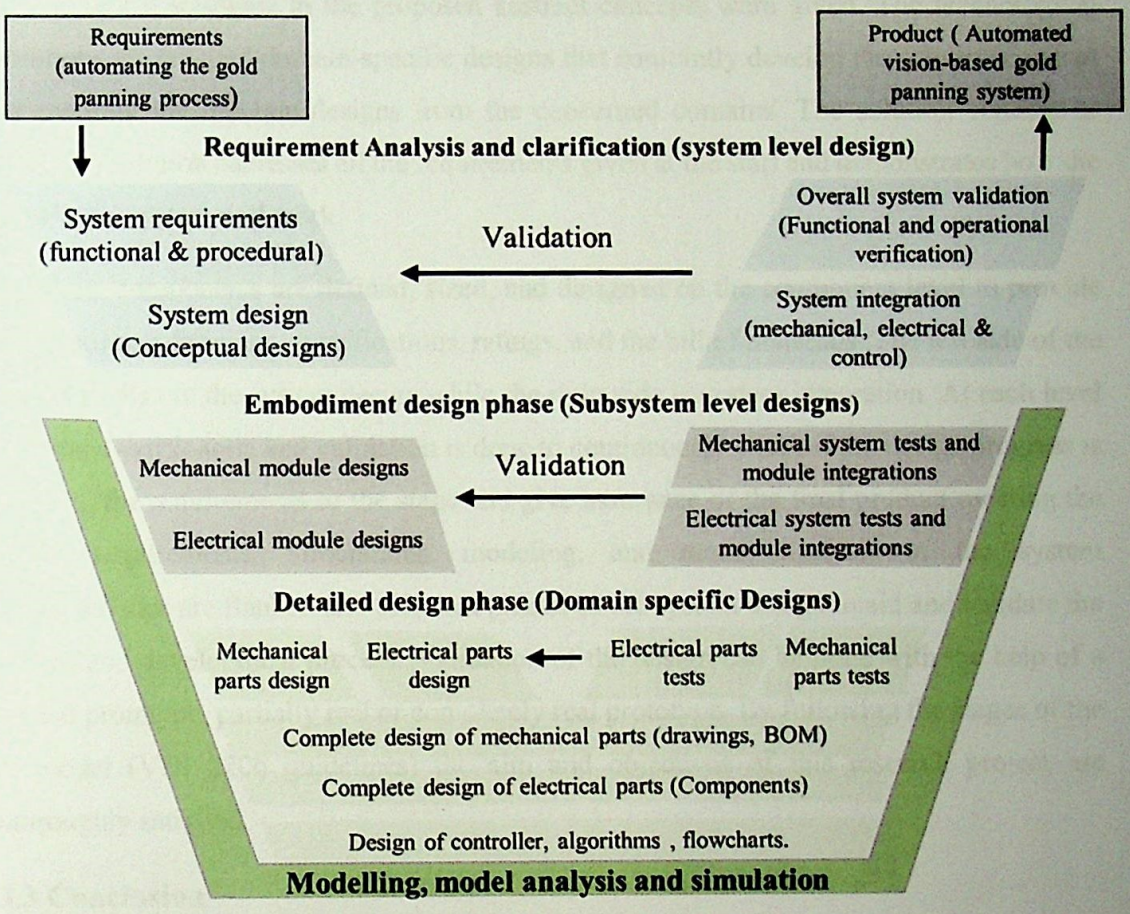


Figure 3. 1 :Customized process model for the design of an automated vision-based gold panning system [153]

3.2 Work done using the V-model for mechatronics system design methodology

Fig 3.1 above shows the customized process model for the design of an automated vision-based gold panning system [169][170]. The process model was initiated by formulating a requirement list for the intended system. Through guided observations, process reviews, and document reviews, data was gathered to formulate a requirement list. Both the technical and procedural requirements for the automated system to be developed were noted and this data was used for problem characterization and solution formulation.

The requirements (what needs to be done/ problems to be solved) were defined and clarified on the functional level and these were transformed to system requirements that aim at establishing a cross-domain solution and also provide a system test plan for verification and validation of the product later. A requirement list was used to abstract the product function. After the functional and procedural requirements were well defined and clarified at the

system level, abstract and technical concepts that were capable of solving the requirements were proposed. From the conceptual design phase, the embodiment step which provides technological solutions to the proposed abstract concepts were given. The technological solutions are detailed domain-specific designs that conjointly develop the solution concept by merging the separate designs from the concerned domains. The solution concept or principal solution addresses all the requirements given at the start and demonstrates how the developed system will work.

Different components are defined, sized, and designed on the component level to provide the necessary drawings, specifications, ratings, and the bill of materials. The left side of the model spells out the system design while the right side is system integration. At each level and stage verification and validation is done to continuously check if the design progress is meeting the requirements of the stage and give assurance of the final product meeting the initial requirements. Simulations, modeling, and model analysis of the system characteristics are flanked into different phases of the system design to aid and validate the design and development process. Validation of the design can be done with the help of a virtual prototype, partially real or completely real prototype. By following the stages of the V model (VDI 2206 guidelines) the aim and objectives of this research project are thoroughly satisfied.

3.3 Conclusion

A fitting methodology for the system being designed was presented and justifications for the selection of the chosen methodology were provided in this chapter. Customization and adaptation of the methodology to the particular design and how it was applied to the problem at hand were outlined together with the work done through the selected methodology.

CHAPTER 4

CONCEPTUALIZATION, DESIGN, AND MODELING

4.0 Overview

This chapter presents the conceptualization and the design of an automatic vision-based gold panning machine. The chapter expounds and expatiates the points mentioned in chapter 3 under system design and seeks to perform the actual work those points entail. Both procedural and functional requirements of the system will be generated in this chapter and conceptualization of the solutions that meet the requirements will be laid out in this chapter. The outcome of the conceptualization is a concept design that is principally defined together with the domain-specific designs that form the final product. The computer-aided drawings of the system being designed are presented in this chapter. The design of the gold detection and localization framework under the software domain was also performed in this chapter. Modeling setup for the mechanical subsystems designed was also presented in this chapter.

4.1 Generating requirement list

As presented in the methodology, the chosen process model is initiated by a clear understanding and definition of the system requirements. Under this section, relevant information for the design of an automated vision-based gold panning machine and its related specifications were obtained. Guided observations and surveys were carried out to gather necessary parameters needed in the gold panning process such as the panning duration, process sequence, indicators of a successful washing procedure, etc. During these observations, the current panning process was analyzed to gather all the necessary information needed in the design process. Documents review from the ore milling companies was done to gather the time needed for the panning process. In formulating the requirement list, it was important to understand the panning process, the involved inputs, and outputs. The black box model below depicts the gold panning process.

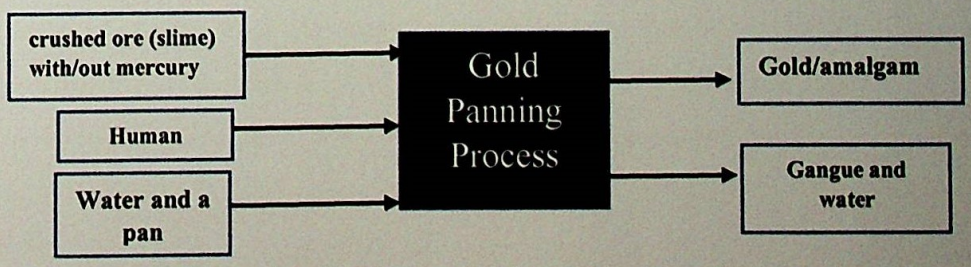


Figure 4. 1 : Blackbox model of the gold panning process

Through observations and inquiry, necessary information on the gold panning process from the customer's view was acquired to identify, understand and discover potential needs, interests, requirements, and systems functions.

4.1.1 The gold panning process

The gold panning process receives the crushed mineral ore in slime form and water to wash the ore to recover gold particles. The purpose of panning is the separation of gold from gangue. Mercury is sometimes used to amalgamate the gold to ease the separation process. The human operator systematically shakes the pan (dish) containing the crushed ore and water to expose the gold particles by taking advantage of the weight of gold particles compared to that of the ore (gravimetric separation). Through the systematic shaking more of the gangue is ejected out of the panning platform and the gold particles can be seen accumulating in different locations in the pan. The appearance of gold sets it apart from the rest of the gangue and through tilting the platform or handpicking the gold particles or gold-mercury amalgam can be separated from the gangue. This whole process is somewhat tedious.

Through the understanding of the process, the requirement list was formulated to have a clear design specification list. The requirement list provided functional specifications and procedural specifications in the gold panning process. The requirement list also serves as the measure against which the final output is assessed. The requirements were derived from the function of the human operator during the panning process since it is his operation that is being automated. The application of force (centripetal force) to the panning platform through systematic shaking and rotation of the pan, supply of the needed energy, control of the panning process, gold detection, and recognition, and picking operations are solely performed by the human. The panning process is usually accompanied by ergonomics and poor safety issues due to the repetitive and straining nature of the process. The table 4.1 below shows the functions of the human person which were concealed in the black box above.

Table 4. 1: Inputs, outputs, and processing in the gold panning process

Inputs	Gold panning process "Human input"	Outputs
Wet crushed ore "slime" with/out mercury	• Mixes the water and slime. • Systematically and intelligently shakes the pan/dish to create a force that promotes ejection of the lighter gangue particle from the pan. • tilt the dish to remove excess water to have a better view of the process. • Provide support to the pan /dish	Gold particles / gold-mercury amalgam
Water	• Scans the platform optically to look for the target objects (gold particles/ mercury/amalgam)	Gangue
Panning platform	• Recognition of the gold/ amalgam by appearance.	Water
	• Separating the gold/amalgam from the gangue(localization) through sorting and picking. Hand-eye coordination	
	• Processing (roasting and smelting)	

The above human functions in the gold panning were used for planning and clarification of tasks as they were transformed into system requirements. The human operations during the gold panning process were reviewed, analyzed, and transformed into verifiable system requirements. These requirements were analyzed, elicited, validated, and documented.

4.2 Design requirements

4.2.1 System requirements

Narrative requirements

- A system that will mimic the washing process of the crushed ore, automatically detect and localize gold/amalgam/mercury in the panning platform using vision sensors and separate the wanted materials from the mining waste using visual information without polluting the environment and harming the miner.

The narrative requirements were analyzed and formulated to become abstract, unambiguous, verifiable, and traceable so that they can fit well into the V model design process.

Characteristics:

- The system will have a mechanical structure acting as a chassis to provide support for the washing system and separating system.
- Vision sensors will be used to detect the contents of the panning platform
- Easy to operate (plug and play system)
- Efficiently mimic the current panning process and mitigate human involvement in the process.
- Heed to environmental and water pollution. (Avoid mercury emissions and mercury pollution)
- Ease of maintenance (usage of modules/subsystems to allow for ease of retrieval for maintenance schedules and repair)
- Minimum work envelope

4.2.2 Initial requirements setup

The human operations in the panning process formed the initial requirements of the system. Table 4.2 below summarizes the initial requirements for the automated system.

Table 4. 2: Initial requirements for the vision-based automated gold panning system

Abbr.	Requirements
R1	Controlled delivery of slime and water to the panning platform, mechanically perform the washing process (systematic shaking of the panning platform).
R2	Capture the image of the gold panning scene, extract the necessary features from the visual information, perform image processing to detect and localize the target objects.
R3	Extract coordinates of the target objects from the processed image.
R4	Communicate a signal that will servo the tool piece in the working area to the extracted x-y-z coordinates, to remove the target objects from the panning platform.
R5	Minimum energy consumption and minimum time in servoing and positioning of the tool piece from the home configuration to the target position and orientation.
R6	Modular designs for ease of maintenance and quick troubleshooting
R7	Ease of communication between the controller and image processor using serial communication or USB
R8	Minimum human involvement.

R9	Bottom-up building approach with chassis providing support to all the involved sub-systems
R10	Utilization of locally available or processed materials (Import only when necessary)
R11	Minimum work envelope based on the area of the panning platform. (preferably >> 600mm * 600 mm)
R12	Manually load or fix the end effector tool piece with hard-wired tool compensation.
R13	Minimum achievable image resolution from the vision sensor.
R14	Usage of artificial illumination to ease image processing efforts.
R15	Make use of prismatic joints.
R16	Minimize pollution /avoid mercury emission to the water bodies nor atmosphere

Knowledge-rich requirement checklists were used in the formulation of requirements to eliminate personal preferences and bias during this stage. The Pahl and Beitz requirement checklist [171] was used together with the initial requirements to formulate the design specifications of the system.

4.2.3 Part of Pahl and Beitz requirement checklist [171]

Table 4. 3: Part of Pahl and Beitz requirement checklist

Axioms	abbr	Examples
1. Geometry	C_1	Size, height, breadth, length, diameter, space requirements, number, arrangement, connections, extension
2. Kinematics	C_2	Type of motion, direction, velocity, acceleration
3. Forces	C_3	The direction of force, the magnitude of force, frequency weight, load, deformation, stiffness, elasticity, stability, resonance
4. Energy	C_4	Output, efficiency, loss, friction, ventilation state, pressure, temperature, heating, cooling, supply, storage, capacity, conversion
5. Material	C_5	Physical and chemical properties of the initial and final product, auxiliary materials, prescribed materials (food regulations etc.)
6. Signals	C_6	Inputs and outputs, form, display, control equipment
7. Safety	C_7	Direct safety principles, protective systems, operational, operator, and environment safety

8. Ergonomics	C_8	Man, machine relationship, type of operation, clearness of layout, lighting, aesthetics
9. Production	C_9	Factory limitations, maximum possible dimensions, preferred production methods, means of production, achievable quality, and tolerances.
10. Quality control	C_{10}	Possibilities of testing and measuring, application of special regulations and standards.
11. Assembly	C_{11}	Speed regulations, installations, siting, foundations
12. Transport	C_{12}	Limitations due to lifting gear, clearance, means of transport (height and weight), nature, and conditions of dispatch
13. Operation	C_{13}	Quietness, wear, special uses, marketing, and destinations (e.g. sulfurous atmosphere, tropical conditions.)
14. Maintenance	C_{14}	Servicing intervals (if any), inspections, exchange and repair, painting, cleaning, planned, preventive, reactive, hybrid
15. Recycling	C_{15}	Reuse, reprocessing, waste disposal, storage,
16. Costs	C_{16}	Maximum permissible manufacturing costs, cost of tooling, investment, and depreciation
17. Schedules	C_{17}	End date of development, project planning, and schedules, delivery date (<< 24 months)

An incidence matrix was used to check for correspondence and identify the interaction between the Pahl and Beitz requirement checklist and the initial requirements to make sure that all the requirements are well categorized and none is neglected in the design specification process [172].

4.2.4 Incidence matrix representing the interaction between the requirement checklist and the initial requirement.

Table 4. 4: Incident matrix

		R1	R2	R3	R4	R5	R6	R7	R8	R9	R10	R11	R12	R13	R14	R15	R16
Function	C_1	e_1	e_1	e_1	e_1				e_1			e_1					
kinematics	C_2	e_2															
Force	C_3	e_3															
Energy	C_4					e_4											
Material	C_5									e_5	e_5	e_5					
Signals	C_6				e_6			e_6						e_6			
Safety	C_7								e_7								e_7
Ergonomics	C_8																
Production	C_9																
Quality control	C_{10}													e_{10}	e_{10}		
Assembly	C_{11}						e_{11}			e_{11}							
Transport	C_{12}																
Operation	C_{13}								e_{13}				e_{13}				
Maintenance	C_{14}						e_{14}										
Recycling	C_{15}																
Cost	C_{16}														e_{16}	e_{16}	e_{16}
Schedules	C_{17}																

Where e_i is the entity concept that depicts the attribute of the initial requirement which corresponds to the main heading of the requirement checklist. The design specification list was derived from the selected entity concepts of the incidence matrix.

4.2.5 Design specification list for the automated gold panning system

Table 4. 5: Design specification table for the automated gold panning system

Date	Design specification sheet (Automated gold panning system)
	Functional Performance • Washing - Systematic shaking of the panning platform (circular motion) • Controlled introduction of the inputs to the panning platform. • Image capturing and image processing. • Gold/mercury/amalgam detection and localization • Image coordinates extraction and servoing of the tool-piece to remove the targets from the platform
	Constraints *Geometry* • *Length ≤ 750mm* • *Width ≤ 750mm* • *Height ≤ 1200mm* • *Panning platform diameter < 500mm* *Workpiece envelope (work stroke)* *500mm * 500mm*
	Kinematics • only x, y, and z-axis translations for positioning of the end-effector tool piece • the systematic circular motion of the washing/separation system – single-axis horizontal.
	Energy • efficient energy use (electrical energy, mains voltage) • artificial lighting
	Signals • 0-5V for control signals • 4-20 Ma • Serial communication and USB. • Industrial standards
	Assembly • Use of subsystems, modules, plug-and-play systems, top-down approach. • Simple sensor configuration without an obstructed field of view.
	Safety • No leakages of mercury to the water bodies and environment **Maintenance** • Simplify maintenance and troubleshooting.

The validation of the established requirements and the design specifications is an iterative process that is confirmed and verified by the generation of functional and physical models. Through modeling, model analysis, and simulations the performance of the generated models will be tested and the design specification can be endorsed or updated till the design specifications are well-formed and established.

4.3 CONCEPT GENERATION

Following the V-model guidelines, having established the requirements and specifications, concept generation follows. The automation of the gold panning system calls for a definition of a wide range and selection of parameters. To provide full coverage of all the requirements and specifications, a decision analysis tool is required to ease the process. And to do this morphological analysis was used to explore the possible solutions from a pool of available technologies and techniques. The morphological analysis will be used to assist in the exploration of design options amid uncertain and vast parameters. The morphological analysis procedure will be accomplished through the following steps:

a) Identification of the sub-systems from the basic functions of the automated system being designed.
b) Formation of all possible solution elements/working principles/variants lists
c) Evaluation and identification of possible combinations for the optimal solution concept

4.3.1 Functional Analysis system Technique for the automated system

The human operations during the gold panning process mentioned above were translated to functions of the system being developed. The expressed requirements were converted and decomposed to functions, sub-functions, technical and elementary functions using the Functional Analysis System Technique (FAST). The functional analysis of the system designed guarantees that all the needed functions were considered, as the automated gold panning system will be accomplished through a series of interacting sub-functions. Through the Functional Analysis System Technique (FAST) diagrams, the complex gold panning process was decomposed to gain clarity on how the automated panning process will come about from the interaction of separate functions/tasks. The functional analysis through functional decomposition aided in the production of the functional architecture, functional block diagram, product tree, and connection matrix which suits the desired functional requirements.

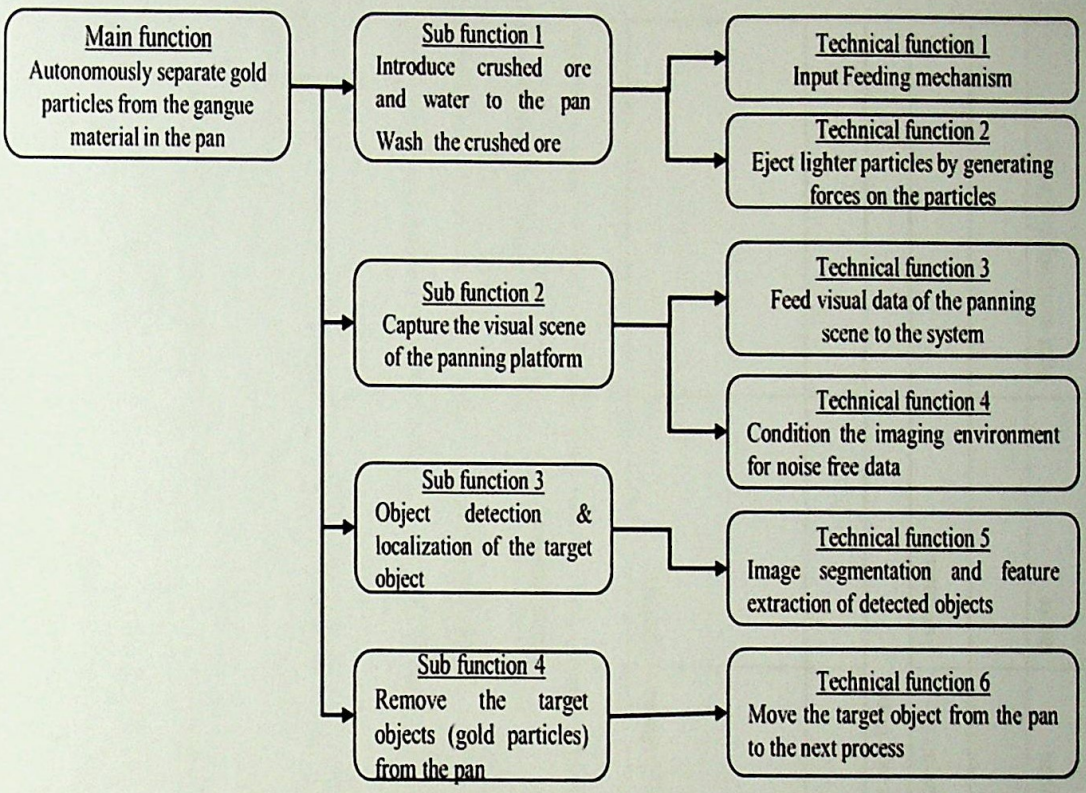


Figure 4. 2: Function Analysis System Technique (FAST) diagram of the automated gold panning system

4.3.2 Morphology Analysis

Having established the basic functions and the required subsystems to meet these functions, an extensive search for new and existing ideas for achieving the required functions excellently was gathered and processed through morphological analysis. In this work, the morphology analysis was used not only as a decision-making tool but was applied creatively, adapted, and modified as a methodology to meet the requirements and solve the design issue at hand. Through this methodology, a systematic review of existing ideas and systems was done. Integration of suitable working principles or solution elements was done to determine different sets of theoretical solutions which will be analyzed and filtered according to the functional requirements and design specifications to come up with an optimal solution concept ready for development. A morphological chart consists of tabular representations of potential solutions to different individual sub-functions of the overall product. The morphological chart table 4.6 below consists of the critical sub-functions across the first column, the cells of the chart are populated based on existing ideas, solutions, brainstorming activities, and expertise, this activity is based on the participants' interpretation of the design assignment.

Table 4. 6: Morphological Chart

Alternatives ▶ **Functions ▼**	**Solution concepts/alternatives [initial object design knowledge]**				
Feeding mechanism	Manual loading	Bucket conveyors	Screw feeders	Chute conveyors	
Washing system (generating forces on particles and water)	Cyclic shaker	Direct drive Cam based shaker	Electro-dynamic shaker	Direct drive eccentric rotating shaker	
visual sensor	Light-fields cameras	C-MOS	CCD		
Sensor configuration	Eye-in-hand	Multi-vision	Stereo vision	Monocular vision	
	Eye and hand				
Image processor	PC	FPGA	SOC	GP	
Handling manipulator	Articulated Arm	SCARA	Cartesian	Gantry system	
Drive mechanism	belt	Lead screw	pneumatic	Rack and pinion	Crank slider
Joint actuators	Servo motor	Stepper motor	Encoders		
End-effector tooling	Gripper	Suction nozzle (vacuum / negative pressure)	Tilting mechanism	scoops	
robot controller	PC	FPGA	SOC		
Space execution	Task space execution		Joint space execution		
Control	Manual	online	Semi - automated	Automated	
Visual servoing scheme	PBVS	IBVS	hybrid		
Artificial lighting	incandescent lamps	fluorescent lamps	quartz halogen	lasers	light-emitting diodes

4.3.3 Design Questions Checklist

Table 4. 7: Design Questions Checklist

Design Question checklist	Requirements	Constraints	Functions	Components/ subsystem	Evaluation measures
What defines a good ore washing procedure?	-Should be able to mimic the manual panning process effectively. -Should be able to systematically reject many gangue particles to remain with heavier particles especially gold.	-The amount of material to be washed should be controlled per time. -The force exerted for gangue rejection should not overthrow the panned material.	Systematically separates the lighter particles from heavier particles. - uncover the heavier particles from the gangue. -generate the forces on the particles.	-Feeding mechanism -Washing System	Systematically generates forces on the particles. - Ability to produce stable cyclic motions or patterns
What factors influence the detection and localization of the target?	-Visibility of target. -Ambient lighting -the resolution of the image sensor. -Image processing algorithm. -Type of image features	-the field of view of the camera. -occlusion of the target. -cost of the image processor. -Minimum resolution of the image sensor. -Appearance-based features not geometric.	-capture or record of the panning platform. -feature extraction of the image features. -image processing	-Image sensor. -image processor -Artificial lighting system	Configuration of the camera. -fixed or dynamic camera -Overhead non-shiny illumination. - low-cost image processor and camera
How to remove the wanted materials from the platform to the next step in the process?	-handling of the wanted materials. -Transferring the materials from the panning platform to the next process.	-The size and form of crushed particles (small sawdust-like particles).	Handling and transportation of particles (picking and placing operation)	- end-effector tooling. - Handling manipulator	- simple kinematics for the manipulator. -Ease of programming for servoing the end effector. -Ease of integration and configuration

		- no particular shape of particles			
How is the designed system going to be operated	-Fully automated or online operated	. The technology and approach should be practically achievable. -User-friendliness	-Be able to carry the washing process autonomously. -automatic visual detection and localization. -Automatic movement of the end–effector to the desired positions	- Control unit -User interface.	-Maintainability - ease of integration. -Adaptability
What level of maintenance will be required?	-Robust -The components should be readily and easily available locally. -usage of modules and plug and play systems	- technical know-how of the operator. -simple architectures for easy diagnostics and troubleshooting	- Overall functions	-all components and subsystems	- plug and play systems and components. -Industrially robust components (moisture and dirt)
What type of technology is required to operate the system	Current industrial technology, neither too advanced nor outdated for the African context.	Technologically trending and supported. Standard compatible technology	All functions	All components	Locally Available operability-ability Scalable technologies. Adoptable to the African context
The level of the cost required	Inexpensive	As per budget	Overall functions	All components and subsystems	Adaptable to the African context and for small-scale mineral processing. Affordability Profitability
Material needs.	Industrial standard. Resistant to corrosion.	Cost	overall functions	washing system and handling system	

4.3.4 Evaluation of variants lists

Table 4. 8: Selection of solution concepts from variants lists

FUNC.	CRITERIA	Alternatives/ solution concepts			
Handling manipulator		**Articulated robotic arm**	**SCARA**	**Cartesian**	**Gantry system**
	Ease of customization	3	3	5	5
	Stroke/reach	3	1	3	5
	Payload	5	2	4	5
	versatility	3	4	5	5
	Speed	3	5	3	3
	Ease of use	3	3	5	5
	Total Points	20	17	25	28
	Rank	3	4	2	1
Washing System		**Cyclic shaker**	**Cam based shaker**	**Electro-dynamic shaker**	**Eccentric rotating shaker**
	Effectiveness	3	5	3	4
	Cost	4	4	1	4
	Ease of control	3	5	2	3
	Points scored	10	14	6	11
	Rank	3	1	4	2
Image Processor		**PC**	**FPGA**	**SOC**	**GP**
	Cost	3	4	5	3
	Application specific	3	5	4	5
	Customization	3	4	5	4
	size	2	4	5	4
	Power Consumption	3	3	4	3
	Points scored	14	20	23	19
	Rank	4	2	1	3

Drive mechanism		**belt**	**Leadscrew/ power screw**	**pneumatic**	**Rack and pinion**	**Ball screw**	**Direct Drive**
	Accuracy	4	4	3	5	5	5
	Integration	3	3	2	5	5	5
	performance	3	4	3	5	5	4
	Efficiency	3	5	3	3	5	3
	Size	3	4	2	3	4	4
	Smooth motion	3	4	3	3	5	5
	Precision	4	4	3	5	5	5
	Rigidity	2	4	3	4	4	5
	Point scored	25	32	22	33	38	36
	Rank	5	4	6	2	1	2

Image sensor configuration		**Camera in hand**	**Camera and hand**	**hybrid**
	Ease of computation	3	5	2
	Fixed field of view	3	5	5
	Cost	5	5	2
	Ease of integration	3	4	2
	Points scored	14	19	11
	Rank	2	1	3

Image sensor type		**C-MOS camera**	**CCD Camera**	**Light field cameras**
	cost	5	3	3
	Power consumption	5	3	2
	Higher integration	5	4	1
	High-speed application	5	4	3
	Points scored	20	14	9
	rank	1	2	3

End-effector tooling/handling		**Gripper**	**Suction nozzle (vacuum / negative pressure)**	**Tilting mechanism**	**scoops**

FUNC.	CRITERIA	Alternatives/ solution concepts			
	Ability to handle small particles	2	5	4	4
	Ease of control	4	5	4	3
	Mounting requirements	3	5	2	3
	Minimum weight	3	5	3	3
	Maximum rigidity	3	5	2	2
	Minimum size	2	5	4	2
	Ease of design	3	5	3	3
	Points	20	35	22	20
	grade	3	[illegible]	2	3

lighting		fluorescent	incandescent	Quartz halogen	lasers	LED
	Light output	5	5	5	5	3
	Lumens per watt	4	4	5	5	4
	Surface brightness	5	5	5	5	4
	Life span	3	1	3	3	5
	Dimmability	2	3	3	5	5
	Size and design flexibility	4	2	3	3	5
	Energy saving	4	2	2	1	5
	Cost	3	4	1	1	5
	Minimum additional equipment	2	3	2	2	4
	Points	32	29	29	30	40
	grades	2	4	4	3	[illegible]

To evaluate among the solution concepts and select the optimal working principle or solution concept, the initial requirements, requirements checklist, constraints were used together with design questions. These provided an evaluation criterion, measures, and basis for the elimination or selection of components/concepts/working solutions. Much emphasis was placed on the functional aspect to check for the feasibility of the technique and approach. From the morphological chart, different alternatives can be merged to realize the needed function. From the populated morphological matrix, the possible number of combinations can be approximated using (5):

$$C = \prod_{j=1}^{n} m_j \quad (5)$$

Where C is the number of combinations, m is the number of possible alternatives for each function n. For this work the number of possible combinations was approximated to be above:

$$C = \prod_{j=1}^{n} m_j = 4*4*3*3*2*4*4*5*3*4*3*4*3*5$$

$$= 49766400$$

To select the optimal concepts or working solutions, the alternatives or solution variants were evaluated against different criterions such as technical, economic, etc. The provided evaluation criteria for a function or sub-function provided the measure and basis for elimination or selection of components/concepts/alternative as shown in Table 4.8 above. Technical design attributes such as maintainability, reliability, compatibility, scalability, repeatability, speed, payload, stroke/reach, power consumption, etc. were used to select the optimal solution for a given function. The evaluation criteria were different for each function and some attributes had different weights compared to others. Table 4.9 below shows a selection of optimal solution variants for the design of an automated vision-based gold panning system after the evaluation process.

4.3.5 Principle working solution

From the selected working principles that satisfied the requirements and constraints, the working structure was established. Fig 4.3 shows the block diagram for the principal solution. All the sub-systems are connected to the main controller. The washing system consists of a pan that is attached to motors. The motors cause the pan to rotate systematically to generate forces on the particles and eject lighter gangue particles out of the pan and cause the heavier gold particles to accumulate in close positions in the pan. The imaging system consists of artificial lighting, an image sensor, and an image processor which capture noise-free images used in the detection and localization of target objects. The main controller receives the coordinates of the detected objects from the image processor and sends signals to the handling system (gantry manipulator), to move the end-effector (suction nozzle) to the gold particles to transfer them from the pan to the next process. All the components of the sub-systems derive energy from the power supply. The controller also controls the delivery of the inputs (crushed ore and water) through the feeding system and controls the movements of the washing system.

Table 4. 9: Selected solution concepts

Alternatives ▶ Functions ▼	**Solution concepts/alternatives [initial object design knowledge]**				
Feeding mechanism	Manual loading	Bucket conveyors	Screw feeders	Chute conveyors	
Washing system (generating forces on particles and water)	Cyclic shaker	Direct drive Cam based shaker	Electro-dynamic shaker	Direct drive eccentric rotating shaker	
visual sensor	Light-fields cameras	C-MOS	CCD		
Sensor configuration	Eye-in-hand	Multi-vision	Stereo vision	Monocular vision	
	Eye and hand				
Image processor	PC	FPGA	SOC	GP	
Handling manipulator	Articulated Arm	SCARA	Cartesian	Gantry system	
Drive mechanism	belt	Lead screw	pneumatic	Rack and pinion	Crank slider
Joint actuators	Servo motor	Stepper motor	Encoders		
End-effector tooling	Gripper	Suction nozzle (vacuum / negative pressure)	Tilting mechanism	scoops	
robot controller	PC	FPGA	SOC		
Execution space	Task-space execution		Joint–space execution		
Control	Manual	online	Semi - automated	Automated	
Visual servoing scheme	PBVS	IBVS	hybrid		
Artificial lighting	incandescent lamps	fluorescent lamps	quartz halogen	lasers	light-emitting diodes

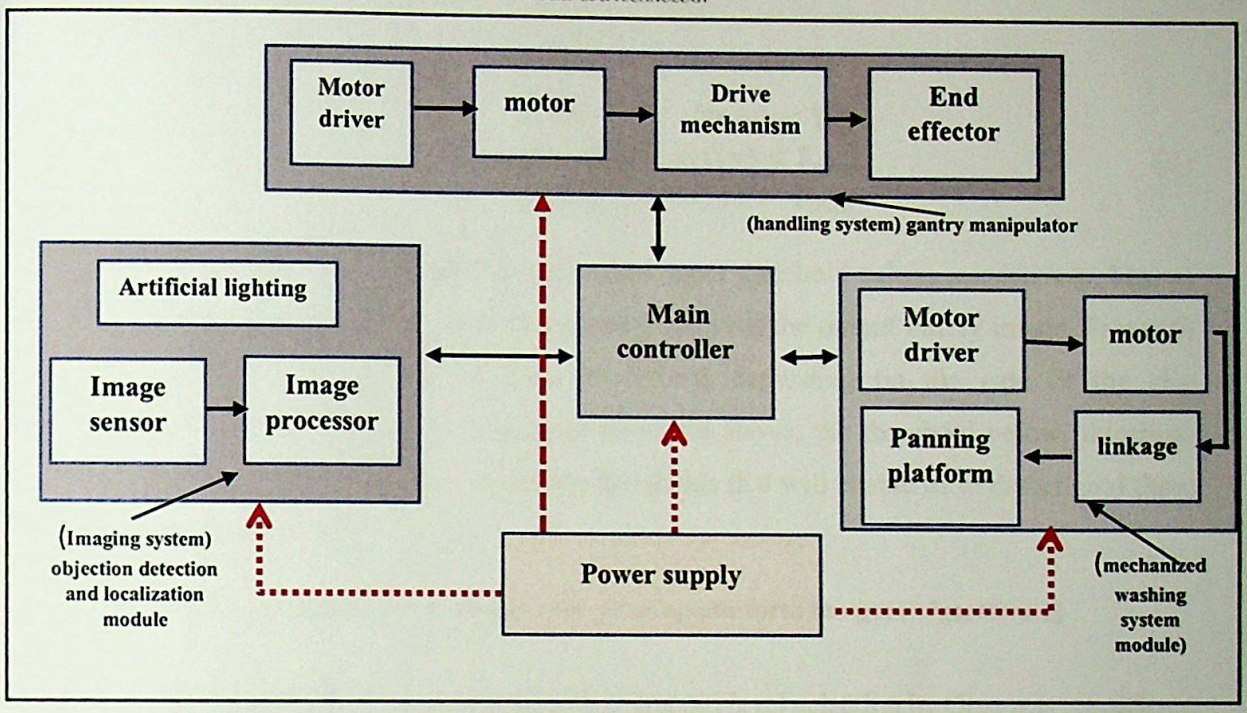


Figure 4. 3 : Principal solution functional block diagram

4.4 Domain-Specific Designs

Having the functional structure layout and preliminary decisions about the overall mechanical properties, sensor configurations, choice of materials, functional sequences, procedural sequences, and parameters needed for a successful design from the requirements, specifications, and morphological analysis the domain-specific designs were initiated. The development of the gold detection program was conducted first since the success of the whole design is hinged on the ability to detect gold particles in the image

4.4.1 Gold detection and localization framework (software domain)

This section is in line with objective 2 which focuses on the application of machine vision principles to detect and localize gold using visual information. With so many segmentation techniques and algorithms available, this presents the challenge of choosing the best and most appropriate technique for the problem at hand. No segmentation technique or object detection framework for the gold panning platform images has been developed to date, hence this section seeks to apply some of the known techniques to segment gold panning platform images to detect and localize the gold particles in the images. Three thresholding techniques are first explored for this problem as they are widely applied and they are computationally less complex and easy to implement and they are user friendly [140]. Equation (6) will be used to segment images using the threshold technique, this will apply both on monochrome images and color images.

$$O_{(x,y)} = \begin{cases} 0, & I(x,y) < T_{min}, \\ 1, & T_{min} < I(x,y) < T_{max}, \\ 0, & I(x,y) > T_{\max} \end{cases} \quad (6)$$

Where T_{min} and T_{max} are lower threshold and upper threshold values respectively, I (x, y) is the intensity value of the input image and O (x, y) is the output binary image. From (6) four categories of thresholding can be defined depending on the side of the clip level/threshold considered and these are threshold above, the threshold below, threshold inside, and threshold outside. To find the thresholds that will enable us to detect gold three techniques were used.

4.4.1.1 Otsu's global thresholding on gold panning platform images (Algorithm 1)

Global thresholding based on automatic threshold level selection by Otsu was considered first because of its popularity and competence. Otsu's automatic thresholding was considered as it seeks to automatically choose the optimal threshold that minimizes the intraclass variance. Otsu's method was used to learn a clip level that can maximize the between-class variance. Otsu's segmentation was done on the grayscale images so the images were first converted from RGB image to grayscale image. After the conversion of the image to a grayscale image the histogram of that image was computed and normalized [173]. Equation (7) was used to normalize the grayscale histogram which was used as the probability distribution.

$$p_i = {}^{n_i}/_{N}, \quad p_i \geq 0, \quad \sum_{i=1}^{L} p_i = 1 \quad (7)$$

n_i represent the number of pixels at level i of L gray levels and p_i is the probability distribution. For bi-level thresholding which results in two classes C_0 and C_1 corresponding to background class and foreground class, the probabilities of class occurrence and mean class levels according to Otsu [173] are denoted by (8), (9), (10), and (11) as :

$$\omega_0 = P(C_0) = \sum_{i=1}^{k} p_i = \omega(k) \quad (8)$$

$$\omega_1 = P(C_1) = \sum_{i=k+1}^{L} p_i = 1 - \omega(k) \quad (9)$$

And

$$\mu_0 = \sum_{i=1}^{k} \frac{ip_i}{\omega_0} = \mu(k)/\omega(k) \tag{10}$$

$$\mu_1 = \sum_{i=k+1}^{k} \frac{ip_i}{\omega_1} = \mu_T - \mu(k)/1 - \omega(k) \tag{11}$$

Here $\mu(k) = \sum_{i=1}^{k} ip_i$ *and* $\omega(k) = \sum_{i=1}^{k} p_i$ *and* $\mu_T = \mu(L) = \sum_{i=1}^{L} ip_i$ *and* ω_0 and ω_1 are the probabilities of class occurrence for C_0 and C_1 respectively, μ_0 and $\mu_1$are the mean class levels, μ_T is the total mean level of the whole image. The class variances are computed using the mean and probability distributions above using (12) and (13):

$$\sigma_0^2 = \frac{\sum_{i=1}^{k}(i-\mu_0)^2 p_i}{\omega_0} \tag{12}$$

$$\sigma_1^2 = \frac{\sum_{i=k+1}^{L}(i-\mu_1)^2 p_i}{\omega_1} \tag{13}$$

These variances are used to calculate the 'good' class separability parameters which are used in the discriminant analysis of the threshold. The most commonly used separability measure is the within-class variance (σ_B^2) which is computed using (14):

$$\sigma_B^2(k) = \frac{[\mu_T\,\omega(k) - \mu(k)]^2}{\omega(k)[1-\omega(k)]} \tag{14}$$

And k is the optimal threshold that maximizes the interclass variance (σ_B^2). So, Otsu's method is an optimization problem that automatically finds the threshold/intensity level that maximizes the interclass variance formulated by (15):

$$J(k) = \max \sigma_B^2\ (k), 0 \le k \le L-1 \tag{15}$$

Where J(k) is the objective function and k is the intensity level being calculated. The automatically determined threshold was used to segment the images. Below are the steps followed using Otsu's global segmentation technique.

Steps for Otsu's thresholding-based segmentation

1. Read image data
2. Convert the image from RGB image to grayscale image (equation 3).
3. Compute image histogram
4. Normalize the image histogram (equation 4)
5. Compute good class separability parameters (equation 5 -11).
6. Define the threshold value that matches the computed good class separability measure (equation 12).
7. Assign pixels to either background or foreground using the "above threshold" criteria.
8. Perform post segmentation processing
9. Perform feature extraction.

Fig 4.4 below shows these steps using a flow diagram for Otsu's threshold method and its application on one of the gold panning platform images. The results and analysis of this approach are presented in the preceding chapter.

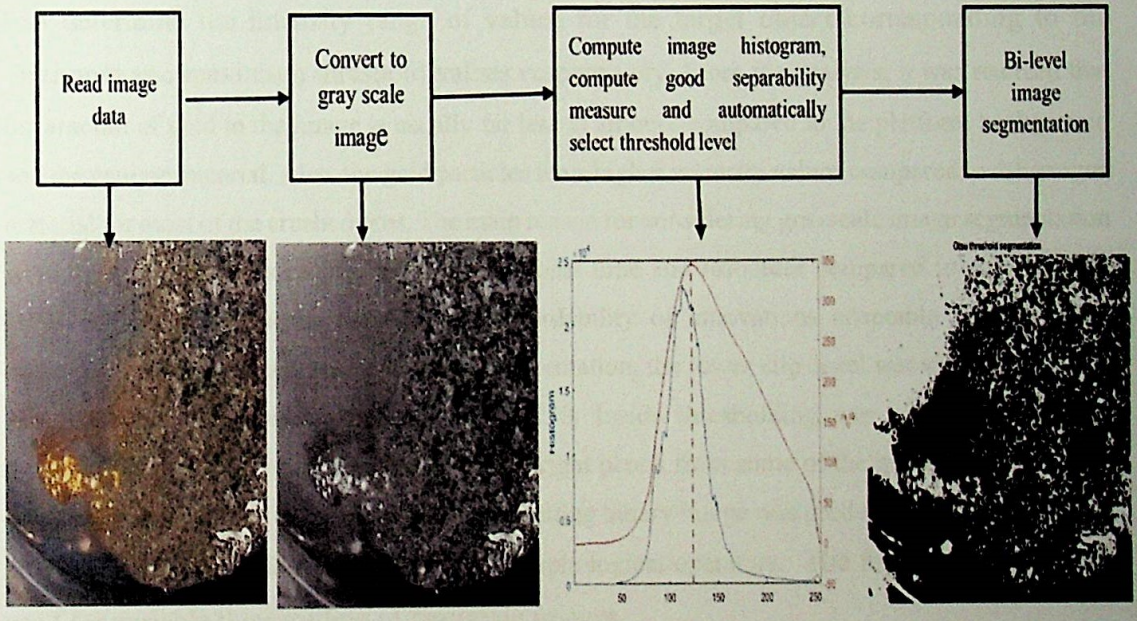


Figure 4. 4: Otsu's thresholding segmentation flowchart and application example on a gold panning platform image

4.4.1.2 Grayscale image variable thresholding of gold panning platform scenes (Algorithm 2)

From the histogram analysis of grayscale images of the gold panning platform images the thresholds were obtained and were used in the segmentation process. The monochrome images contain a grayscale data matrix representing the intensity values of the image. The intensity of a pixel is represented with a range of values from 0 to 255, where 0 represents black and 255 represents white, and any other value between represents varying shades of gray. From the panning images captured

in the primary color system, the YIQ conversion was performed to have the intensity value using the following equation:

$$Y = 0.2909R + 0.507G + 0.1140B \quad (16)$$

Where Y is the luminance value of the output grayscale image obtained by the weighted sum of the red, green, and blue components of the input image. Having converted the image to a grayscale image the thresholding procedure was done to obtain the segmented image using the values obtained from the histogram analysis. The following rule was used for segmentation:

$$Y_b = \begin{cases} 1\,(gold) & if\ Y_l \leq Y_g \leq Y_h \\ 0\,(Background) & else \end{cases} \quad (17)$$

Where Y_b is the binary image after thresholding, Y_l and Y_h are the two threshold values that determine the intensity range of values for the target object corresponding to the minimum and maximum threshold values respectively. From the analysis, it was realized that the amount of gold in the image is usually far less in amount compared to the platform background and the gangue material. Also, the gold particles have higher intensity values compared to the gangue material for most of the crushed ores. The main reason for considering grayscale image segmentation is that grayscale images require less computational time and resources compared to color images [174], which can influence the cost and affordability of innovations adaptable to developing countries. From histogram analysis and experimentation, the lower clip-level was chosen to be 130 and the upper clip-level was chosen to be 250. Inside thresholding was chosen over above thresholding to avoid specular reflections and bright pixels from some of the gangue material. The thresholds were applied to the image and the resulting binary image was produced. The binary image produced had noise so it was cleaned using morphological operators. The following steps were used for variable thresholding of grayscale images.

Algorithm 1: thresholding based on monochromatic images

1. Capture the image of the gold panning platform
2. Read the image dataset I (i, j).
3. Convert the image from RGB to grayscale image using equation (3):
   $$Y = 0.2909R + 0.507G + 0.1140B$$
4. Perform the thresholding procedure with the minimum intensity value Y_l=130 and maximum intensity value Y_h = 250
5. Assign 1 (white/object) to all the pixels in the range (130 -250) and 0 (Background) to all the pixels outside the range.
6. Perform morphological operations to clean and filter out unwanted noises.
7. Extract the wanted statistical information of the objects using region properties

Binary morphological operations

For step 6 above the morphological operations were used to clean up the segmented image. Morphological operations are non-linear image processing activities performed on the detected features. The operations depend on the relative structuring of pixel values rather than their numerical values, which make them applicable to binary or grayscale images. The structuring element is used to probe the image by comparing it to all possible image neighboring pixels. The probing tests whether the element fits in the neighboring pixels or whether it intersects the neighborhood and based on the result the binary image is altered.

After the thresholding rule was applied to the image and the pixels of the gold panning platform were assigned as either gold particles (target object) or background material (gangue) to form a binary image, the binary morphological operations were carried out to 'clean up' the segmented image by removing some unwanted specs. This was a necessary step in easing and speeding the future processes of robot control. The small spots in the background were wiped out by setting the smallest acceptable size of the gold particles discernible in the further application. Any gold particle blob less than the acceptable size was wiped out. Also, the holes or gaps inside the detected object were filled. Binary morphological erosion and dilation operations were used during the post-segmentation process to clean up the image.

Binary morphological Dilation

This operation was responsible for expanding the regions, that is, it sets to the maximum value the output pixels of all the pixels in the input pixel neighborhood. This operation is performed by the structuring element. The dilation operation is denoted by the following equation:

$$B \oplus S = \cup_{b \in B} S_b \tag{18}$$

Where B is the segmented binary image to be cleaned and S_b is the structuring element. S is shifted to B such that when S touches a bright pixel (1) of B it expands that region.

Binary morphological erosion

This operation is responsible for shrinking regions, that is, it sets to minimum value the output pixels of all the pixels in the input pixel neighborhood. This is denoted by the following equation:

$$B \ominus S = \{b | b + s \in B, \forall_s \in S\} \tag{19}$$

In the erosion operation as S sweeps over B, any region where S is completely contained in B shrinks the region by outputting a 1 (bright pixel) on the origin of that region.

Opening and Closing operation

The sequence of these two morphological operations can perform the opening and closing of regions on a binary or gray image. Morphological dilation followed by morphological erosion operation performs the flood-filling operation (closing operation) on the background pixels of the segmented binary image. It fills the holes and gaps in background pixels that cannot be reached by filling in the background from the edge of the image. Usually, holes are sets of dark pixels surrounded by light pixels. The closing operation is denoted by:

$$B \bullet S = (B \oplus S) \ominus S \tag{20}$$

Erosion followed by morphological dilation eliminates the small projections, regions, and objects (Opens the region). This operation smoothens the border of large objects. The opening operation is denoted by the following equation:

$$B_o S = (B \ominus S) \oplus S \tag{21}$$

After the cleaning process feature extraction of the detected gold particles was performed to extract features that will be necessary for further control processes. Fig 4.5 shows the flowchart for the variable thresholding segmentation process of grayscale gold-panning platform images and its application on the sample images. The results and analysis of this approach and feature extraction results are presented in the preceding chapter.

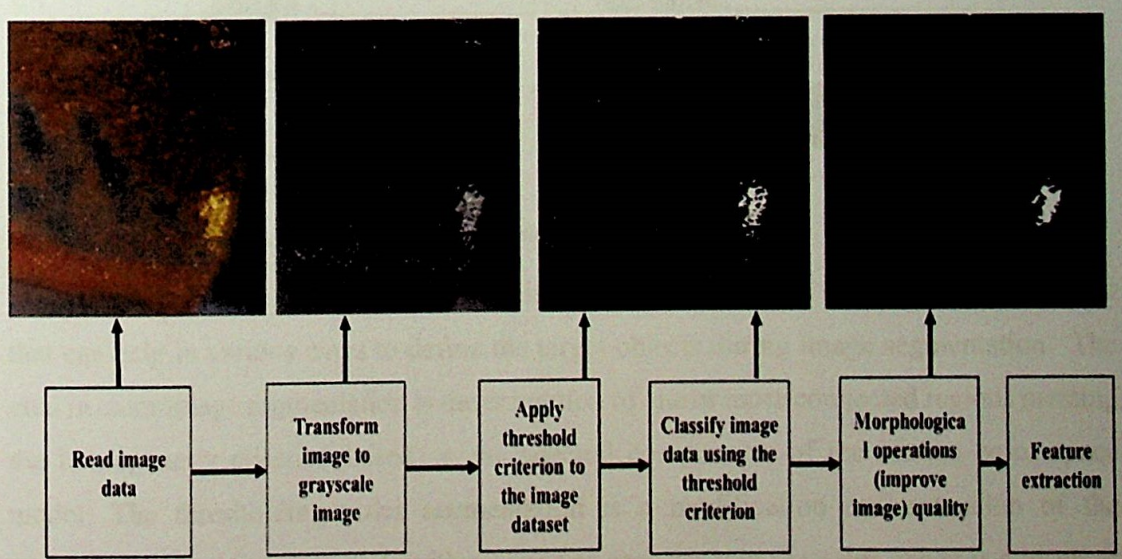


Figure 4. 5: Variable thresholding and application on grayscale images

This thresholding method was extended to segment color images since it performed well on grayscale images compared to Otsu's automatic global thresholding method.

4.4.1.3 Colour image thresholding-based segmentation of gold panning platform images (Algorithm 3)

Colour is the only attribute that the miners use to detect gold from the gangue material in the panning platform. There are many color models used to represent color images. For color-based segmentation, color histograms of the separate channels of the RGB color space, HSV color space, and the CIELAB color space were first analyzed and the appropriate color space for the required application was chosen. Figure 4.6 shows an example of the histogram analysis of the channels of the 3 color spaces of the captured images.

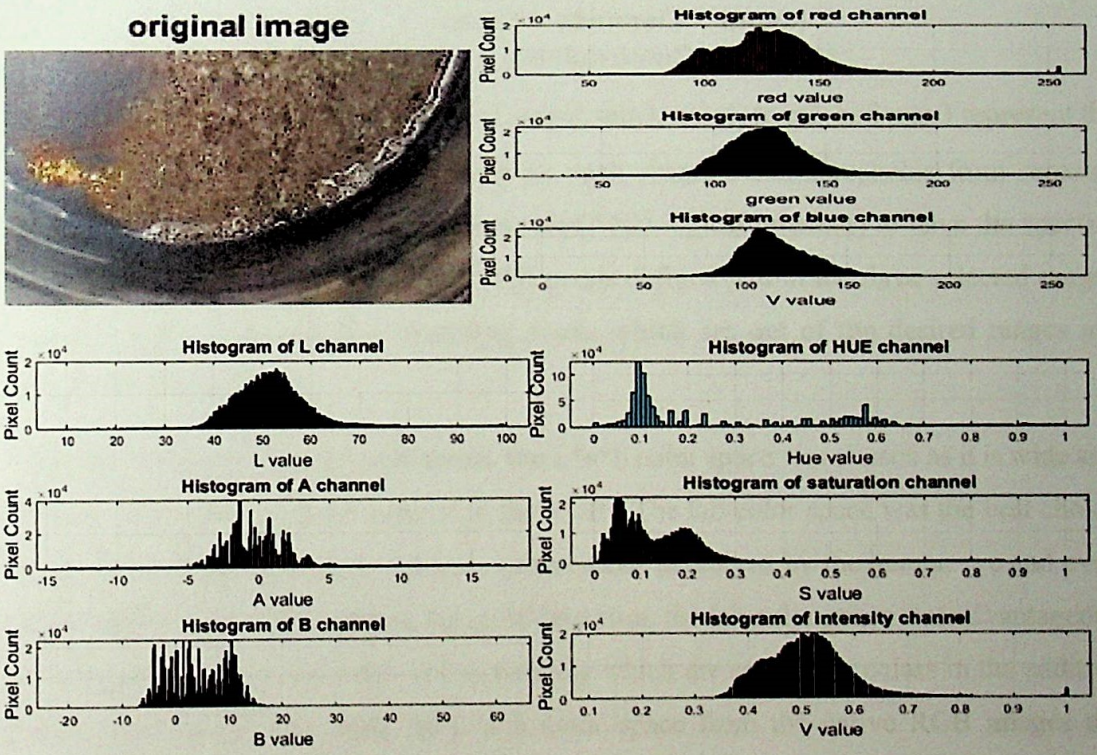


Figure 4. 6: Histogram analysis of an image in 3 color space model

As witnessed in the analysis of the color histograms, color images bear a lot of information that can help in various ways to define the target objects during image segmentation. The goal in color image segmentation is the extraction of one or more connected regions meeting the homogeneity criterion based on the spectral components of the chosen color space model. The thresholding color segmentation is a modification and extension of the monochromatic thresholding algorithm above as each pixel in the color image is a result of the 3 channel components [143]. Colour image thresholding was done to filter out gold

particles from the gangue materials by taking advantage of the distinct color difference of the materials. Using histogram analysis and different plots of the different channels of the reference images containing gold particles and gangue material. The effect of the different channels on gold detection was studied and channel thresholds were established. For the task at hand, thresholding was used to determine the channel values belonging to gold particles and pixels/intensities belonging to non-gold particles. The pixel was detected as gold if its spectral components are found between the chosen thresholds values otherwise it was detected as the non-gold particle. The segmentation results were obtained using the rule:

$$O_{(x,y)} = \begin{cases} \mathbf{1} \quad (\boldsymbol{gold})\ \boldsymbol{if}\ \ldots\ldots \\ (\boldsymbol{min1} \leq \boldsymbol{channel1} \leq \boldsymbol{max1})\ \cap \\ (\boldsymbol{min2} \leq \boldsymbol{channel2} < \boldsymbol{max2})\ \cap \\ (\boldsymbol{min3} < \boldsymbol{channel3} < \boldsymbol{max3}) \\ \mathbf{0}\ (\boldsymbol{background})\ \ \boldsymbol{else} \end{cases} \tag{22}$$

$O_{(x,y)}$ is the resulting binary image, min1, min2, min3, max1, max2, and max3 represent the lower and upper thresholds respectively for each channel. The thresholds from separate channels are fused using the intersection rule (AND logical operator) to have the spectral components fitting for gold detection. All pixels defined within the three selected ranges are assigned as gold and the remaining pixels which are out of the desired ranges are assigned as background.

After several experimental verifications, the L*a*b color space was chosen as it is wide and contains more color fields compared to the RGB. The lab color space was the best choice for the application as it expressed colors that can be perceived by the human eye and even those outside human perceptions. For gold detection, the lab color space was advantageous as it contained yellow and other colors natively which are secondary colors in the additive RGB color model. To realize the L*a*b color space from the native RGB images the following conversion equations were used. From the three channels of the RGB color model and their range of values $(0-255)$

$$L^* = \begin{cases} 116\left({}^{Y}/_{Y_n}\right)^{1/3} - 16\ ;\ {}^{Y}/_{Y_n} > 0.008856 \\ 903.3\left({}^{Y}/_{Y_n}\right)\ ;\ otherwise \end{cases} \tag{23}$$

$$a^* = 500\left[f\left({}^{X}/_{X_n}\right) - \left({}^{Y}/_{Y_n}\right)\right] \tag{24}$$

$$b^* = 200\left[f\left({}^{Y}/_{Y_n}\right) - \left({}^{Z}/_{Z_n}\right)\right] \tag{25}$$

Where

$$\begin{bmatrix} X \\ Y \\ Z \end{bmatrix} = \begin{bmatrix} 0.412453 & 0.357800 & 0.180423 \\ 0.212671 & 0.715160 & 0.072169 \\ 0.019334 & 0.119193 & 0.950227 \end{bmatrix} \begin{bmatrix} R \\ G \\ B \end{bmatrix} \tag{26}$$

And

$$f(t) = \begin{cases} t^{1/3} \; ; \; t > 0.08856 \\ 7.787t + \left({}^{16}/_{116}\right) ; otherwise \end{cases} \tag{27}$$

Where L^* component is the lightness of the color, a^* component is a position between red/magenta and green, b^* component is the position between yellow and blue, f is the calibration function, X, X_n, Y, Y_n, Z, Z_n are coordinates of the CIEXYZ color model.

After the conversion to the lab color space, the different channels were separated and the thresholding values are applied to each channel according to the equation (22). The results of the thresholding process under different channels are combined using the AND logical operator to produce the segmented binary image which is further processed using the morphological operations.

Algorithm 3: thresholding based on color images

1. Capture the image of the gold panning platform
2. Read the image dataset I (x, y, i).
3. Convert the image from RGB color space to CIELAB color space using the equations
4. Separate the channels of the Lab color space.
5. Apply thresholds to the individual channels of the colour space:
   4.0 < L* channel < 99.3
   -6.7 < a* channel < 23.2
   39.7 < b* channel < 65.4
6. Combine the channel thresholds using logical AND operator.
7. Assign 1 (white/object) to all the pixels that satisfy the homogeneity criterion above (steps 5 and 6) and 0 (Background) to all the pixels outside the range to create a binary image.
8. Perform morphological operations to clean and filter out the unwanted noises- closing and opening operations.
9. Extract statistical information of the objects using region properties

The channel thresholds were established through experimentation and analysis of channel histograms of several gold panning scenes captured under different imaging conditions. Table 4.10 below shows the thresholds that were used:

Table 4. 10: CIELAB Threshold values

CIELAB channel	Threshold used	
	Lower threshold	Upper threshold
L*-channel	4.0	99.3
A*- channel	— 6.7	23.2
B*- channel	39.7	65.4

The results of this approach and analysis and comparisons with the other approaches above are presented in chapter 5. Image segmentation was done to understand the image data clearly and it led to gold detection. After the detection features which aid in localization were extracted.

4.5 Mechanical sub-system

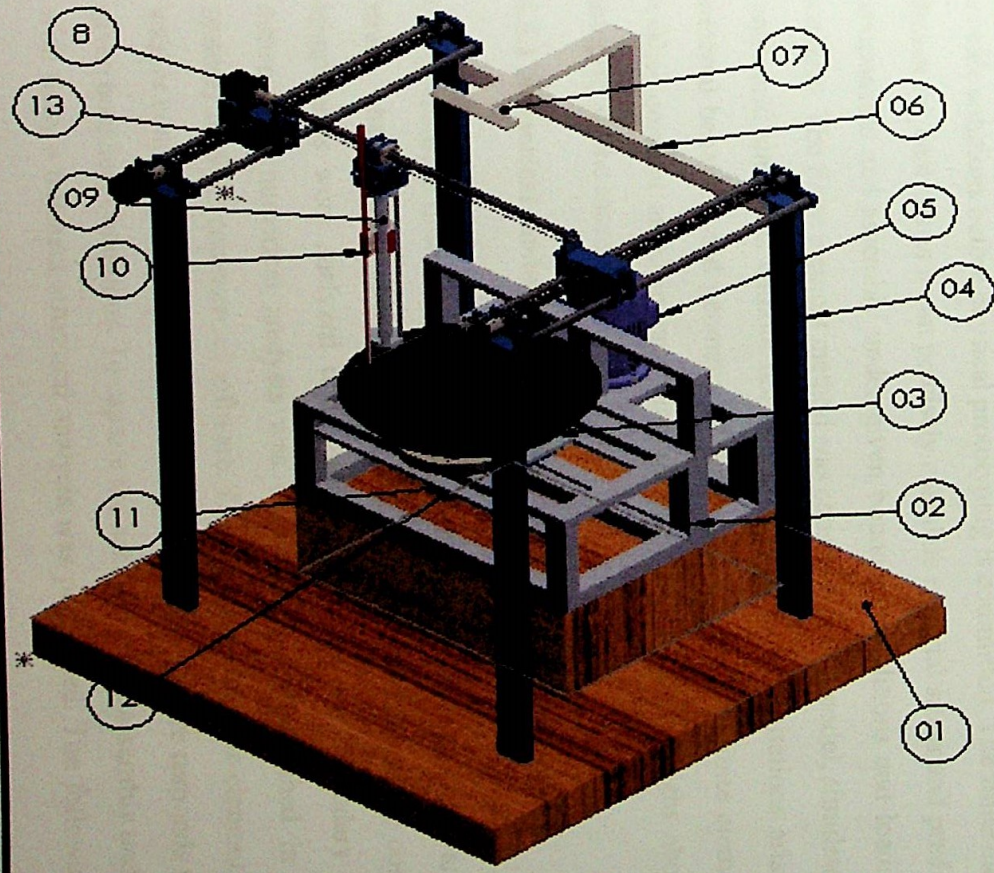
The mechanical part is the basis and skeleton of the automated vision-based gold panning system. The other domains are there to monitor, control, and provide information on the state of the process. The mechanical design of the system considered all the physical aspects of the system in full detail to satisfy the requirements and this included the structure, mechanisms, properties, and parameters. Sensor and actuator configuration and positioning together with their hardware integration matters were considered during this design phase. 2D and 3D models of the automated vision-based gold panning system were designed and validated using computer-aided design (CAD) and computer-aided engineering (CAE) tools before physical prototyping. To convey the details of the mechanical design of the automated gold panning system a series of working drawings were produced. Fig 4.7 shows the drawing of the entire assembly and how all the sub-assemblies of the system interact. The complete details of the entire working drawings, geometries, back-of-envelope calculations of the design are presented in Appendix A. The mechanized ore washing system and the gold handling system in the form of a gantry manipulator formed the mechanical component of the system

The entire assembly consists of the handling system in a gantry configuration which also provided a structure for the imaging system. The fixed 'camera and hand' configuration was assembled for the imaging system. The x-y-z translations of the end-effector are made possible by the lead screw drive mechanism of the gantry manipulator. The suction nozzle

end-effector is connected to the suction mechanism that is energized when the nozzle is above the detected gold particles to suck them out of the pan.

The designed 3D CAD mechanical model was used to study the performance of the mechanisms, components, and assemblies under different conditions to refine the design. Through the designed mechanical subsystem, the interactions of various parts and assemblies

of the model were studied and refined. Mechanical stimulation of the model was used to test the kinematic, static, and dynamic behavior. Motion analysis study was done to analyze the motion of various parts of the design and to probe if they were providing the needed motion.



Item no	Part Name	Description
13	Leadscrew	stainless steel 15mm diameter
12	Big pulley	steel alloy pulleys
11	Pulley Belt	durable nylon rubber
10	End-effector nozzle	Nozzle
09	z-axis link holder	machined
08	servo motor	NEMA 34
07	camera & lighting	LED Lights and camera
06	camera holder	Aluminium
05	electric motor for washer	18.5 kW 4P 180M
04	frame for handling system	Base frame for the handling system
03	Grooved gold pan	Rigid PVC pan
02	Washer frame	fabricated frame for washing system
01	Base	Hard mahogany/teak wood

Notes:
1. All dimensions are in mm unless stated
2. All permanent joints are welded unless stated
3. Finish is as machined unless stated

Scale1:15	GENERAL ASSEMBLY	
BIUST	Automated vision based gold panning	
	Drawn by: Blessing Chipfurwe Makoni	
	Checked and approved by:	Dr M. Namoshe Dr O. Matsebe
	Date 09/20	Sheet 1/7

Figure 4. 7: 3D assembly drawing of the automated gold panning system

4.6 Modelling, model analysis, and simulation of the mechanized gold-washing system.

As per the requirement of the design methodology (VDI 2206), modeling and model analysis was done for the designed gold washer concept. The finite element method (FEM) which is a computational technique used to approximate solutions to boundary value problems (field problems) was used to analyze the designed washer. Boundary value problems are numerical problems in which one or more dependent variables must satisfy a differential equation everywhere in a known domain of independent variables and satisfy the provided conditions on the boundary. This analysis is significant in exploring and understanding the design functionality and fidelity and improving the design at an early design phase.

This section focuses on the study of the designed washer assembly and its components, and identify the problems which might be faced while performing the gold washing process, and provide solutions before physical prototyping is committed. The finite element method was chosen for analysis as it can precisely calculate material stress and predict the behavior of components and assembly under given boundary conditions and loading in a quasi-real scenario. The finite element method was chosen as it can model, simulate and evaluate near real-world situations without non-linear characteristics limitations arising from contacts, material behavior, and geometry of the design easily. The Finite element analysis of the washer concept aided in providing reliable insight and foresight about the mechanical integrity of the assembly.

4.6.1 Numerical modeling and analysis of the gold washer system

Comprehensive finite element analysis of the washer was conducted and the deformation, strain, stress, strain energy, elastic strain, stress concentration, contact status of the components were analyzed under the applied load and boundary conditions. Three-dimensional numerical analysis was developed and established in ANSYS (Analysis system) 2019 R3 commercial software. The main goal of finite element analysis of the gold washer concepts was to evaluate how the assembly structure responds to loading under the given boundary conditions. To capture the behavior of the assembly under the provided load with time, a transient structural analysis was performed. The following procedure which

included pre-processing steps, processing steps, and post-processing steps was performed to carry out the analysis.

1) Pre-processing

The 3D model of the gold-washer designed in SolidWorks in section 4.5 was converted into an Initial Graphics Exchange file format (IGES) and imported into the ANSYS analysis environment. Each component of the imported file was assigned to the corresponding material selection and its stiffness behavior was defined. Only the pulley transmission belt was modeled as flexible material made of nylon rubber. Having assigned materials and defined their behavior the contacts and joints between the various components were established. Bonded contacts or fixed joints were preferred between components that have no relative motion between them. The frictional contact with a co-efficient of 0.2 was established between the belt and the two pulleys. Revolute joints with their torsional stiffness were provided for the connection between the supporting structure and both the motor rotor and the shaft that connects the larger pulley to the pan-holder.

Having defined the materials and the contacts between the components of the assembly discretization of the assembly were performed. Default mesh was first applied to the whole assembly and then refined mesh was used on components and areas which bear greater loading conditions. Non-uniform meshing was preferred since meshing has a strong influence on the reliability and accuracy of the results as well as the computational time of the solution. Coarse/low-density mesh was applied on non-critical areas while fine/high-density mesh was employed on critical paths to speed up the solver time and reduce computational cost while maintaining the accuracy of the results. The meshing procedure of the designed gold-washer outputted a finite element model with 35499 elements connected by 65679 nodes.

The final step in pre-processing was the application of the boundary conditions and loads to the model being analyzed. The boundary conditions entail how the model interacts with its environment and define the loading and constraints applied to the model. The main structure was fixed to the ground to restrict the rigid motion of the whole assembly and the revolute joints were restricted to axial rotation along the z-

axis without any translational motion. The pulley belt was constrained by the frictional contact with the pulley to always be in the pulley groove.

2) ***Processing***

This is where the finite element analysis procedure calculates/solves the model based on the provided boundary conditions and loads. It is a computational solution procedure that is heavily dependent on the lengthy numerical calculations required for the analysis based on the number of elements and nodes. An incremental iterative solving technique was used to solve the non-linear problem and ensure its convergence. The total revolute joint load was divided into smaller loads which were applied incrementally and iterative cycles were performed to obtain a converging solution that corresponds to the stage of the loading. The time steps (sub-steps) over which to apply the incremental loads were specified for the solver to compute several equilibrium iterations which lead to a converged solution. Force convergence, displacement convergence, line search, and moment convergence criteria were used to check for the convergence of the non-linear solution. After removing the unnecessary features of the model, it took 179 minutes to solve for stress analysis, strain analysis, deformation analysis, and contact status analysis of the gold-washer analysis on a 10-processor core i5 computer, operating on a normal license.

3) ***Post-processing***

This was the main goal of the finite element analysis procedure as it enables the user to visualize the results of the analysis. The results in the form of deformed geometries, stress-strain curves, stress/strain/deformation distribution maps were produced. These helped to analyze the design by identifying failure-prone areas, hot spots, and contact status graphically. The results of this finite element analysis are presented in the next chapter.

4.7 Modelling and simulation of the handling system, control, motion planning, and analysis.

The modeling and simulation of the handling system were done as one of the validations and verification ways in the mechatronic design approach (VDI 2206 process model). Much work on this section was done to address the technical optimization of the gold picking process (sorting process). This process involves the coordination of the imaging system and the suction nozzle (end-effector) movement. Vision-based control was utilized in this section. To fulfill this task, the following steps were followed:

- Kinematic modeling and analysis of the handling system – representation of the kinematic link, computation of forward and inverse kinematics, computation of the Denavit Hartenberg parameters, and workspace analysis
- Physical modeling and simulation of the handling system based on the kinematic modeling and analysis above.
- Controller design of the handling system
- Motion planning and analysis – path planning, trajectory generation, trajectory following task space and joint space trajectories and their comparisons
- Vision-based control of the handling system – task planning operations; combining of the image processing, trajectory generation, trajectory following, and control of the handling system.

Model setup of the handling system and its analysis was performed in MATLAB Simscape add-in and the control elements were implemented in MATLAB Simulink. The above steps together with their setup's and their results are presented in the result section in the next chapter for coherence's sake.

4.8 Conclusion

Following the design process model presented in chapter 3 both functional and procedural requirements for the automated gold panning machine were generated with the help of the Pahl and Beitz Requirement checklist. Conceptualization was performed using the FAST technique and morphology analysis which resulted in an optimal concept design that is principally defined. The domain-specific designs were carried out in this chapter resulting in computer-aided drawings for the mechanical subsystem and a gold detection and localization framework for the software domain. The modeling setup for the mechanical subsystems and control elements was laid out at the closing of the chapter.

CHAPTER 5

RESULTS, ANALYSIS, AND EVALUATION

5.0 OVERVIEW

This section presents the results, analysis, and discussion of this design work. The results of the developed gold detection framework are presented in this chapter. Modeling, model analysis, and simulation of the system designed were presented in this chapter. This was done to explore the design of the mechanical subsystem and control elements. Physical modeling was done to facilitate the simulations' efforts and extraction of results. The subsystems will be modeled separately and after the modeling process, the control elements will be included. Comparisons and discussions of the results, modeling, and simulations are also presented. Lastly, the design work is evaluated based on the work done and the results of the modeling and simulation.

5.1 Results and comparative study of the image segmentation

Figure 5.1 below shows the sample results of image segmentation work presented in section 4.4.1. of Otsu's segmentation, variable thresholding in gray-scale images, and the variable thresholding in color images. As witnessed on the analysis of several gold panning platform images, the automatically selected thresholds computed by Otsu's method (Algorithm I) are image dependent and could not segment the gold panning platform images in such a way that would detect the gold particles from the panning platform and the gangue. This is mainly because the global thresholding by Otsu's method works well for bi-modal image histograms and when classes are equal or nearly equal. Many of the gold panning images contain complex data that cannot be bi-modal unless all the gangue material is thoroughly washed to leave only the gold and the pan. The method could not handle the non-uniform backgrounds associated with some of the gold panning scenes. Automatic global thresholding could not handle the background non-uniformities and class inequality prevalent in gold panning images.

Algorithm 2 performed better than algorithm I in the segmentation of gold particles though it had some false detections and produced noisy results and could not handle illumination variations well in some images. Algorithm 1 is best suited for gold detection in darker ores where the contrast between the gold particles and the gangue material is high. Algorithm 3 outclassed the other two techniques and was robust to illumination variations and could

differentiate between bright speckles and gold particles. Algorithm 3 could segment all the gold particles even under various shades.

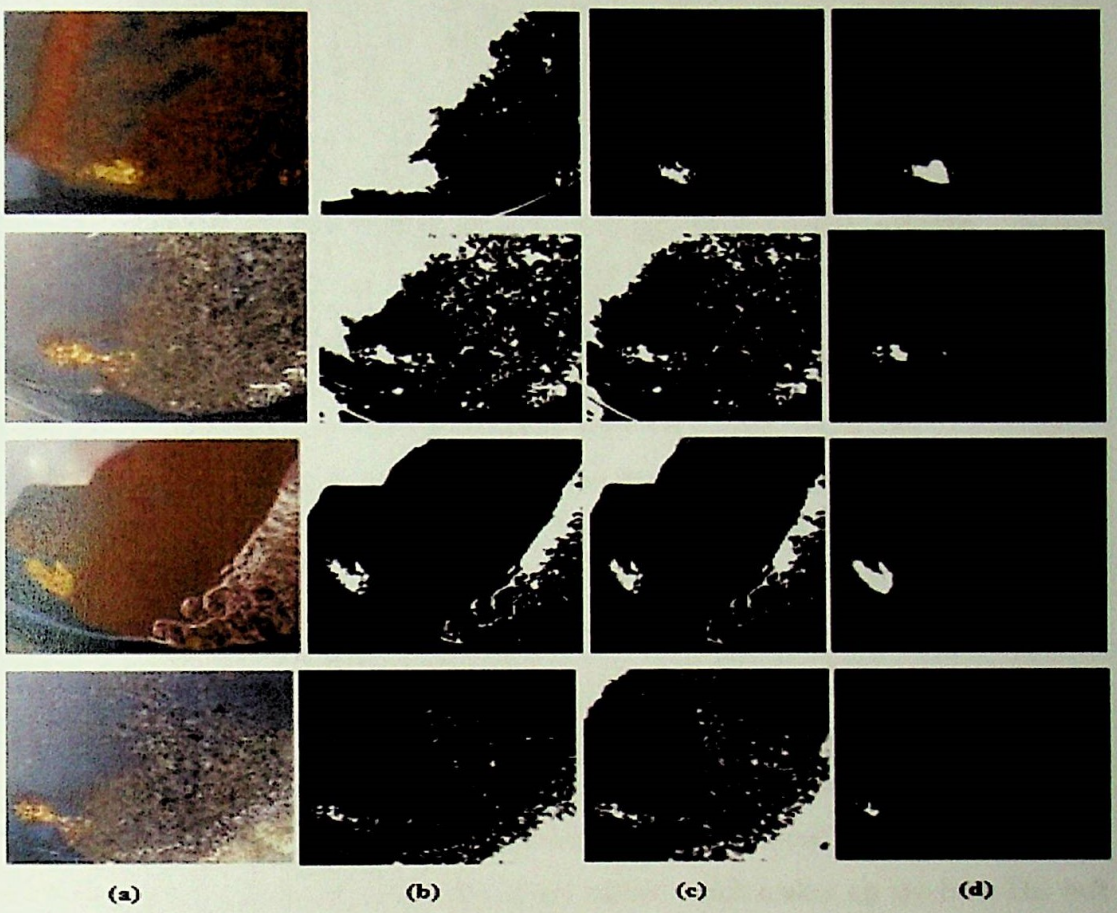


Figure 5. 1: Sample results of the segmentation process: (a) original image, (b) segmented mask for an algorithm I, (c) segmented mask for algorithm II, (d) segmented mask for algorithm III

From the segmented images, it was witnessed that algorithm 3 would detect gold better than the other two algorithms. So, through qualitative analysis of the segmented images, color-based thresholding in the CIELAB color space was proposed as the front-end technique for automated gold detection and localization in the automation of the gold panning process. Features were extracted from the segmented images from the color thresholding algorithm. These features were used for object localization and extracting other statistical information about the detected regions. Figure 5.2 below shows the images with regions that were detected and located as gold using the color thresholding algorithm. The objects detected are surrounded by a bounding box and their positions will be used to control the end-effector of the handling system.

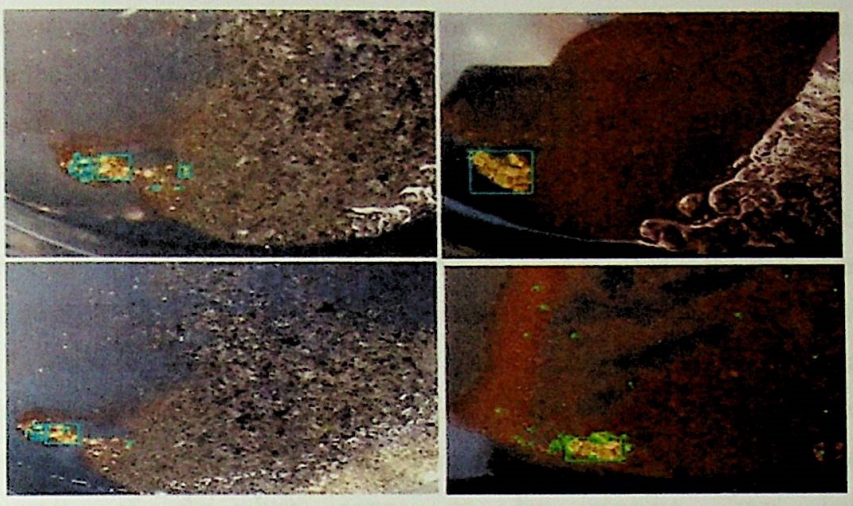


Figure 5. 2: Feature extraction and localization of detected gold particles

5.2 Gold- washer finite element analysis results and discussion

The results below show the color-graded distribution maps of the gold-washer stress analysis, strain analysis, deformation analysis, and contact analysis under the provided transient load. The color distribution map for the equivalent stress (Von mises). Figure 5.3 below shows a stable and uniform stress distribution. It is important to note the high stress and strain in the transmission belt. The stress and strain in the transmission belt are uneven as the belt is moving and high stress is experienced at the contact points between the tight side of the belt and the pulley. The maximum stress experienced in the belt is far less compared to the tensile strength of the nylon rubber which makes up the belt. The belt geometry and mechanical properties suited the proposed design and will be able to perform its function of driving the bigger pulley and the pan based on motor rotation.

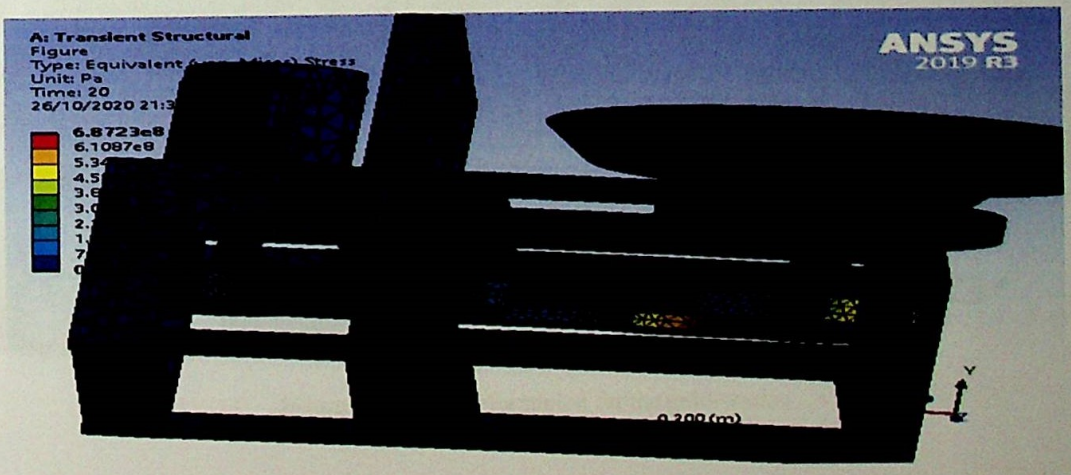


Figure 5. 3: Stress distribution of the gold-washer

The strain distribution in the assembly follows the same pattern as was depicted by the stress distribution as the materials respected the stress-strain relationship. Figure 5.4 below shows the

elastic strain analysis result. As expected, the areas of high stresses exhibited high strain and it was domiciled in the belt. The deformation results were also analyzed as shown in figure 5.5, the deformation pattern shows the flexible nature of the belt since it is flexible. The total deformation predicted in the belt is within the elongation percentage range of the nylon rubber used for the belt and shows that the belt will always engage the pulley groove and will not fall out. From the deformation results, it was noticed that high deformation is experienced at the slack side of the belt compared to the tight side which is dependent on the direction of rotation of the drive pulley. As can be seen on the graph in figure 5.6 and the map distribution in fig 5.5, the total deformation of the whole structure and other components is zero except for the belt. The deformation of the belt on the slack side is negative and greater than that on the tight side which is positive since the direction of the movement of the belt seems to be opposite from both sides.

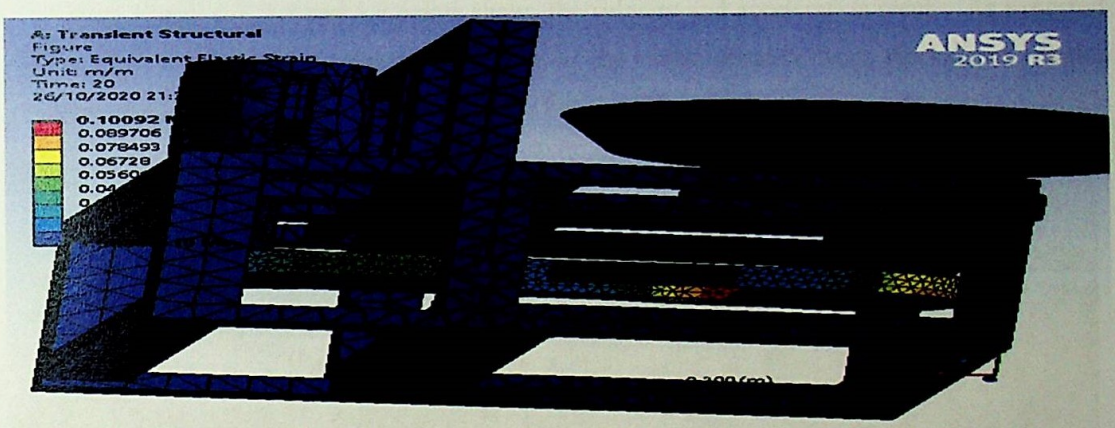


Figure 5. 4: Equivalent elastic strain of the gold-washer

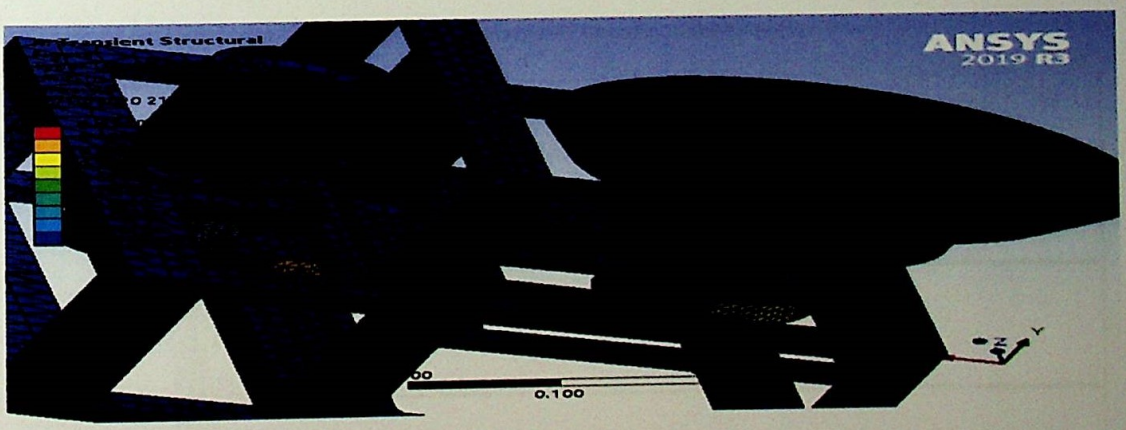


Figure 5. 5: Total deformation for the gold-washer

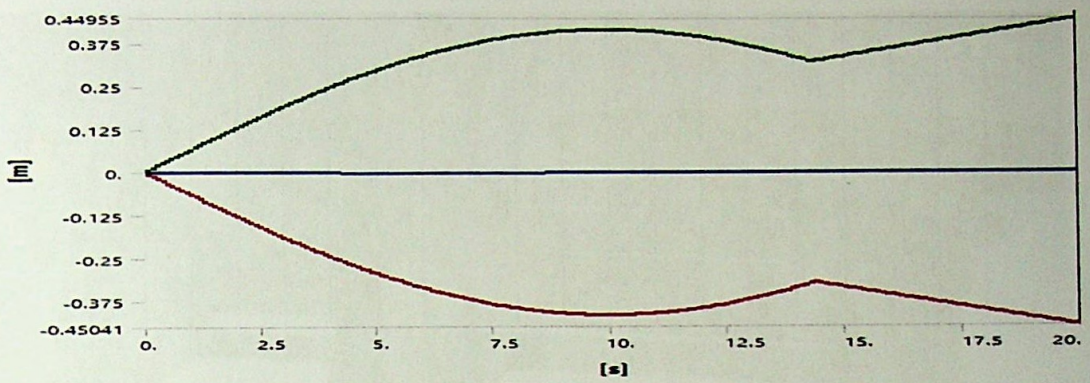


Figure 5. 6 : Maximum total deformation {green}, average total deformation [blue], minimum total deformation [red]

The dynamic behavior of the assembly under the provided load and boundary conditions were also evaluated. Figure 5.7, 5.8 and 5.9 below shows the velocity and acceleration results. As expected, the angular velocity and acceleration increase as the radial distance from the axis of rotation increases. It was noticed that the velocity of the belt is uniform.



Figure 5. 7: Total velocity of the components in motion

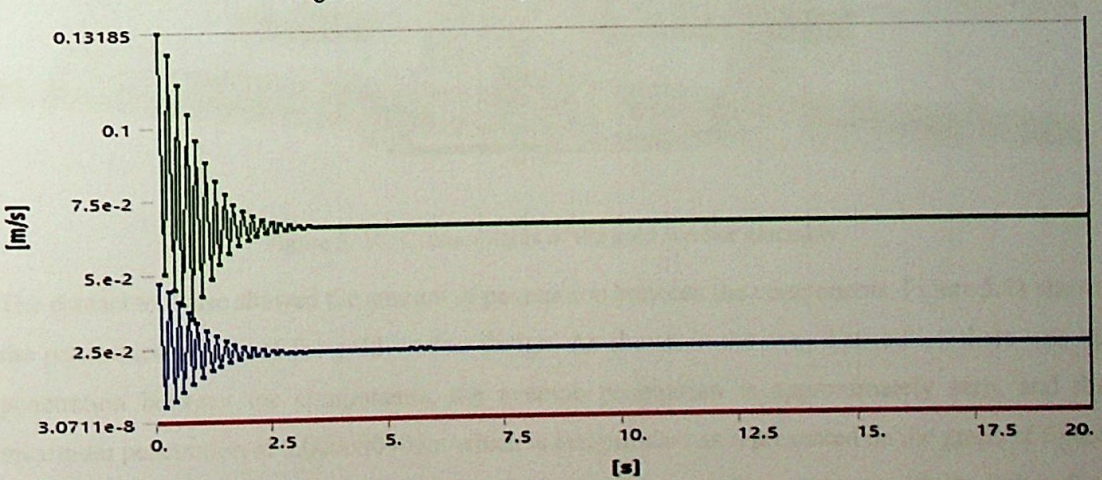


Figure 5. 8: Minimum total velocity(blue), Maximum total velocity (Green), and average total velocity (red)

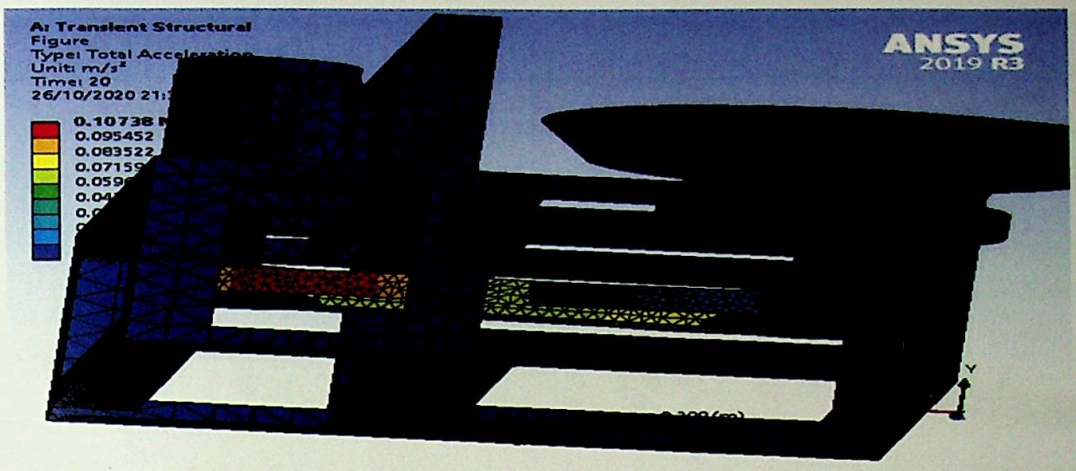


Figure 5. 9: Total acceleration results of the gold-washer

To investigate how the various moving components of the assembly were interacting with each other, the contact tool was used. The contact tool helped to evaluate the movement of the mating parts relative to each other. Fig 5.10 below shows the contact status of the assembly, as can be witnessed none of the parts were sticking together. Of note was the contact status between the belt and the pulley, the belt was not sticking which is important in the transmission of motion.

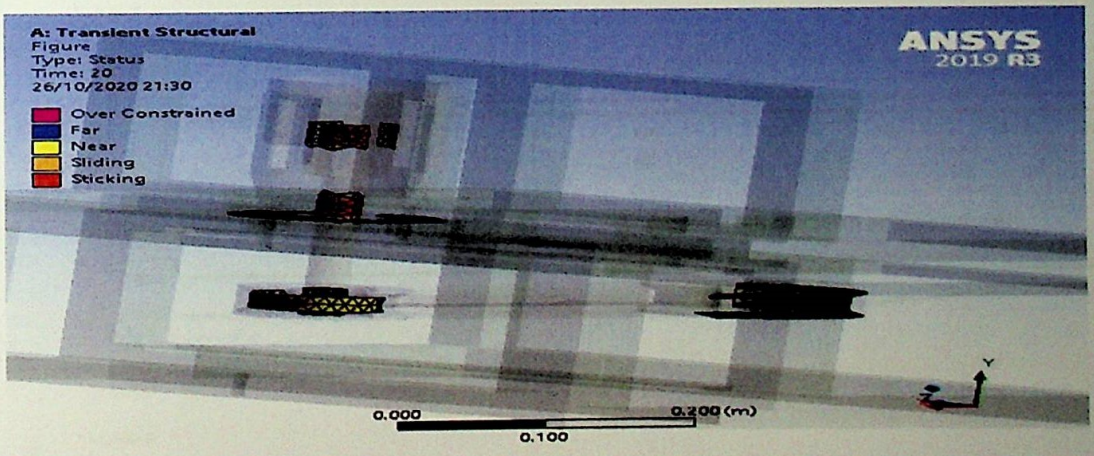


Figure 5. 10: Contact status of the gold-washer assembly

The contact tool also showed the amount of penetration between the components. Figure 5.11 shows the penetration details of the gold-washer design. As shown in the map distribution there was no penetration between the components, the average penetration is approximately zero, and the maximum penetration of 0.000080405m which is insignificant as represented on the graph of figure 5.12. Figure 5.13 present the results of the sliding distance mainly concerned with the belt-pulley connection. The slack side of the belt slides as it engages with the pullies while there is no sliding on the other side.

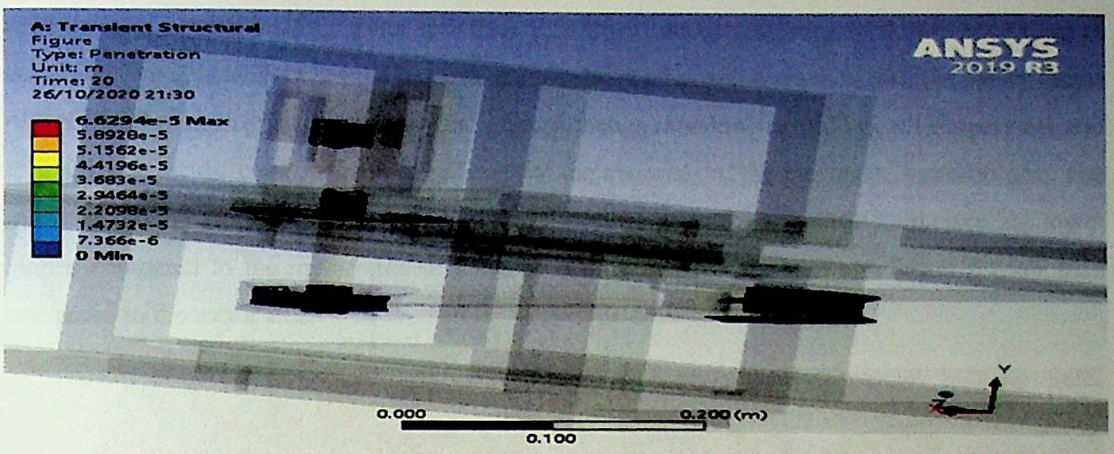


Figure 5. 11: Penetration information of the gold washer

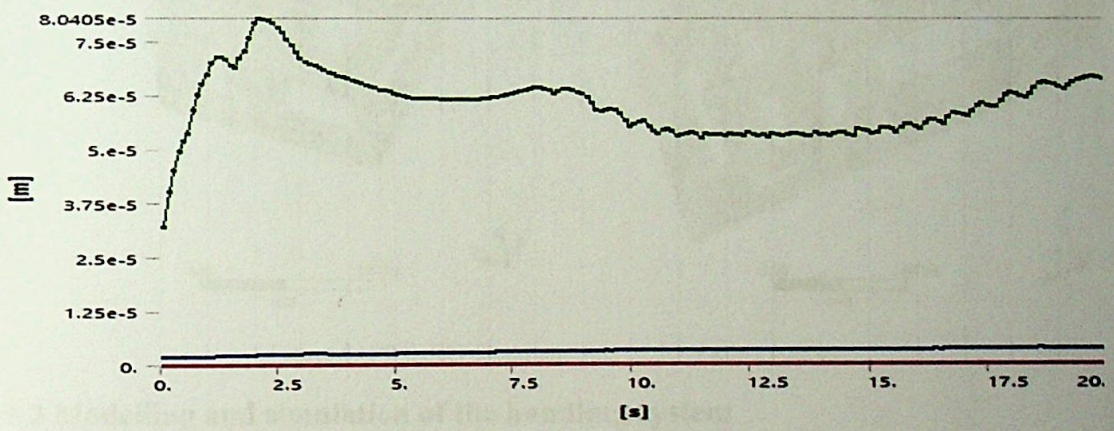


Figure 5. 12 : Maximum penetration{green}, average penetration [blue], minimum penetration[red]

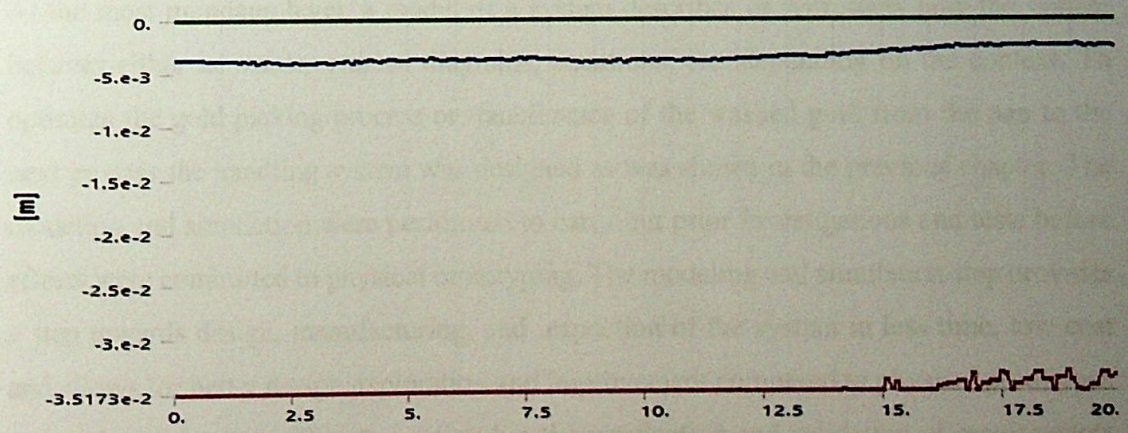


Figure 5. 13 : Maximum sliding distance {green}, average sliding distance [blue], minimum sliding distance[red]

Finally, the safety factor of the designed assembly was investigated as shown in figure 5.14 below. As can be seen, the majority of the assembly has a safety factor above one, meaning much of the assembly has stress in the permissible range which is safe for the operator. Only the belt has some

sections of it having a safety factor less than 1 and that means it's prone to failure according to analysis. The contact between the pan and the pan-holder has some patches with the safety factor of less than 1 meaning that contact may face abrupt change (breaking or sliding) when operating and this is due to the different stiffness co-efficient of the materials of the pan and the pan-holder. The map distribution of the safety factor shows that the half-side of the supporting structure has lower values compared to the motor side and this is mainly because the pan side bears greater load compared to the motor side.

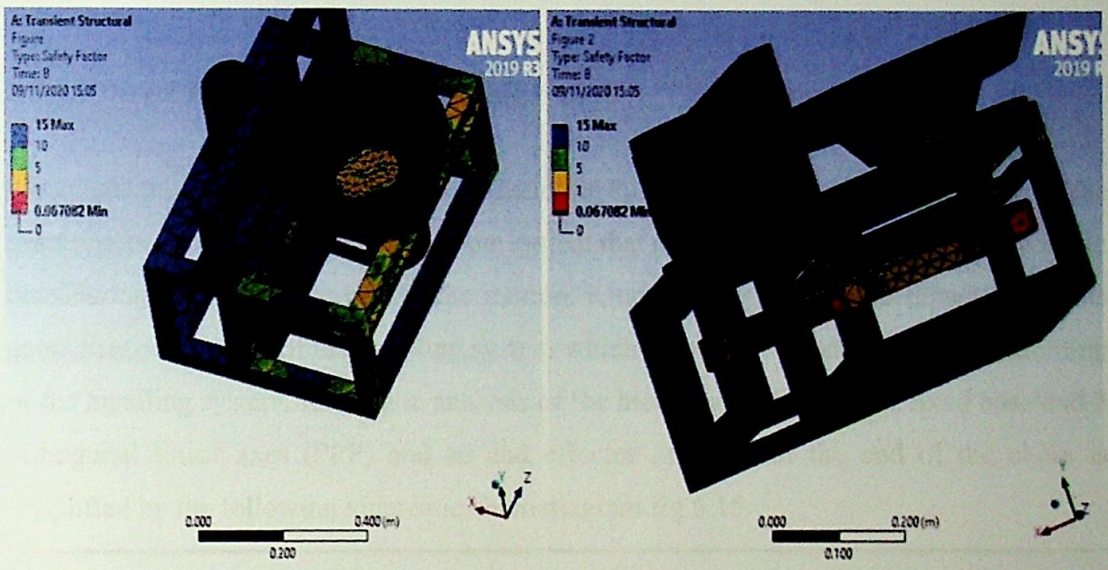


Figure 5. 14: Safety factor analysis of the washer concept

5.3 Modelling and simulation of the handling system

At the most mundane level, a model of a system describes or represents how the system behaves either in words, graphs, diagrams, equations, etc. depending on the context. To optimize the gold picking process or transference of the washed gold from the pan to the next process the handling system was designed as was shown in the previous chapter. The modeling and simulation were performed to carry out prior investigations and tests before efforts were committed to physical prototyping. The modeling and simulation step provides a step towards design, manufacturing, and inspection of the system in less time, low cost and allows for better design exploration and improvement compared to physical prototypes and real-world setups. This step assisted in the verification and validation of requirements and specifications through evaluation and prediction of the system behavior.

5.3.1 kinematic modeling and analysis of the handling system

The handling system was fashioned in the form of a gantry robotic manipulator in a 2X-Y-Z configuration. The handling system consists of 3 prismatic joints actuated by servo motors powering the leadscrew drive mechanism which activates axial motions. The chosen configuration had the advantage of a large workspace, better positioning accuracy, and lesser complexity concerning motion programming[175]. The handling system performs transverse motion across the horizontal plane (x-y – plane) and vertical motion in the z-direction based on the position and orientation of the detected gold particles.

5.3.1.1 Direct kinematics of the handling system

Kinematic modeling and analysis of the handling system sought to study the motion of the links apropos a fixed reference coordinate system that makes up the handling system without considering the forces that caused the motion. Kinematic modeling was done to give the geometric description of the handling system which helps in the control and programming of the handling system. Kinematic analysis of the handling system with a fixed base and 3 orthogonal linear axes (PPP) and an end effector mounted at the end of the chain is simplified by the following kinematic chain diagram fig 5.15.

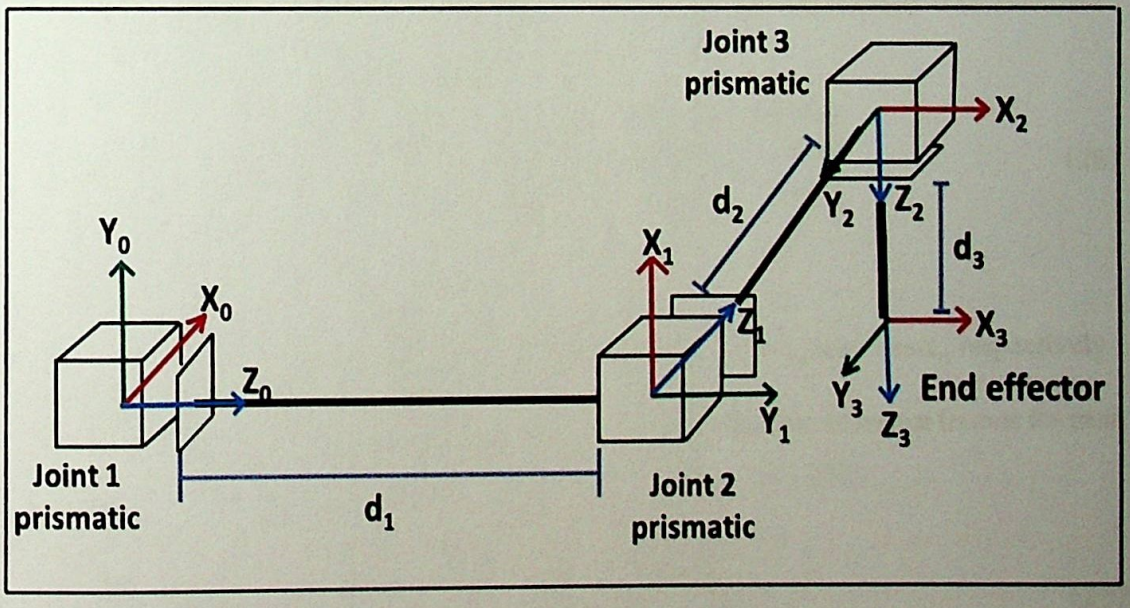


Figure 5. 15: kinematic chain for the handling system

The analytical relationship between the joint positions and the end-effector in the above kinematic chain and the frame assignment was established using the Denavit-Hartenberg (DH) convention. The table below shows the D-H parameters of the handling system, these four parameters are adequate in establishing the relationship between consecutive frames.

Table 5. 1:D-H parameters for the handling system

The frame (n)	a_n	α_n *(radians)*	d_n	Θ_n *(radians)*
1	0	$\pi/2$	d_1	$\pi/2$
2	0	$-\pi/2$	d_2	$\pi/2$
3	0	0	d_3	0

The above parameters are a representation of the relationship between the cartesian coordinate system and the joint coordinate system of the handling system which help in the formulation of the position and orientation of the end-effector regarding the base frame. The z-axes (joint axis) represent vectors that indicate link displacement of link (n) in relation to link (n-1). As shown in the table above the transformation of the end-effector frame relative to the base frame is described using four parameters: Θ_n, d_n, a_n, and α_n. The perpendicular distance along the x-direction between the joint axes of link (n) and link (n-1) denotes the link length (a_n). The link offset (d) describes the distance between two links (link lengths) along a joint axis (z-direction) while the joint angle (Θ_n) is the rotation from the link (n-1) to the link (n) following the right-hand screw rule about the common axes. α_n is the rotation about the x_n axis that matches the current and previous z-axis. From the established D-H parameters the homogeneous transformation matrix between the frames was calculated using the 4-parameter transformation matrix below:

$$ {}^{n-1}_{n}T = \begin{bmatrix} c\theta_n & -s\theta_n c\alpha_n & s\theta_n s\alpha_n & r_n c\theta_n \\ s\theta_n & c\theta_n c\alpha_n & -c\theta_n s\alpha_n & r_n s\theta_n \\ 0 & s\alpha_n & c\alpha_n & d_n \\ 0 & 0 & 0 & 1 \end{bmatrix} \quad (28) $$

$c\theta_n$,$s\theta_n$, $s\alpha_n$ *and* $c\alpha_n$ are shorthands for $cos\theta_n$, $sin\theta_n$, $sin\ \alpha_n$ *and* $cos\alpha_n$ respectively.

By substituting the DH parameters into equation 28, we obtain the reference frames for each link as follows. Accordingly, the transform for link 1 is given by (29):

$$ {}^{0}_{1}T = \begin{bmatrix} 0 & 0 & 1 & 0 \\ 1 & 0 & 0 & 0 \\ 0 & 1 & 0 & d_1 \\ 0 & 0 & 0 & 1 \end{bmatrix} \quad (29) $$

Link 2 is given by

$$ {}^{1}_{2}T = \begin{bmatrix} 0 & 0 & -1 & 0 \\ 1 & 0 & 0 & 0 \\ 0 & -1 & 0 & d_2 \\ 0 & 0 & 0 & 1 \end{bmatrix} \quad (30) $$

Link 3 is given by

$$ {}^{2}_{3}T = \begin{bmatrix} 1 & 0 & 0 & 0 \\ 0 & 1 & 0 & 0 \\ 0 & 0 & 1 & d_3 \\ 0 & 0 & 0 & 1 \end{bmatrix} \tag{31} $$

The overall handling system transformation matrix that relates the base frame to the end-effector frame is the matrix product of each homogeneous transformation matrix, that is

$$ {}^{0}_{N}T = {}^{0}_{1}T * {}^{1}_{2}T * {}^{2}_{3}T \ldots {}^{N-1}_{N}T \tag{32} $$

Therefore, the overall transformation matrix that describes the suction nozzle (end-effector) position relative to the handling system's base frame is:

$$ {}^{0}_{3}T = \begin{bmatrix} 0 & -1 & 0 & d_2 \\ 0 & 0 & -1 & -d_3 \\ 1 & 0 & 0 & d_1 \\ 0 & 0 & 0 & 1 \end{bmatrix} \tag{33} $$

From equation 33 it can be witnessed that since the handling system is void of revolute joints the rotational matrix does not contain rotational variables and only the variable link parameters for the prismatic joint are involved in the translation vector. This implies that the velocity of the end-effector relative to the base frame is defined by the variable link parameters as:

$$ V_3^0 = \dot{d}_2 i - \dot{d}_3 j + \dot{d}_1 k \tag{34} $$

End-effector acceleration is also a derivative of the end-effector velocity, with gravity effect (g) along the y_0-axis. The following equation represents the acceleration of the end-effector relative to the base frame:

$$ a_3^0 = \ddot{d}_2 i - (\ddot{d}_3 + g) j + \ddot{d}_1 k \tag{35} $$

The forward kinematics and the computed parameters were validated using the MATLAB robotics toolbox and the possible workspace was analyzed. The workspace encompassed the overall reachable space the end-effector tip could reach. The workspace provided by the handling system is a cuboid in nature with dimensions of 600*600*350 millimeters. Figure 5.16 shows some of the forward kinematics configurations of the handling system and its workspace.

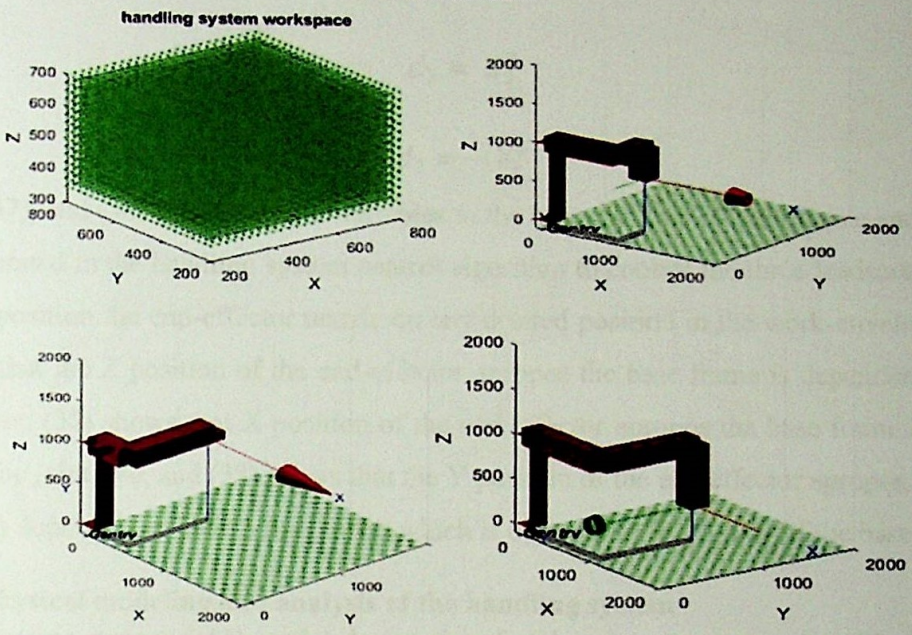


Figure 5. 16: top left is the workspace, top right is the handling system configuration for end-effector point (800 500 400), bottom left configuration for end-effector point (200, 1000, 100), and bottom right (1000, 1000, 700).

5.3.1.1 Inverse kinematics of the handling system

The handling system inverse kinematics solves for joint parameters given the required end-effector position (gold particle position in the washing platform). This computation is vital since the control of the handling system is based on the reception of the desired locations of the gold particles in the washing platform from the imaging system. In inverse kinematics, the joint variable determination is reduced to finding a set of coupled algebraic equations which are mainly nonlinear either using analytical or numerical methods. This formulation assists in the positioning and orientation of the end-effector during the transfer of gold particles from the washing platform to the next process.

For a manipulator with revolute joints, the problem of multiple solutions is prevalent but for the designed gantry the problem of multiple solutions is done away with by the prismatic joints. For the designed handling system, the analytic solution of inverse kinematics based on the kinematic diagram (fig 5.15) was carried out. In the positioning part of the inverse kinematics, the formulation of equations that relate the joint variables as inputs to the spatial location (x, y, z coordinates) of the end-effector was carried out. For the designed handling system, the inverse kinematics formulation determines the joint extension (d_1, d_2, d_3) that gets the end-effector to the location of the gold particles in the washing platform as a function of the end-effector frame relative to the base frame.

$$d_1 = Z_3^0 \tag{36}$$

$$d_2 = X_3^0 \tag{37}$$

$$d_3 = -Y_3^0 \tag{38}$$

(36), (37), and (38) relate the joint variables to the base and end-effector frame and will be incorporated in the handling system control algorithm to control the three leadscrew joints which position the end-effector nozzle on any desired position in the work-envelope. (36) shows that the Z position of the end-effector apropos the base frame is dependent on the first joint, (37) shows that X position of the end effector apropos the base frame is solely driven by joint two, and (38) shows that the Y position of the end effector apropos the base frame is depended on joint 3 movement which is opposite to the Y-axis of the base frame.

5.3.2 physical modeling and analysis of the handling system

The handling system CAD model designed in Solidworks was exported to SimScape (a MATLAB add-in package) as a physical modeling XML file. The SimScape physical network model which represented the mechanical system was used for simulation in MATLAB. This physical network of the mechanical system is a set of rigid bodies connected through joints and bound by kinematic constraints. SimScape provided the main simulation environment for the handling system as it provided forces, torques, or motion inputs to actuate the various rigid bodies and a means of including the control elements. The rigid bodies of the physical network provided the solid properties of the parts/assembly/sub-assemblies and all the geometry, inertia, and axial information that encode positional and orientational details of the model. All these physical properties were imported from the CAD/CAM environment (Solidworks).

The multibody system block diagram below (fig 5.17) shows the SimScape model of the handling system. The five rigid blocks representing the base, link 1, link 2, the end effector (link3), and end-effector nozzle. The rigid bodies are translated and rotated by the rigid transform block to their proper positions and orientations. The mechanism configuration defines the gravitational constant in the model and the inertial reference frame of the model is provided by the world frame. The solver configuration block provides the SimScape local solvers needed to compute complex mathematical relations needed in the simulation. The prismatic joints actuate the model by applying a force or torque to the associated links/rigid bodies.

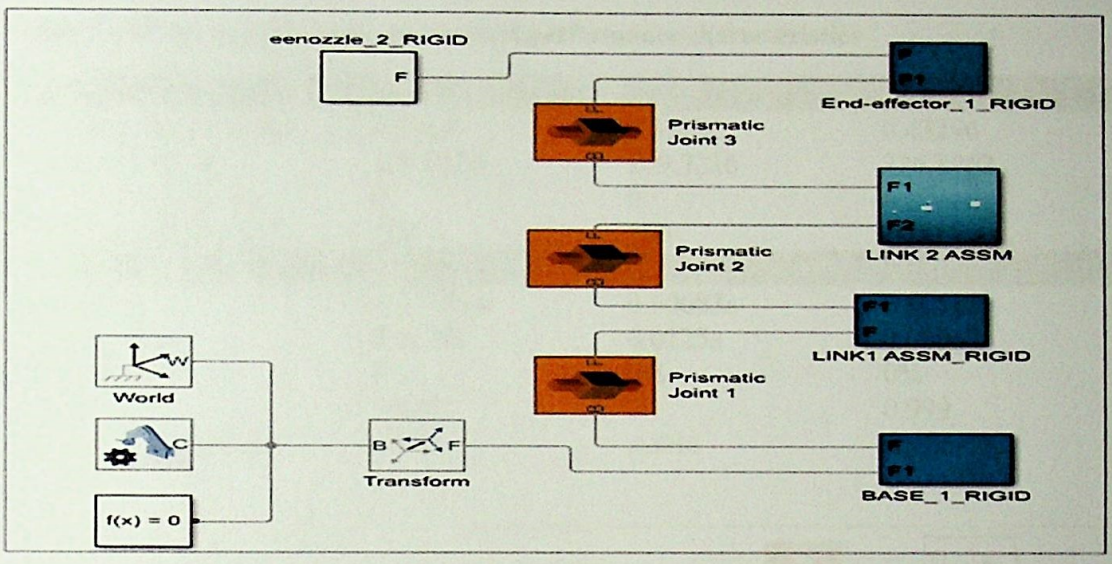


Figure 5. 17: SimScape multibody physical model of the handling system

5.3.2.1 Handling system controller design

The above physical model of the handling system manipulator exhibits unstable behavior without a controller. MATLAB Simulink was used to design the controller for each joint of the handling system manipulator. The joint controllers designed in Simulink were coupled with the SimScape multibody model. This was done to infer on controller effect on the displacements, velocity, acceleration, actuator force, and torques for the various key points of the mechanisms. Each joint was controlled by an individual PID controller, this configuration was chosen to reduce the deviation between the desired and actual motion for each joint. Fig 5.18. shows the physical model of the handling system with the control elements. The controllers were tuned automatically using the PID tuner in MATLAB and the desired performance characteristics were established. The gain values for the joints were different due to the difference in link geometries. The gain values for the joints were different due to the difference in each link's geometry, damping, and co-efficient of friction. Table 5.2 below presents the controller parameters and performance characteristics for each joint. Fig 5.19 shows the reference tracking of the block response and the tuned response of the joint controllers for joint 1 and joint 2.

Table 5. 2: Joint controller parameters and performance characteristics

Controller Parameter	*Joint 1 controller*	*Joint 2 controller*	*Joint 3 controller*
Proportional gain (k_p)	0.2114	0.32736	0.43296
Integral gain (k_i)	229.0326	259.3216	326.8962
Derivative gain (k_d)	0	0	0
Filter co-efficient (N)	100	100	100
Performance Characteristic			
Rise time	0.00735 s	0.00683s	0.00517s
Settling time	0.0128s	0.0125s	0.00947s
Overshoot	0%	0%	0%
Peak	0.999	1	0.999
Closed-loop stability	stable	stable	stable

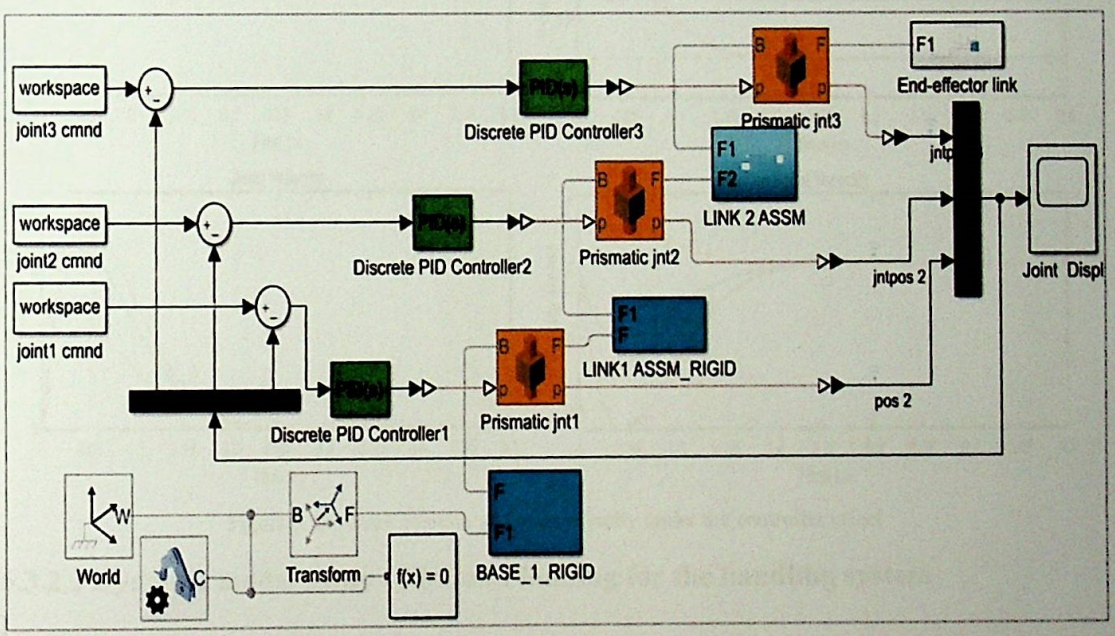


Figure 5. 18: SimScape multibody model of the handling system with joint controllers.

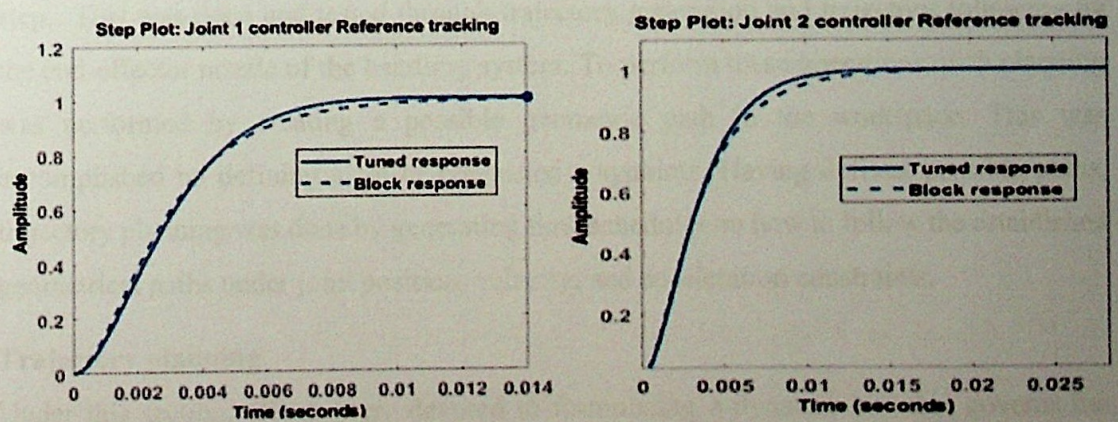


Figure 5. 19: Step plot for block response and tuned response for joint controllers

The graphs below (figure 5.20 a and b) show the controller effect on joint motion behavior in the simulation environment as the end-effector traverse from (a) home position (0, 0, 0) to (0.45, 0.55, 0.25) to (b) (0.25, 0.1, 0.35) and the corresponding joint link velocity. The dashed lines present the target position to be reached and the solid line presents the actual position in time. The difference in joint velocity profile is due to the difference in the displacements being traversed for the same duration.

(a) (b)

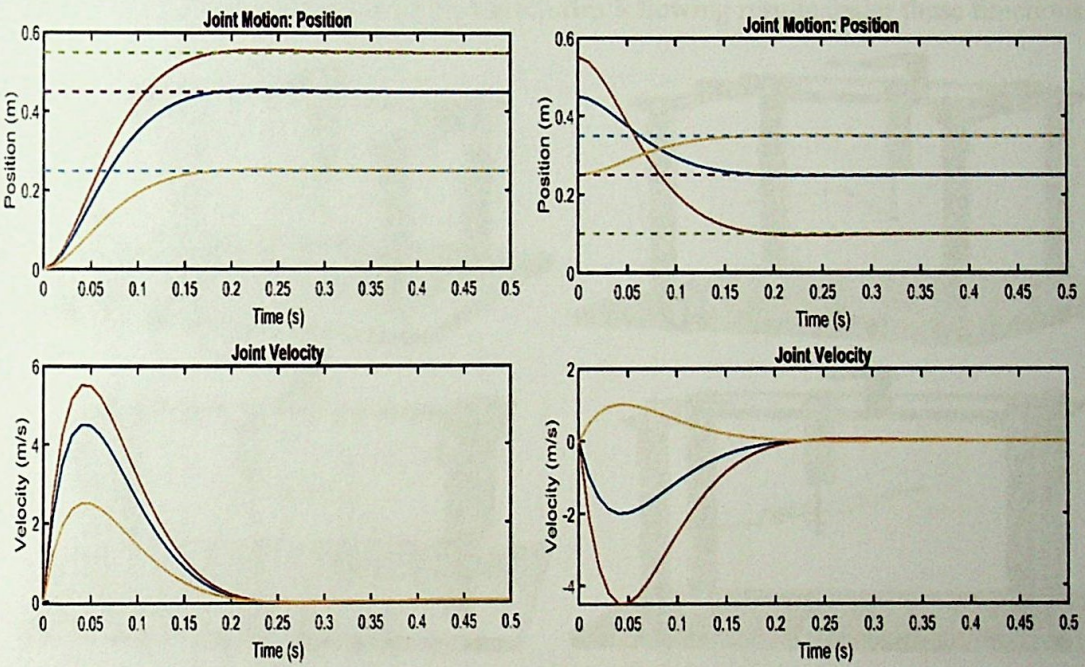


Figure 5. 20: Joint position and joint velocity under the controller effect

5.3.2.2 Dynamic model study - Motion Planning for the handling system

In the simulation of the dynamic model of the handling system, motion planning was a vital step. This was done and tested through trajectory generation and trajectory following by the end-effector nozzle of the handling system. To perform these operations, path planning was performed by creating a possible geometric path in the workspace. This was accomplished by defining a set of connected waypoints. Having defined possible paths, trajectory planning was done by generating time schedules on how to follow the established geometrical paths under joint position, velocity, and acceleration constraints.

Trajectory planning

Under this section, efforts were devoted to formulating a dynamic law that governs the motion of the handling system when its end-effector is moving along a geometric path under

given constraints. In the formulation, the geometric path to be followed, the kinematic and dynamic constraints of the handling system are the inputs, and the time sequence of the manipulator's joints/end-effector position, velocity, and acceleration are the outputs. The resulting trajectories (time sequences of position, velocity, and acceleration) of the joints or end-effector are based on the chosen interpolation functions that satisfy the provided constraints kinematically and dynamically. Trapezoidal and cubic interpolation functions were tested under the same constraints to choose the best function for the task at hand. Figure 5.21 below shows some of the trajectories following results under these functions.

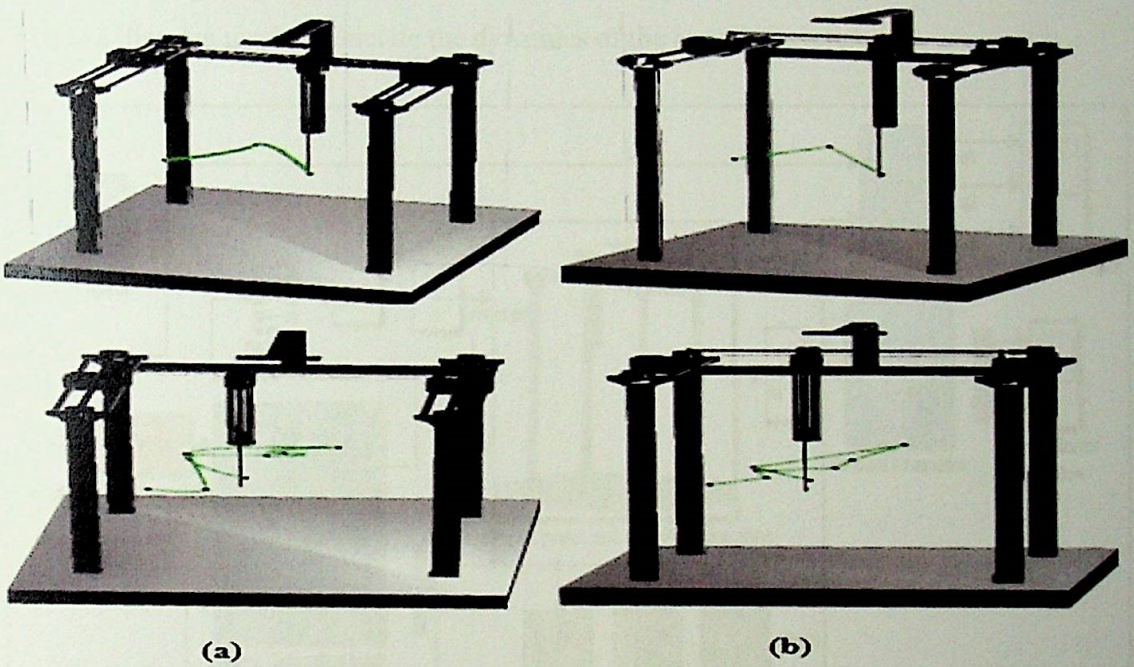


Figure 5. 21: simulation capture of the handling system executing (a) cubic trajectory (b) trapezoidal trajectory

The above figure 5.21 presents a capture of simulation results of the handling system when following a set of points, this was done to check the behavior of the model in trajectory following. Column (a) demonstrates trajectory following in following a 3 points geometric path and a 7 points geometric path using cubic polynomial interpolating function and (b) demonstrates trajectory following of the identical geometrical paths using trapezoidal function. The cubic polynomial interpolating function offers a non-zero velocity trajectory following as depicted by the curved trajectory while trapezoidal interpolating functions guarantees trajectories with zero velocities at the waypoints which might be an important characteristic in pick and place operations. The generated trajectories must satisfy the maximum torque requirements and must be void of mechanical resonances. This requirement was made to reduce the wear of the robot structure that is accompanied by

induced vibrations that damage the actuators. Stable trajectories are needed in performing accurate operations.

Execution of trajectory following was done in joint space. This was preferred to task space execution since joint space execution acts directly on the joints which allow smooth actuator motion. Joint space execution makes it easy to modify trajectories according to the design requirements and specifications and allows for the avoidance of kinematic singularities. The chosen gantry configuration helped in removing the non-linearities which usually arise when converting joint trajectories into end-effector trajectories. Figure 5.22 below shows the block diagram used to simulate the dynamics of the handling system.

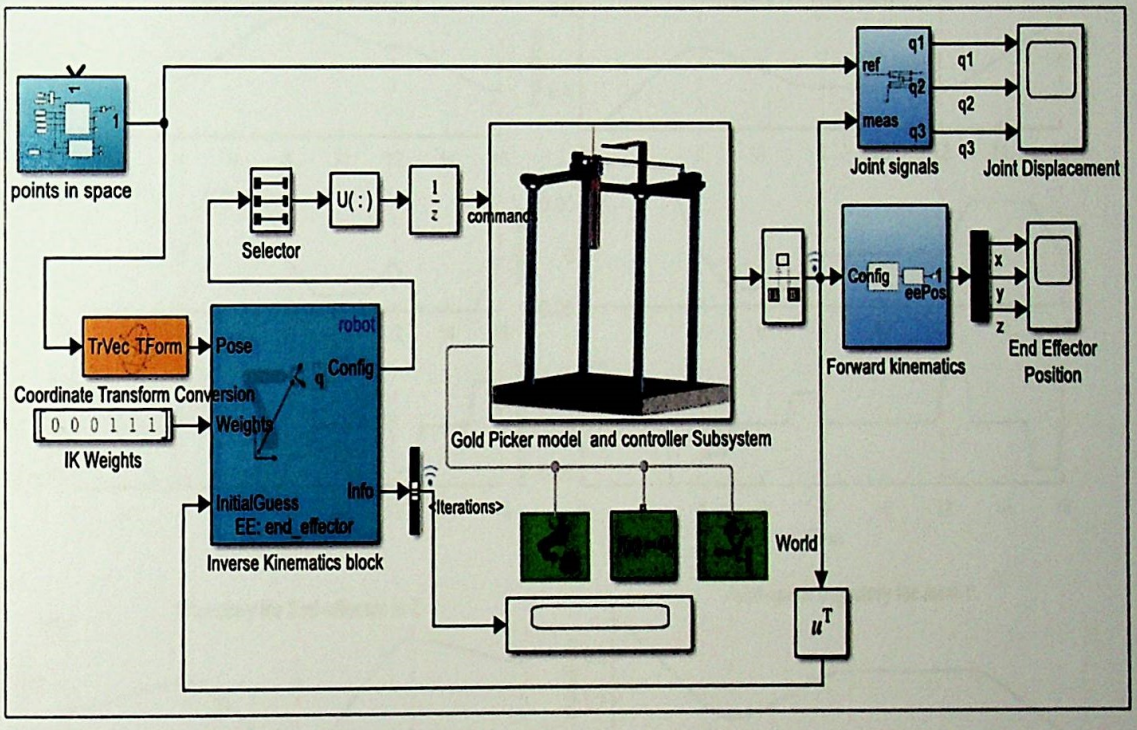
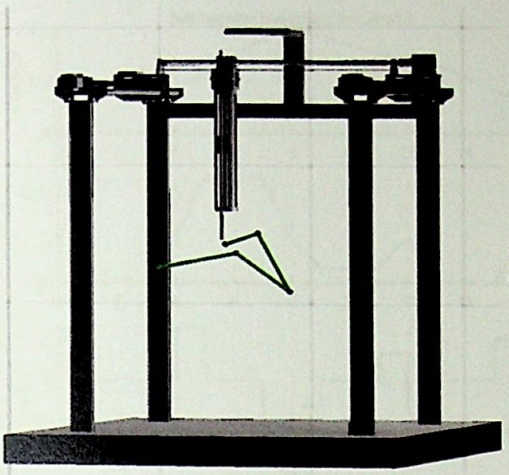
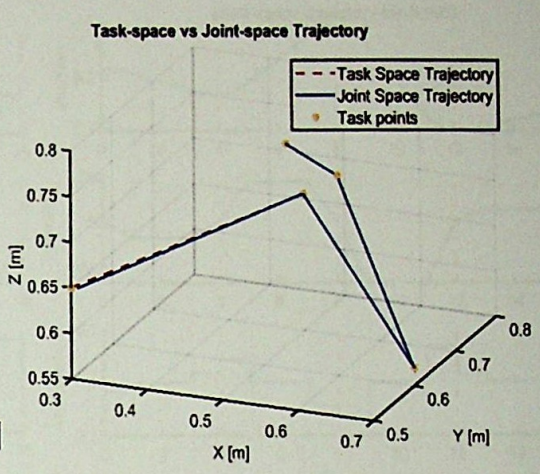
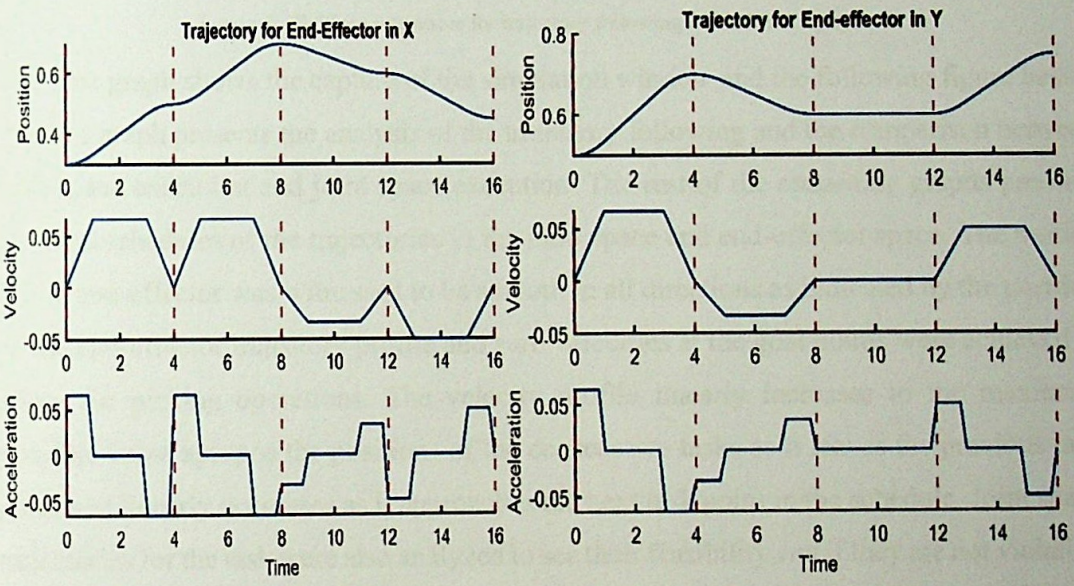


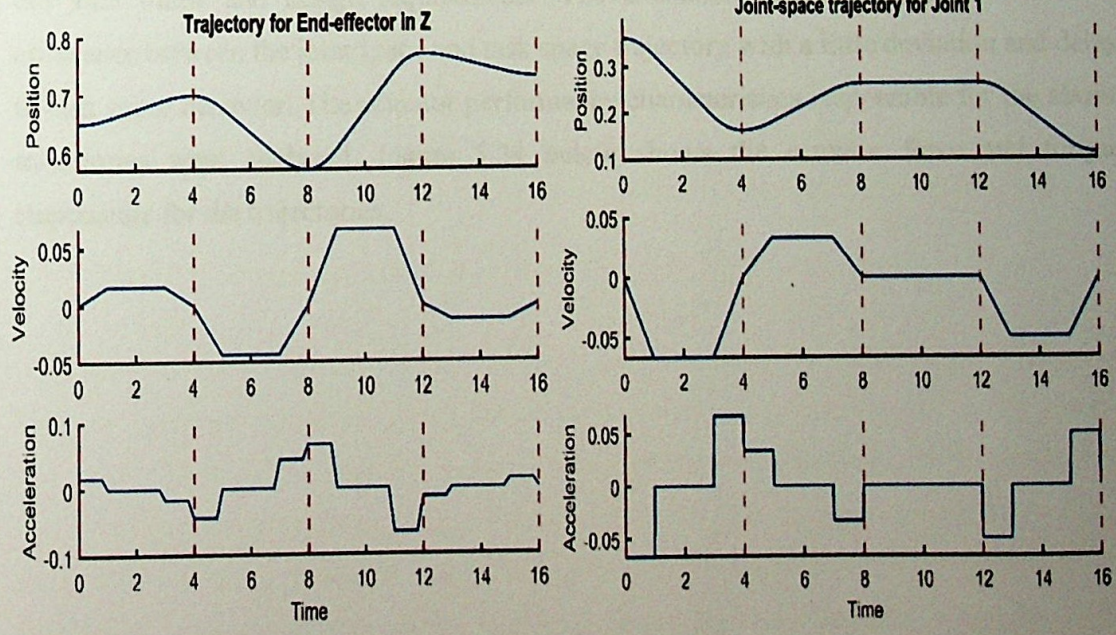
Figure 5. 22:Dynamic modeling and simulation of the handling system

As shown in figure 5.22 above the geometric path is established first and kinematic inversion of the path is performed to generate the handling system's joint configurations that are utilized by direct kinematics to position and orientate the end effector in the work-space. Figures 5.23 below present some of the resulting time schedules of the joint's and end-effector's position, velocity, and acceleration when following the given geometric path.




Task-space vs Joint-space Trajectory
Task Space Trajectory
Joint Space Trajectory
Task points
Z [m]
X [m]
Y [m]


Trajectory for End-Effector in X
Trajectory for End-effector in Y
Position
Velocity
Acceleration
Time


Trajectory for End-effector in Z
Joint-space trajectory for Joint 1
Position
Velocity
Acceleration
Time

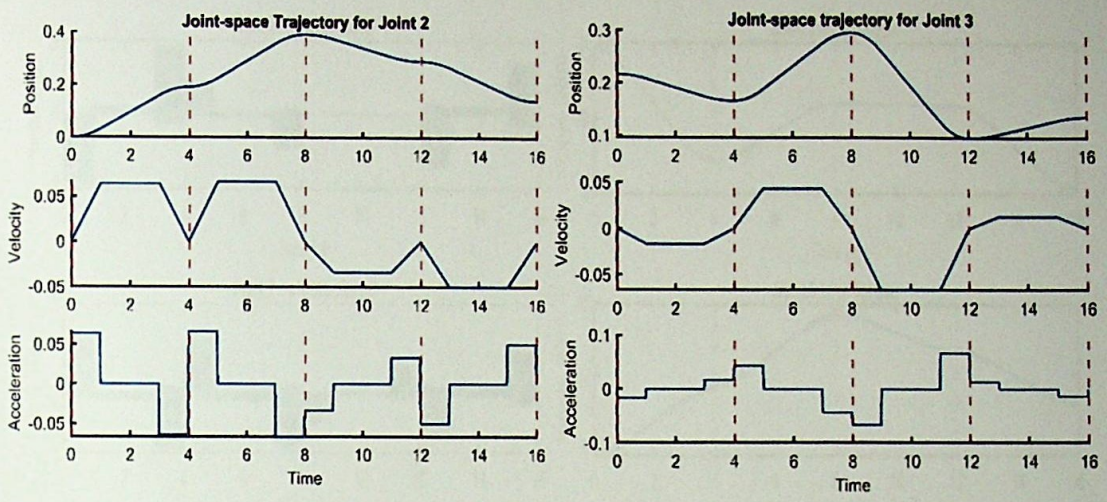


Figure 5. 23: Time sequences for trajectory following of the handling system

The first graph shows the capture of the simulation window and the following figure beside the first graph presents the analysis of the trajectory following and the comparison between task-space execution and joint space execution. The rest of the remaining graphs presents the time schedules of the trajectories in the joint space and end-effector space. The motion of the end-effector was witnessed to be smooth in all directions as indicated by the position of the end-effector trajectory profile and zero velocities at the goal points were achieved to allow for picking operations. The velocity profile linearly increases to the maximum possible value apropos the positions of the consecutive tasks as it leaves the previous task point and linearly decreases as it approaches the next task point in the schedule. Joint space trajectories for the task were also analyzed to see their feasibility and if they are not violating the joint limits and design requirements. The execution space comparison witnessed coherence between the joint space and task space trajectory with a little deviation and delay in task space behavior. The actuator performance characteristics responsible for the above trajectories were analyzed. Figure 5.24 below shows the actuator force and torque responsible for the trajectories.

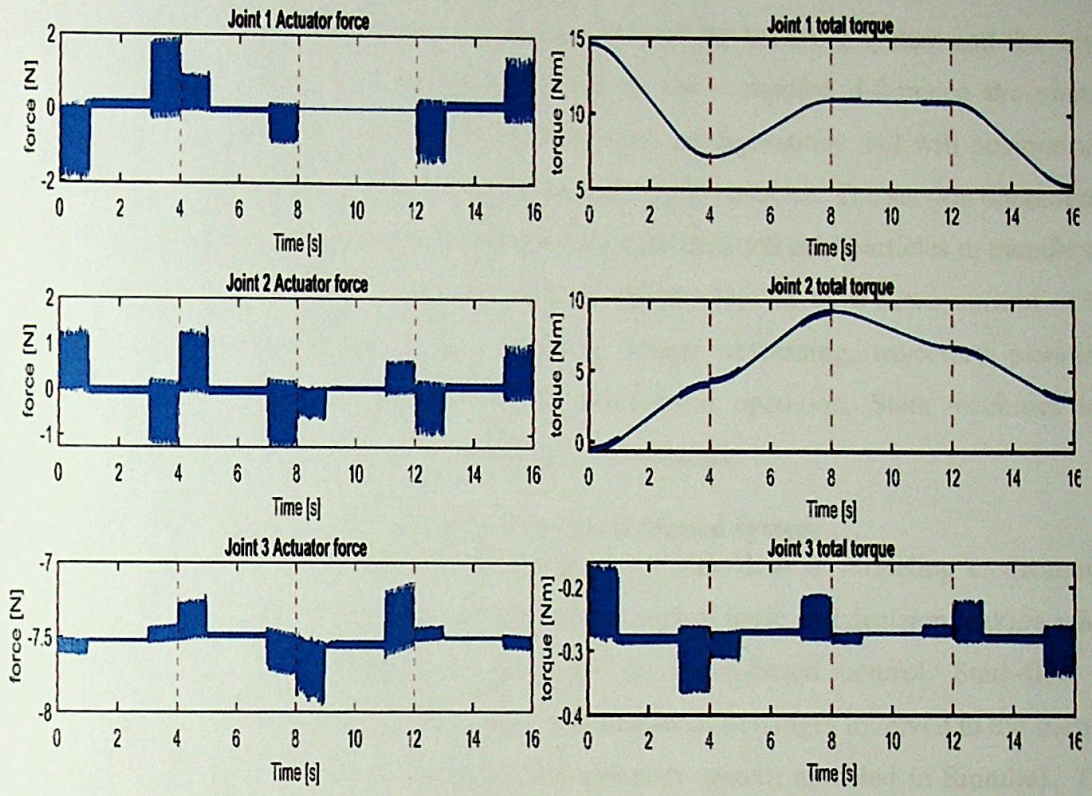


Figure 5. 24: Actuator force and Torque for trajectory following

From the joint torque and actuator force graphs, it can be noticed that effort is required to take the joint from the previous task to the next and a counter reluctance is witnessed as we approach the next task to stop the joint motion. Joint 1 experienced greater force followed by joint 2 and lastly joint 3, this is because joint 1 carries and supports the other 2 joints and their links, and joint 2 and carries the last joint and its links. The negative actuator force in joint 3 is to counter the gravitational force since their line of action is along the same axis. The same narrative goes for the joint torques. The smaller joint torques experienced by joint 3 are due to the smaller force and short strokes it performs compared to the XY joints.

5.4 Vision-based control of the handling system (Task planning)

Having established the kinematic model, physical model, and simulated trajectory following of the handling system over a geometric path, vision-based control simulations were initiated and tested on captured images. The captured images of the gold panning scenes were segmented to detect the gold particles using the gold detection framework developed in section 4.4.1. The detected blobs and their spatial information are decoded by the control program into the target pose of the end-effector of the handling system. The vision-based control algorithm

minimizes the difference between the current pose of the handling system and the target pose derived from the detected blobs. Based on the computed difference the control algorithm uses inverse kinematics to provide joints configurations that will position and orientate the end-effector nozzle above the detected gold particles. The suction operation is activated when the end effector nozzle hovers over the detected gold particles to transfer the gold particles from the pan to the next stage in the process. To have better control of the tasks and operations involved in combining image processing, trajectory planning, trajectory following, kinematic inversion, and suction operation, State machines and flowcharts were used for decision making and control logic.

5.4.1 Decision making and control logic of the designed system

State machines and flowcharts were developed in State-flow ® modeling environment together with Simulink to model and simulate the control logic and decision making when interfacing the various components involved in vision-based control. State-flow ® environment made it possible to interface the instantaneous changes involved in the suction operation and the continuous changes in the dynamic system modeled in Simulink. The handling system's kinematics and dynamics were modeled in Simulink and SimScape as presented in the previous section but the various operations involved in task manipulation were accomplished in State-flow.

Various modes of operation of the system such as manipulator motion, gold detection, suction operation, etc. were handled and modeled by state machines of the State-flow. The conditions and combinatorial behavior of the system such as transitioning from one operation to the other or which modes to combine were handled and managed by the flowcharts. Figure 5.25 below shows the state-flow chart that was developed to interface the gold detection framework which was written as a MATLAB function and the rigid body tree of the handling system to maneuver the end-effector through the workspace and perform the suction operation.

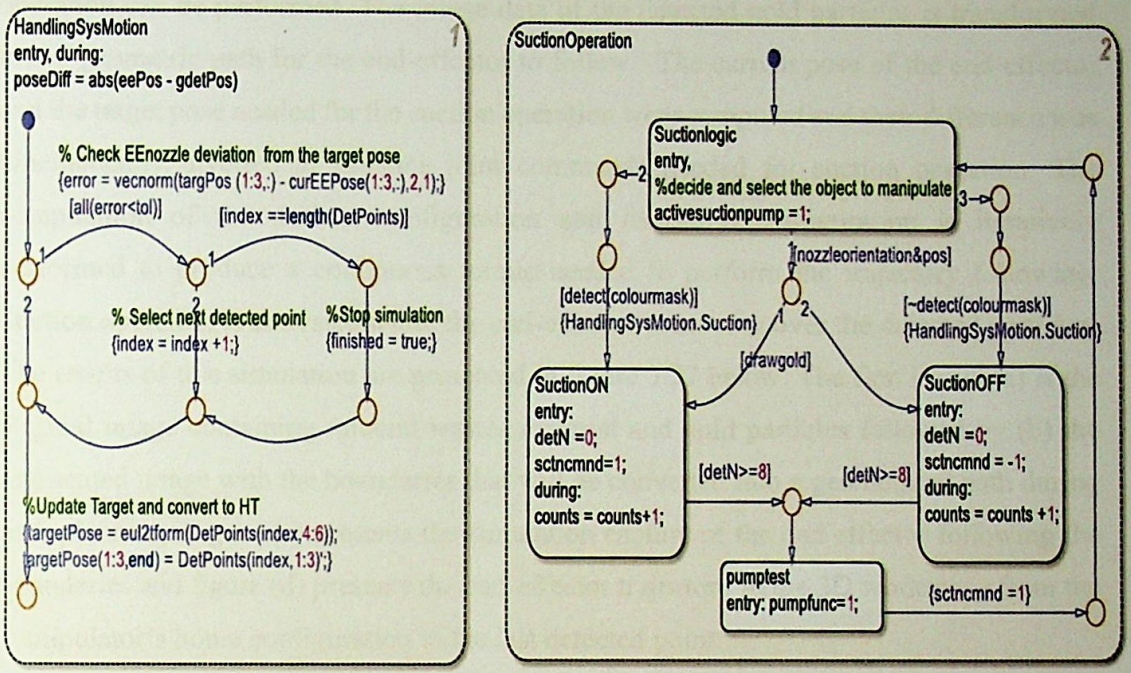


Figure 5. 25: Part of the Stateflow chart for the handling system's control.

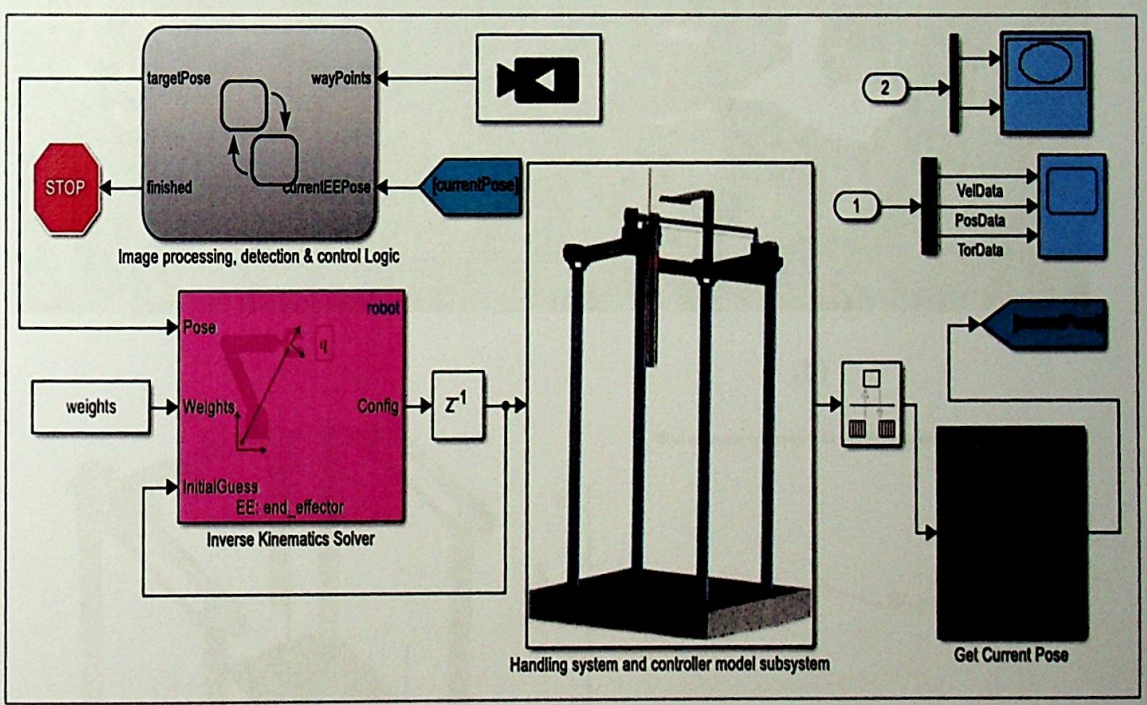


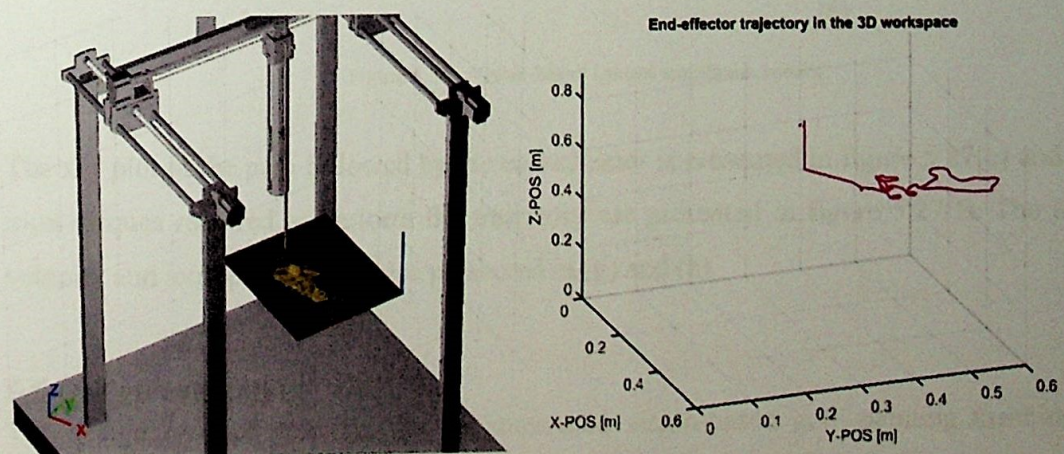
Figure 5. 26: Vision-based control block diagram

Figure 5.26 shows the block diagram with the added elements which was used to model and simulate vision-based control operation. The above state-flow chart is cascaded in the image processing, detection, and control logic block. The visual information from image data was used to generate the pose and orientation of the end-effector nozzle so that the picking

operation can be performed. The image data of the detected gold particles is transformed into a geometric path for the end-effector to follow. The current pose of the end-effector and the target pose needed for the suction operation were computed and their difference was kinematically inverted to produce joint commands needed for suction operation. The computation of the desired configuration and measured configuration is iteratively performed to produce a continuous torque needed to perform the trajectory following. Suction operation is activated while the end-effector is moving over the detected particles. The results of this simulation are presented in figure 5.27 below. The first image (a) is the original image containing mineral wastes material and gold particles followed by (b) the segmented image with the boundaries that will be converted into a geometrical path during path planning. Figure (c) presents the simulation capture of the end effector following the boundaries and figure (d) presents the end-effector trajectory in the 3D workspace from the manipulator's home configuration to the last detected point.



(a) (b)



(c) (d)

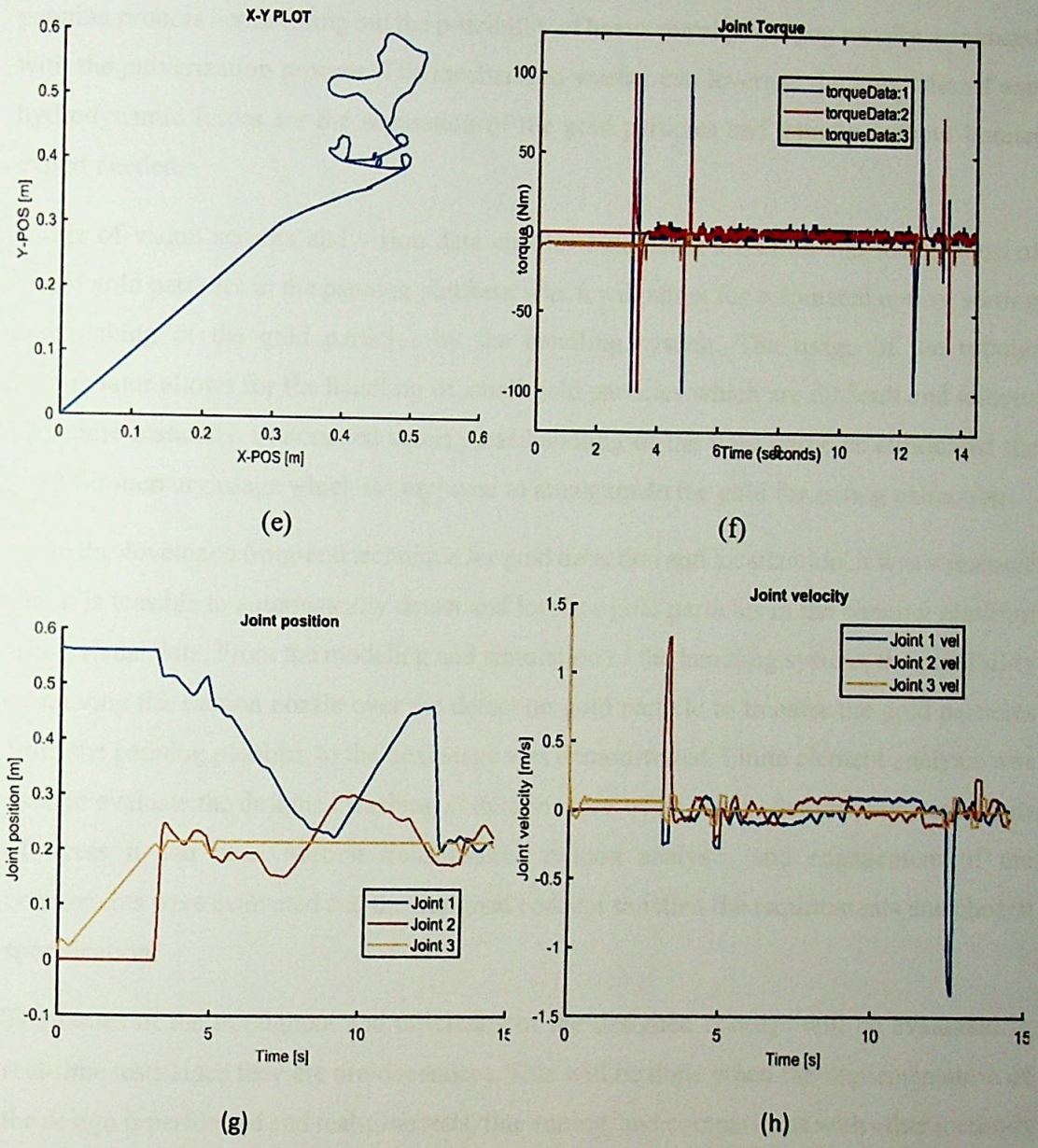


Figure 5. 27: Vision-based control simulation results

The x-y plot of the path followed by the end-effector is presented in figure 5.27(e) and the joint torques required to perform the trajectory are presented in figure 5.27(f). The joint velocity and joint position are also presented in (g) and (h).

5.5 Design evaluation

The design concept presented for an automated vision-based gold panning machine if implemented can mitigate the mercury pollution and mercury poisoning problem while increasing the effectiveness of the gold panning procedure. The mechanized gold washing system will ensure that no human effort will be needed to carry out the repetitive gold

panning process hence ruling out the possibility of heavy metal poisoning usually associated with the pulverization process. The mechanized washer can leverage the gravitational and hydrodynamic forces for the separation of the gold particles and gangue without human expert needed.

Usage of vision sensors and vision data enables automated detection and localization of visual gold particles in the panning platform which will allow for automated optical sorting and picking of the gold particles by the handling system. The usage of the robotic manipulator allows for the handling of small gold particles which are difficult and tedious to handle manually. Automated sorting and handling of the gold particles eliminated the need for mercury usage which is employed to amalgamate the gold for easing extraction.

From the developed front-end technique for gold detection and localization, it was witnessed that it is feasible to automatically detect and localize gold particles in the panning platform using visual data. From the modeling and simulation of the handling system, the possibility of moving the suction nozzle over the detection gold particle to transfer the gold particles from the panning platform to the next stage was demonstrated. Finite element analysis was used to evaluate the designed washing system in terms of its safety, deformation, and limits of stress it can bear. Motion transmission, motion analysis, and engagement of the components were evaluated and the designed concept satisfied the requirements and chosen specification.

The issues of the throughput and efficiency of the designed concept will be evaluated in real-time tests since they are ore-dependent. This will be done when the implementation of the design is performed and real-time tests, fine-tuning, and comparisons with other methods will be performed.

5.6 Conclusion

The results, analysis, and evaluation of the various subsystems of the design were presented in the chapter. Binary masks and bounding boxes were used to present the results of the gold detection and localization. 2D and 3D computer-aided drawings were used to present the results of the design work. Color distribution maps were used to show the stresses, deformations, contact status, and safety factor analysis for the finite element procedure. Trajectory schedules, workspace analysis graphs, force, and torque curves, and model block diagrams were used to present the modeling and results of the handling system's simulation.

CHAPTER 6
CONCLUSION

6.0 Overview

This chapter outlines the summary of the design of a vision-based automatic gold panning system by concluding the work that was accomplished and presenting recommendations on this area of study. Comments and remarks on objectives and design requirements are also detailed in this chapter. Future works on the presented work are also outlined in this chapter.

6.1 Conclusion

From the activities done in methodology, the automated gold panning system was designed successfully using the mechatronic design approach (VDI 2206). The system was designed and validated in a modular way to ensure the functionality of the involved subsystems. The color thresholding technique in the CIELAB color space was used for image segmentation as a front-end technique for gold detection. Gold detection and localization were performed successfully through image segmentation and extraction of the spatial information of the detected gold blobs. Finite element analysis of the designed washer concept was performed to analyze the behavior of the designed concept under loading. Simulation and modeling were done to validate the functionality of the designed system. The results of the modeling and simulation of the handling sub-system from the mechanical design view, controller design, trajectory planning, trajectory following, and vision-based control showed that the designed handling system is achievable, efficient, and feasible in terms of speed, dexterity, manipulation, and control.

6.2 Future work

Future work will focus on the implementation of the designed system on real hardware and performing real-time tests. Machine learning techniques will be considered for the gold detection front-end technique. Cascaded control for the joints will be considered instead of the individual joint control which was done in this system since each joint activity affect the other. Further improvement on the overall algorithm for task planning can address product functionality that is typically solved at the assembly level rather than component level. For future work, the granular separation process will be modeled and simulated using the discrete element method and computational fluid dynamics (DEM-CFD) coupling to visualize particle behavior under the operation of the mechanized washer system.

BOTSWANA INTERNATIONAL UNIVERSITY OF SCIENCE & TECHNOLOGY

Publications

1. B. C. Makoni, M. Namoshe and O. Matsebe, "A front-end technique for visual gold detection and localization – Towards automation of the gold panning process.," 2021 Southern African Universities Power Engineering Conference/Robotics and Mechatronics/Pattern Recognition Association of South Africa (SAUPEC/RobMech/PRASA), 2021, pp. 1-6, doi:10.1109/SAUPEC/RobMech/PRASA52254.2021.9377246.

References

[1] L. I. Y. Director-general, U. UNDP, A. Maarten, S. World, and T. Organisation, "and Value Chains and Industrialisation," vol. 3, no. 5, 2014.

[2] H. F. and P. M. Hentschel Thomas, *Artisanal and Small-Scale Mining - Challenges and Opportunities*, no. January. 2003.

[3] G. Hilson, *Artisanal and small-scale mining and agriculture Exploring their links in rural sub-Saharan Africa*, no. March. 2016.

[4] M. and S. D. (IGF) Intergovernmental Forum on Mining, Minerals, "GLOBAL TRENDS IN ARTISANAL AND SMALL-SCALE MINING (ASM): A REVIEW OF KEY NUMBERS AND ISSUES Secretariat hosted by Secretariat funded by," 2018.

[5] M. M. Hassan, A. A. Nuhu, M. S. Sallau, H. M. Majiya, and A. K. Mohammed, "Zamfara lead poisoning saga: Comparison of lead contamination level of water samples and lead poisoning in Bagega Artisanal gold mining district, Nigeria," *J. Chem. Pharm. Res.*, vol. 7, no. 3, pp. 7–12, 2015.

[6] S. J. Mallo, "Mitigating the Activities of Artisanal and Small-Scale Miners in Africa : Challenges for Engineering and Technological Institutions," *Int. J. Mod. Eng. Res. (IJMER*, vol. 2, no. 6, pp. 4714–4725, 2012.

[7] Y. Liu, B. Wan, and D. Xue, "Sample Digestion and Combined Preconcentration Methods for the Determination of Ultra-Low Gold," 2019.

[8] A. Falconer, "GRAVITY SEPARATION : OLD TECHNIQUE / NEW METHODS," vol. 12, no. 1, pp. 31–48, 2003.

[9] R. Vieira, "Mercury-free gold mining technologies: Possibilities for adoption in the Guianas," *J. Clean. Prod.*, vol. 14, no. 3–4, pp. 448–454, 2006.

[10] N. J. Grigg and G. J. Delemontex, "The Pre-Concentration Of Precious And Base Metal Deposits Using The Inline Pressure Jig (IPJ); Higher Feed Grades And More Metal .," no. xxxxx, pp. 1–14.

[11] S. Lücke, "Comparison of Different Gold Recovery Methods with Regard to Pollution Control and Efficiency," vol. 35, no. 1, pp. 52–61, 2007.

[12] I. J. Corrans, P. Eng, and P. D. M. Se, "Wet high-intensity magnetic separation for the concentration of Witwatersrand gold - uranium ores and residues," no. March 1979.

[13] M. Modino, C. López, A. Argüelles, T. Rivas, and J. Taboada, "Recovery of dense minerals as derivative in the exploitation of the alluvial terraces of the miño river," *Dyna*, vol. 77, no. 161, pp. 71–76, 2010.

[14] K. S. Lindley and N. A. Rowson, "Feed preparation factors affecting the efficiency of electrostatic separation," *Magn. Electr. Sep.*, vol. 8, no. 3, pp. 161–173, 1997.

[15] M. O. Bustamante-Rúa, D. M. Naranjo-Gómez, A. J. Daza-Aragón, P. Bustamante-Baena, and J. D. Osorio-Botero, "Flash flotation of free coarse gold using dithiophosphate and dithiocarbamate as a replacement for traditional amalgamation," *DYNA*, vol. 85, no. 205, pp. 163–170, 2018.

[16] T. M. Diane Hayward Grath, "Western Australian School of Mines Department of Metallurgical and Minerals Engineering Flash Flotation and Gravity Recovery," no. November 2014.

[17] M. Veiga *et al.*, "Manual for Training Artisanal and Small-scale Gold Miners," *Man. Train. Artis. Small-scale Gold Miners*, p. 144, 2006.

[18] I. Grewal, M. Lundt, D. Wong, and W. Tse, "Recent Developments in Preconcentration Using Dense Media Separation," *COM 2014 - Conf. Metall. Proc.*, 2014.

[19] K. Telmer, D. Stapper, UNEP, UNIDO, and IUGS-GEM, "A UNEP Global Mercury Partnership document produced in conjunction with the Artisanal Gold Council and with assistance from Commission on Geoscience for Environmental Management," *Iugs-Gem*, 2012.

[20] S. S G S Minerals, "Flowsheet Development for Gold Orebodies," 2014.

[21] W. Stange, "The process design of gold leaching and carbon-in-pulp circuits," *J. South African Inst. Min. Metall.*, vol. 99, no. 1, pp. 13–25, 1999.

[22] I. De Michelis, A. Olivieri, S. Ubaldini, F. Ferella, F. Beolchini, and F. Vegliò, "Roasting and chlorine leaching of gold-bearing refractory concentrate: Experimental and process analysis," *Int. J. Min. Sci. Technol.*, vol. 23, no. 5, pp. 709–715, 2013.

[23] R. Pieters, *Direct Methods for Vision-Based Robot Control. Application and Implementation*. 2013.

[24] S. Hutchinson, G. D. Hager, and P. I. Corke, "A Tutorial on Visual Servo Control," vol. 12, no. 5, 1996.

[25] C. Cai, "6D Visual Servoing for Industrial Manipulators applied to Human-Robot Interaction Scenarios," 2017.

[26] T. T. Wang, X. Han, J. Zhou, and H. Chen, "Path planning for visual servoing with search algorithm," *Adv. Mech. Eng.*, vol. 10, no. 1, pp. 1–11, 2018.

[27] Y. Zhang, "Vision servo of industrial robot: A review," vol. 040125, p. 040125, 2018.

[28] E. Di Stefano, E. Ruffaldi, and C. A. Avizzano, "A multi-camera framework for visual servoing of a collaborative robot in industrial environments," *IEEE Int. Conf. Emerg. Technol. Fact. Autom. ETFA*, pp. 1–8, 2018.

[29] L. Zhang, X. Gao, C. Zhao, and X. Dong, "Research on the technology of extracting 3D face feature points on basis of binocular vision," *Proc. 2009 2nd Int. Congr. Image Signal Process. CISP'09*, no. 1, pp. 3–6, 2009.

[30] H. Li, M. Jin, and L. Zou, "A new binocular stereo visual servoing model," *Proc. - 2008 Pacific-Asia Work. Comput. Intell. Ind. Appl. PACIIA 2008*, vol. 1, pp. 461–465, 2008.

[31] J. Hsiao, C. Hsu, T. Shih, P. Hsu, S. Yeh, and B. Wang, "The Real-time Video Stabilization for the Rescue Robot," *Iccas-Sice*, pp. 4364–4369, 2009.

[32] A. M. B. Aly and M. Sciences, "Implementation of Vision-Based Trajectory Control for Autonomous Vehicles," no. April 2017, 2018.

[33] E. Saldaña and R. Quevedo, "Review : computer vision applied to the inspection and quality control of fruits and vegetables Revisão : visão computacional aplicada à inspeção e ao controle da qualidade de frutas e verduras," *Brazilian J. food Technol.*, vol. 16, no. 4, pp. 254–272, 2013.

[34] P. Vithu, M. Tech, J. A. Moses, M. Tech, and D. Ph, "Trends in Food Science & Technology Machine vision system for food grain quality evaluation : A review," *Trends Food Sci. Technol.*, vol. 56, pp. 13–20, 2016.

[35] I. Visquez, "A VISUAL SERVOING ARCHITECTURE," pp. 35–40, 2001.

[36] Y. Tu and M. Ho, "Design and Implementation of DSP and FPGA-Based Robust," *2010 IEEE Int. Conf. Control Appl.*, pp. 83–88, 2010.

[37] M. Makky and P. Soni, "Development of an automatic grading machine for oil palm fresh fruits bunches (FFBs) based on machine vision," *Comput. Electron. Agric.*, vol. 93, pp. 129–139, 2013.

[38] S. S. Mehta and T. F. Burks, "Vision-based control of robotic manipulator for citrus harvesting," *Comput. Electron. Agric.*, 2014.

[39] P. Durovic, R. Grbic, and R. Cupec, "Visual servoing for low-cost SCARA robots using an RGB-D camera as the only sensor," *Automatika*, vol. 58, no. 4, pp. 495–505, 2017.

[40] J. A. Brown and D. W. Capson, "A framework for 3d model-based visual tracking using a GPU-accelerated particle filter," *IEEE Trans. Vis. Comput. Graph.*, vol. 18, no. 1, pp. 68–80, 2012.

[41] P. Chatelain, A. Krupa, and M. Marchal, "Real-time needle detection and tracking using a visually servoed 3D ultrasound probe To cite this version : HAL Id : hal-00821231 Real-time needle detection and tracking using a visually servoed 3D ultrasound probe," 2013.

[42] Q. Bateux *et al.*, "Training Deep Neural Networks for Visual Servoing To cite this version : HAL Id : hal-01716679 Training Deep Neural Networks for Visual Servoing," 2018.

[43] C. Zang and K. Hashimoto, "Using GPUs to improve system performance in visual servo systems," *IEEE/RSJ 2010 Int. Conf. Intell. Robot. Syst. IROS 2010 - Conf. Proc.*, pp. 3937–3942, 2010.

[44] G. Pascoe, W. Maddern, and P. Newman, "Robust Direct Visual Localisation using Normalised Information Distance," *Bmvc*, pp. 1–13, 2015.

[45] T. Nammoto, K. Hashimoto, S. Kagami, and K. Kosuge, "High speed/accuracy visual servoing based on virtual visual servoing with stereo cameras," *IEEE Int. Conf. Intell. Robot. Syst.*, pp. 44–49, 2013.

[46] I. Radivojevic, J. Herath, and W. S. Gray, "Architectures for Intelligence and Control Applications," pp. 49–55.

[47] L. E. Ramos-velasco, "Visual Servoing Using Discrete Wavelet Transform," *World Autom. Congr. 2012*, pp. 1–6, 2012.

[48] R. Dahmouche, N. Andreff, Y. Mezouar, O. Ait-Aider, and P. Martinet, "Dynamic visual servoing from sequential regions of interest acquisition," *Int. J. Rob. Res.*, vol. 31, no. 4, pp. 520–537, 2012.

[49] S. J. Ralis and B. J. Nelson, "Visual servoing frameworks for micro-assembly of hybrid MEMS Barmeshwar Vikramaditya."

[50] K. E. Moorgas and P. Govender, "DSP Systems vs ANN Ensembles for Motion Detection and Filtering," pp. 20–25, 2008.

[51] M. Kumar, "Leveraging multicore processors for machine vision."

[52] A. Alabdo, J. Pérez, J. Pomares, G. J. Garcia, F. Torres, and S. Member, "FPGA-based Framework for Dynamic Visual Servoing of Robot Manipulators," 2015.

[53] C. Kyrkou, "No Title EMBEDDED HARDWARE ARCHITECTURES FOR OBJECT DETECTION,"

2010.

[54] C. Kyrkou, "Real-time hardware acceleration of object detection for intelligent embedded vision systems," University of Cyprus, 2014.

[55] J. Stefan and M. Nickl, "FPGA based Real-Time Visual Servoing," pp. 2–5.

[56] L.-A. F.-G. Miguel-Angel martinez-prado, juvenal rodriguez-resendiz, roberto-augusto gomez-loenzo, Gilberto Herrera-Ruiz, "An FPGA-Based Open Architecture Industrial Robot Controller," vol. 6, pp. 13407–13417, 2018.

[57] S. Solak and E. Do, "Real-Time Industrial Application of Single Board Computer Based Color Detection System," pp. 353–357.

[58] C. Lin, A. T. Wagshum, and T. Le, "Robotic Label Applicator : Design, Development and Visual Servoing Based Control," vol. 1, pp. 1–6, 2016.

[59] Q. Wang and W. Minghua, "Computer Vision-Based Object Grasping 6DoF Robotic Arm Using Picamera," *2018 4th Int. Conf. Control. Autom. Robot.*, pp. 111–115, 2018.

[60] A. Palla, A. Frigerio, G. Meoni, and L. Fanucci, "on Ambient Systems EAI Endorsed Transactions Position-Based Visual Servoing Control of a Wheelchair Mounter Robotic Arm using Parallel Tracking and Mapping of task objects," no. May 2017.

[61] J. A. Lopez, "Image processing based control of mobile robotics," no. August 2016.

[62] I. Tornberg, "Real-time object tracking on Raspberry Pi 2," 2016.

[63] A. Hinas, J. M. Roberts, and F. Gonzalez, "Vision-Based Target Finding and Inspection of a Ground Target Using a Multirotor UAV System," no. 2, 2017.

[64] P. Palungsuntikul, "Object Detection and Keep on a Mobile Robot by using a Low-Cost Embedded Color Vision System," pp. 70–76, 2010.

[65] M. S. Chelva and S. V Halse, "A Performance Study of GPU, FPGA, DSP, and Multicore Processors For Embedded Vision Systems," no. Mimd, pp. 61–66, 2015.

[66] I. Švogor, "An initial performance review of software components for a heterogeneous computing platform."

[67] R. Klobucar, J. Cas, R. SafariC, and B. Miran, "Uncalibrated visual servo control with neural network," *Int. Work. Adv. Motion Control. AMC*, vol. 1, pp. 74–79, 2008.

[68] H. Wu, L. Lou, C. Chen, S. Hirche, and K. Kolja, "A Framework of Networked Visual Servo Control System with Distributed Computation," 2010.

[69] H. Wu, L. Lou, S. Member, and C. Chen, "Cloud-based Networked Visual Servo Control," 2013.

[70] P. et al. Dagnino, G., Georgilas, I., Tarassoli, "Vision-based real-time position control of a semi-automated system for robot-assisted joint fracture surgery," vol. 11, pp. 437–455, 2016.

[71] "Robot Manipulators and Control Systems," *Ind. Robot. Program.*, pp. 35–107, 2007.

[72] M. W. Spong, "Motion Control of Robot Manipulators," *Handb. Control*, pp. 1339–1350, 1996.

[73] F. ; H. S. Chaumette, "Visual Servoing and visual tracking," in *Sensing and Perception*, pp. 563–583.

[74] J. A. Piepmeier, G. V Mcmurray, and H. Lipkin, "Uncalibrated Dynamic Visual Servoing squared," pp. 1–6, 2003.

[75] V. Lippiello, B. Siciliano, and L. Villani, "Position-based visual servoing in industrial multi-robot cells using a hybrid camera configuration," *IEEE Trans. Robot.*, vol. 23, no. 1, pp. 73–86, 2007.

[76] A. Muis and K. Ohnishi, "Eye-to-hand approach on eye-in-hand configuration within real-time visual servoing," *IEEE/ASME Trans. Mechatronics*, vol. 10, no. 4, pp. 404–410, 2005.

[77] S. Hans, "A Brief Comparative Study of Visual Servoing Systems A Brief Comparative Study of Visual Servoing Systems," no. January 2018.

[78] F. Chaumette and S. Hutchinson, "Visual servo control. I. Basic approaches," *IEEE Robot. Autom. Mag.*, vol. 13, no. 4, pp. 82–90, 2006.

[79] R. M. Candeias and S. Santos, "Evaluation of Visual Servoing Techniques for Robotic Applications Dissertation for obtaining the Degree of Master in Electrical and Computer Engineering," no. September 2007.

[80] F. Janabi-Sharifi, "Farrokh Janabi-Sharifi," in *Opto-Mechatronic Systems Handbook: Techniques and Applications : visual servoing theory and applications*, 2003, pp. 1–24.

[81] N. Filipe, M. Kontitsis, and P. Tsiotras, "Extended Kalman Filter for spacecraft pose estimation using dual quaternions," *Proc. Am. Control Conf.*, vol. 2015-July, pp. 3187–3192, 2015.

[82] J. N. Babu, "POSE AND MOTION ESTIMATION USING EXTENDED KALMAN FILTER," vol. 1, no. 2, pp. 246–255, 2012.

[83] T. Söderström, "Using an Extended Kalman Filter for Rigid Body Pose Estimation," *J. Biomech. Eng.*, vol. 127, no. 3, p. 475, 2005.

[84] M. E. Ragab and K. H. Wong, "Extended Kalman Filter Based Pose Estimation Using Multiple Cameras," pp. 1–32, 2007.

[85] G. Kumar, H. Pandya, A. Gaud, and K. M. Krishna, "Pose Induction for Visual Servoing to a Novel Object Instance," pp. 2953–2959, 2017.

[86] A. H. Abdul Hafez and E. Cervera, "Particle-filter-based pose estimation from controlled motion with application to visual servoing," *Int. J. Adv. Robot. Syst.*, vol. 11, 2014.

[87] U. B. Pascal and U. M. R. Cnrs, "COMPARISON OF VISUAL SERVOING TECHNIQUES :"

[88] P. I. Corke and S. A. Hutchinson, "A New Partitioned Approach to Image-Based Visual Servo," vol. 17, no. 4, pp. 507–515, 2001.

[89] Deguchi Koichiro; Noguchi Takashi, "Visual servoing using Eigen-spaces method and dynamic calculation of the interaction matrices," pp. 302–306, 1996.

[90] O. Tahri *et al.*, "Visual Servoing Based on Shifted Moments To cite this version : HAL Id : hal-01485458 Visual Servoing based on Shifted Moments," pp. 798–804, 2017.

[91] F. F. Chaumette, "Potential problems of stability and convergence in image-based and position-based visual servoing," *Conflu. Vis. Control*, vol. 237, pp. 66–78, 1998.

[92] D. Tsai, D. G. Dansereau, T. Peynot, and P. Corke, "Image-Based Visual Servoing With Light Field Cameras," *IEEE Robot. Autom. Lett.*, vol. 2, no. 2, pp. 912–919, 2017.

[93] P. Features, "A Simple Robotic Eye-In-Hand Camera Positioning Parallelogram Features," 2018.

[94] A. Mcfadyen, J. Ford, and P. Corke, "Stable Image-based Visual Servoing with Unknown Point Feature Correspondence," no. Cdc, pp. 4278–4282, 2017.

[95] E. Malis, F. Chaumette, and S. Boudet, "Positioning a coarse-calibrated camera with respect to an unknown object by 2D 1/2 visual servoing," *Proc. - IEEE Int. Conf. Robot. Autom.*, vol. 2, pp. 1352–1359, 1998.

[96] O. Kermorgant and F. Chaumette, "Combining IBVS and PBVS to ensure the visibility constraint," *IEEE Int. Conf. Intell. Robot. Syst.*, no. 1, pp. 2849–2854, 2011.

[97] M. Mitic, M. Lazarevic, B. Babic, and Z. Miljkovic, "Expert Systems with Applications Neural network Reinforcement Learning for visual control of robot manipulators," vol. 40, pp. 1721–1736, 2013.

[98] L. R. Buonocore, J. Cacace, and V. Lippiello, "Hybrid visual servoing for aerial grasping with hierarchical task-priority control," *2015 23rd Mediterr. Conf. Control Autom. MED 2015 - Conf. Proc.*, pp. 617–623, 2015.

[99] D. Kragic and H. I. Christensen, "New shortest-path approaches to visual servoing," in *proceedings of 2004 IEEE/RSJ International conference on intelligent robots and systems*, 2004, pp. 349–354.

[100] C. Collewet and E. Marchand, "Photometric visual servoing," 2008.

[101] K. Deguchi, "A Direct Interpretation of Dynamic Images with Camera and Object Motions for Vision Guided Robot Control," vol. 37, no. 1, pp. 7–20, 2000.

[102] E. Dean-León and G. Cheng, "A new method for solving 6D Image-Based Visual Servoing with virtual composite camera model," *IEEE-RAS Int. Conf. Humanoid Robot.*, vol. 2015-February, pp. 519–525, 2015.

[103] I. P. Vieira, A. A. Neto, and L. A. Mozelli, "Fiducial Markers Applied for Pose Tracking of a Robotic Manipulator: Application in Visual Servoing Control," *Proc. - 13th Lat. Am. Robot. Symp. 4th Brazilian Symp. Robot. LARS/SBR 2016*, pp. 287–292, 2016.

[104] K. Yonemori, A. Yanou, M. Myint, S. Ishiyama, and M. Minami, "Robustness of visual-servo against air bubble disturbance of underwater vehicle system using three-dimensional marker and dual-eye cameras," pp. 1–8, 2017.

[105] B. Nemec, "Robot Grasping using ArToolKit library," vol. 77, no. 1, pp. 1–6, 2010.

[106] C. Fantacci, G. Vezzani, U. Pattacini, V. Tikhanoff, and L. Natale, "Markerless visual servoing on unknown objects for humanoid robot platforms," 2017.

[107] J. Pag, *Assisted Visual Servoing by Means of Structured Light*. 2005.

[108] J. Pages, C. Collewet, F. Chaumette, and J. Salvi, "An approach to visual servoing based on coded light."

[109] T. Heitzmann, C. Doignon, C. Albitar, and P. Graebling, "Position-Based Visual Servoing Using a Coded Structured Light Sensor," no. October, pp. 17–18, 2008.

[110] J. Pagès, C. Collewet, F. Chaumette, and J. Salvi, "Robust decoupled visual servoing based on structured light," *2005 IEEE/RSJ Int. Conf. Intell. Robot. Syst. IROS*, pp. 2676–2681, 2005.

[111] Q. Bateux, "Going further with direct visual servoing To cite this version : HAL Id : tel-01764148 Going further with direct visual servoing," 2018.

[112] A. Ibarguren, J. M. Martínez-Otzeta, and I. Maurtua, "Particle filtering for industrial 6DOF visual servoing," *J. Intell. Robot. Syst. Theory Appl.*, vol. 74, no. 3–4, pp. 689–696, 2014.

[113] Yan-Xi Yang, Ding Liu, and Han Liu, "Robot-self-learning visual servoing algorithm using neural networks," no. November, pp. 739–742, 2003.

[114] F. Wang, Z. Liu, C. L. P. Chen, and Y. Zhang, "Adaptive neural network-based visual servoing control for manipulator with unknown output nonlinearities," *Inf. Sci. (NY).*, vol. 451–452, pp. 16–33, 2018.

[115] Y. Zhang, S. Li, B. Liao, L. Jin, and L. Zheng, "A recurrent neural network approach for visual servoing of manipulators," *2017 IEEE Int. Conf. Inf. Autom. ICIA 2017*, no. July, pp. 614–619, 2017.

[116] H. Hashimoto, T. Kubota, and M. Sato, "Visual Control of Robotic Manipulator Based on Neural Networks," vol. 39, no. 6, 1992.

[117] A. X. Lee, S. Levine, P. Abbeel, and C. Sciences, "Learning visual servoing with deep features and fitted Q-iteration," pp. 1–20, 2017.

[118] I. Lenz, H. Lee, and A. Saxena, "Deep Learning for Detecting Robotic Grasps."

[119] K. Ahlin, B. J. A. Hu, and G. Mcmurray, "Autonomous leaf picking Using Deep Learning and Visual-Servoing," *IFAC-PapersOnLine*, vol. 49, no. 16, pp. 177–183, 2016.

[120] Q. Bateux and E. Marchand, "Visual Servoing from Deep Neural Networks."

[121] S. Levine and A. Krizhevsky, "Learning Hand-Eye Coordination for Robotic Grasping with Deep Learning and Large-Scale Data Collection," 2012.

[122] A. Y. Tamtsia, O. Tahri, Y. Mezouar, H. Djalo, and E. Tonye, "New results in images moments-based visual servoing," *2013 IEEE Int. Conf. Robot. Autom.*, no. 1, pp. 5271–5276, 2013.

[123] O. Tahri, H. Araujo, F. Chaumette, and Y. Mezouar, "Robust image-based visual servoing using invariant visual information," *Rob. Auton. Syst.*, vol. 61, no. 12, pp. 1588–1600, 2013.

[124] A. Burlacu, C. Copot, and C. Lazar, *Predictive control architecture for real-time image moments based servoing of robot manipulators*, vol. 45, no. 6. IFAC, 2012.

[125] C. FRANCOIS, "A first step toward visual servoing using image moments François Chaumette To cite this version : HAL Id : Inria-00352087 A first step toward visual servoing using image moments," pp. 378–383, 2009.

[126] O. Tahri, "Point-based and Region-based Image Moments for Visual Servoing of Planar Objects," vol. 21, no. 6, pp. 1–12, 2005.

[127] R. Ozawa and F. Chaumette, "Dynamic visual servoing with image moments for an unmanned aerial vehicle using a virtual spring approach," vol. 1864, 2013.

[128] C. Collewet and E. Marchand, "Photometric Visual Servoing," vol. 27, no. 4, pp. 828–834, 2011.

[129] C. Collewet, E. Marchand, C. Collewet, E. Marchand, C. Collewet, and E. Marchand, "Visual servoing set free from image processing To cite this version : Visual servoing set free from

image processing," 2008.

[130] A. Dame, "A unified direct approach for visual servoing and visual tracking using mutual information To cite this version : HAL Id : tel-00558196," 2011.

[131] C. Collewet and E. Marchand, "Colorimetry-based visual servoing," pp. 5438–5443, 2009.

[132] S. Tahir, H. Rizvi, M. Y. Javed, K. Shahid, and T. Ahmad, "Wireless Visual-Servoing Using Primary Color Space in MATLAB," no. January 2015, 2016.

[133] S. M. Grigorescu and A. Davidescu, "Colored object detection algorithm for visual-servoing application," no. March 2016.

[134] L. S. Student, "An Object Detection and Pose Estimation Approach for Position-Based Visual Servoing," vol. 12, pp. 34–39, 2017.

[135] Q. Bateux and E. Marchand, "Histograms-Based Visual Servoing," *IEEE Robot. Autom. Lett.*, vol. 2, no. 1, pp. 80–87, 2016.

[136] H. Abidi, M. Chtourou, K. Kaaniche, and H. Mekki, "Visual servoing based on efficient histogram information," *Int. J. Control. Autom. Syst.*, vol. 15, no. 4, pp. 1746–1753, 2017.

[137] K. Haris, S. N. Efstratiadis, and N. Maglaveras, "Hybrid Image Segmentation Using Watersheds and Fast Region Merging," vol. 7, no. 12, pp. 1684–1699, 1998.

[138] N. M. Zaitoun and M. J. Aqel, "Survey on Image Segmentation Techniques," *Procedia Comput. Sci.*, vol. 65, no. Iccmit, pp. 797–806, 2015.

[139] T. Srikanth, P. P. P. Kumar, and A. Kumar, "Color Image Segmentation using Watershed Algorithm," vol. 2, no. 5, pp. 2332–2334, 2011.

[140] M. S. Nikita Sharma, Mahendra Mishra, "Colour Image Segmentation Techniques and Issues: an Approach," *Int. J. Sci. Technol. Res.*, vol. 1, no. 4, pp. 9–12, 2012.

[141] W. X. Kang, Q. Q. Yang, and R. P. Liang, "The comparative research on image segmentation algorithms," *Proc. 1st Int. Work. Educ. Technol. Comput. Sci. ETCS 2009*, vol. 2, pp. 703–707, 2009.

[142] A. S. Chauhan, S. Silakari, and M. Dixit, "Image segmentation methods: A survey approach," *Proc. - 2014 4th Int. Conf. Commun. Syst. Netw. Technol. CSNT 2014*, vol. 6, pp. 929–933, 2014.

[143] N. Kulkarni, "Color Thresholding Method for Image Segmentation of Natural Images," *Int. J. Image, Graph. Signal Process.*, vol. 4, no. 1, pp. 28–34, 2012.

[144] S. Samanta, N. Dey, P. Das, and S. Acharjee, "Multilevel Threshold Based Gray Scale Image Segmentation using Cuckoo Search," *Int. Conf. Emerg. Trends Electr. Commun. Inf. Technol.*, pp. 27–34, 2012.

[145] S. Tatiraju, "Image Segmentation using k-means clustering, EM and Normalized Cuts."

[146] V. Grau, A. U. J. Mewes, M. Alcañiz, R. Kikinis, and S. K. Warfield, "Improved Watershed Transform for Medical Image Segmentation Using Prior Information," vol. 23, no. 4, pp. 447–458, 2004.

[147] A. Kaur, "Image Segmentation Using Watershed Transform," no. 1, pp. 5–8, 2014.

[148] K. Chuang, H. Tzeng, S. Chen, J. Wu, and T. Chen, "Fuzzy c-means clustering with spatial information for image segmentation," vol. 30, pp. 9–15, 2006.

[149] N. Dhanachandra, K. Manglem, and Y. J. Chanu, "Image Segmentation using K -means Clustering Algorithm and Subtractive Clustering Algorithm," *Procedia - Procedia Comput. Sci.*, vol. 54, pp. 764–771, 2015.

[150] S. Yang, P. Li, H. Wen, Y. Xie, and Z. He, "SS symmetry K-Hyperline Clustering-Based Color Image," pp. 1–11, 2018.

[151] X. Zheng, Q. Lei, R. Yao, Y. Gong, and Q. Yin, "Image segmentation based on adaptive K - means algorithm," 2018.

[152] A. Malek, S. S. Yasiran, A. K. Jumaat, and V. Models, "Seed Point Selection for Seed-Based Region Growing in Segmenting Microcalcifications," no. May 2014, 2012.

[153] E. Abderrahmane, M.FAKIR, and N.IDRISSIA.MARBOHA, "Review of Color Image Segmentation," *IJACSA Spec. ISSUE*, pp. 15–21.

[154] H. Wu, T. T. Andersen, N. A. Andersen, and O. Ravn, "Visual servoing for object manipulation: A case study in slaughterhouse," *2016 14th Int. Conf. Control. Autom. Robot. Vision, ICARCV 2016*, 2017.

[155] M. Azizian, "Visual servoing in medical robotics : a survey . Part I : endoscopic and direct vision imaging – techniques and applications," no. September 2013, pp. 263–274, 2014.

[156] A. Krupa *et al.*, "Autonomous 3-D Positioning of Surgical Instruments in Robotized Laparoscopic Surgery Using Visual Servoing," vol. 19, no. 5, pp. 842–853, 2003.

[157] A. Krupa, C. Doignon, and J. Ganglo, "Towards semi-autonomy in laparoscopic surgery through vision and force feedback control."

[158] S. Voros and G. Haber, "ViKY Robotic Scope Holder : Initial Clinical Experience and Preliminary Results Using," vol. 15, no. 6, pp. 879–886, 2010.

[159] C. Staub, T. Osa, A. Knoll, and R. Bauernschmitt, "Automation of Tissue Piercing using Circular Needles and Vision Guidance for Computer-Aided Laparoscopic Surgery," *2010 IEEE Int. Conf. Robot. Autom.*, pp. 4585–4590, 2010.

[160] B. C. Becker, S. Member, R. A. Maclachlan, G. D. Hager, and C. N. Riviere, "Handheld micromanipulation with vision-based virtual fixtures," *2011 IEEE Int. Conf. Robot. Autom.*, pp. 4127–4132, 2011.

[161] B. C. Becker, S. Member, C. R. Valdivieso, J. Biswas, L. A. Lobes, and C. N. Riviere, "Active guidance for laser retinal surgery with a handheld instrument," *2009 Annu. Int. Conf. IEEE Eng. Med. Biol. Soc.*, pp. 5587–5590, 2009.

[162] B. C. Becker, S. Member, S. Voros, R. A. Maclachlan, G. D. Hager, and C. N. Riviere, "Active guidance of a handheld micromanipulator using visual servoing," *2009 IEEE Int. Conf. Robot. Autom.*, pp. 339–344, 2009.

[163] W. Lin-kun and T. U. Zhi-guo, "Hybrid Visual Servoing Control for Robotic Arc Welding Based on," vol. 31, no. 4, 2005.

[164] C. Li, C. Cao, and Y. Gao, "Visual Servoing based object pick and place manipulation system."

[165] T. Timm, N. Axel, H. Wu, T. T. Andersen, N. A. Andersen, and O. Ravn, "Visual Servoing for Object Manipulation : A Case Study in Slaughterhouse," 2016.

[166] T. Rakotomamonjy and Q. H. Truong, "ScienceDirect ship landing using visual Helicopter

Helicopter ship landing visual on platform Helicopter ship visual servoing servoing on a" *IFAC-PapersOnLine*, vol. 50, no. 1, pp. 10507–10512.

[167] C. Fan, B. Song, X. Cai, and Y. Liu, "Dynamic Visual Servoing of a Small Scale Autonomous Helicopter in," pp. 5301–5306, 2009.

[168] A Mcfadyen, L. Mejias, and P. Corke, "Visual servoing approach to collision avoidance for aircraft," *28th Congr. International Counc. Aeronaut. Sci. 2012*, no. September, pp. 24–28, 2012.

[169] J. Gausemeier and S. Moehringer, "VDI 2206- A New Guideline for the Design of Mechatronic Systems," *IFAC Proc. Vol.*, vol. 35, no. 2, pp. 785–790, 2017.

[170] R. Bin Ramhuzaini, U. Pulm, and R. Stetter, "Systematic mechatronic design of a piezo-electric brake," *Proc. ICED 2007, 16th Int. Conf. Eng. Des.*, vol. DS 42, no. August, pp. 1–12, 2007.

[171] G. . Pahl, W. . Beitz, J. Feldhusen, and K. H. . Grote, *Engineering design. [electronic book] : a systematic approach: University of Liverpool Library*.

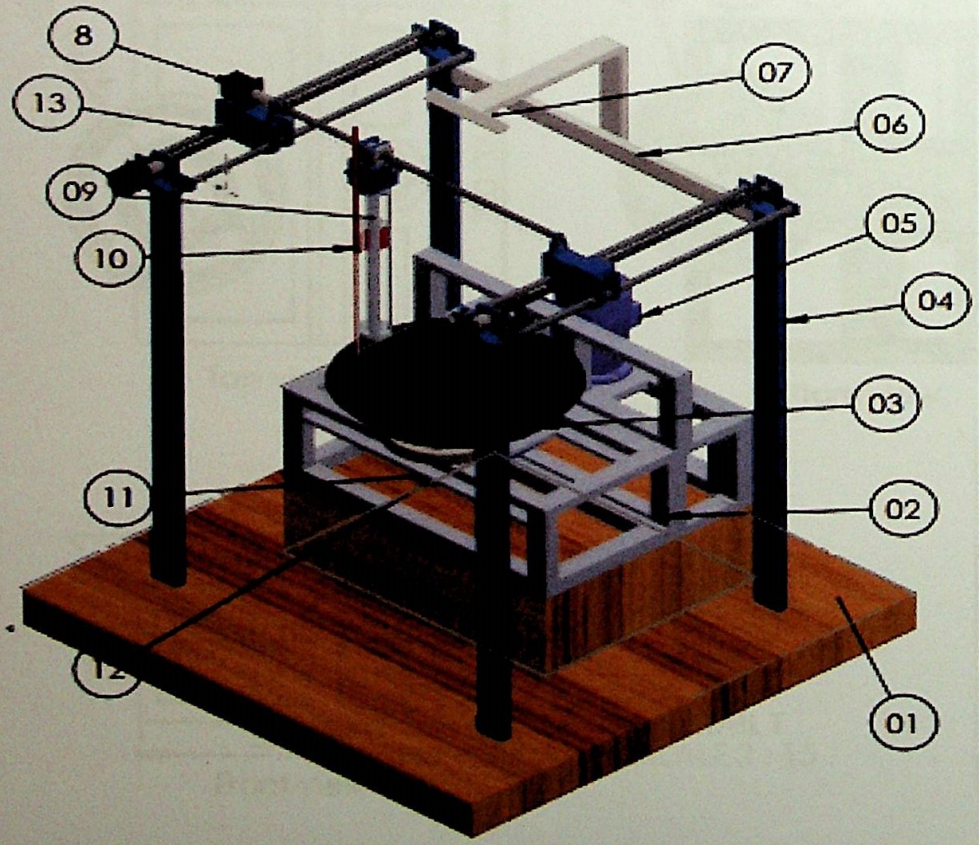
[172] W. Brace and K. Thramboulidis, "Specifications- a Formal Approach," pp. 639–650, 2010.

[173] O. Nobuyuki, "A threshold selection method from gray-level histograms," *IEEE Trans. Syst. Man. Cybern.*, vol. SMC-9, no. 1, pp. 62–66, 1979.

[174] T. Horiuchi, "Grayscale Image Segmentation Using Color Space," no. 3, pp. 1231–1237, 2006.

[175] T. B. Tuli, "Mathematical modeling and dynamic simulation of gantry robot using bond graph," 2018, vol. 244, no. July 2018, pp. 228–237.

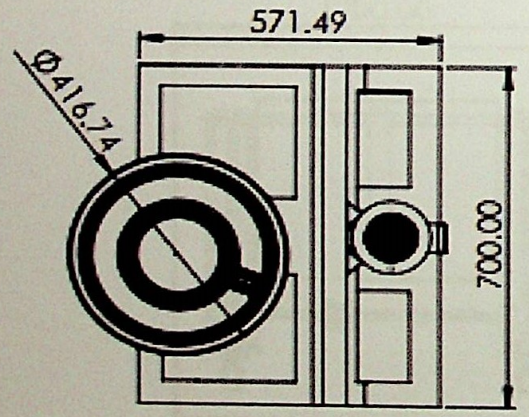
APPENDIX A



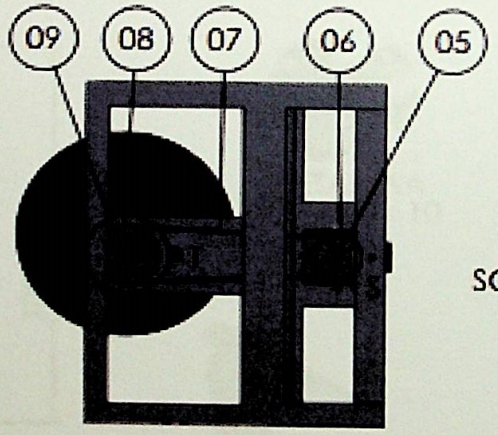
Notes:
1. All dimensions are in mm unless stated
2. All permanent joints are welded unless stated
3. Finish is as machined unless stated

Item no	Part Name	Description
01	Base	Hard mahogany/teak wood
02	Washer frame	fabricated frame for washing system
03	Grooved gold pan	Rigid PVC pan
04	frame for handling system	Base frame for the handling system
05	electric motor for washer	18.5 kW 4P 180M
06	camera holder	Aluminium
07	camera & lighting	LED Lights and camera
08	servo motor	NEMA 34
09	z-axis link holder	machined
10	End-effector nozzle	Nozzle
11	Pulley Belt	durable nylon rubber
12	Big pulley	steel alloy pulleys
13	Leadscrew	stainless steel 15mm diameter

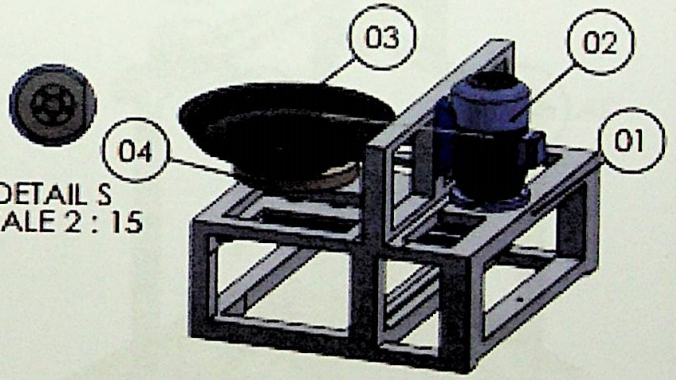
Scale1:15	GENERAL ASSEMBLY	
BIUST	Automated vision based gold panning	
	Drawn by: Blessing Chipfurwe Makoni	
	Checked and approved by:	Dr M. Namoshe Dr O. Matsebe
	Date 09/20	Sheet 1/7



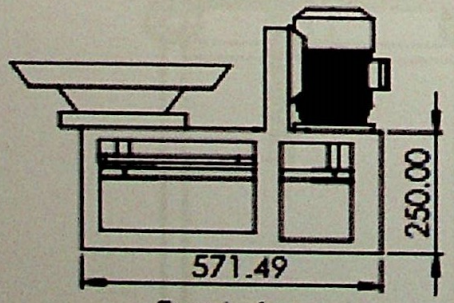
Top view



Bottom view



DETAIL S
SCALE 2 : 15



Front view

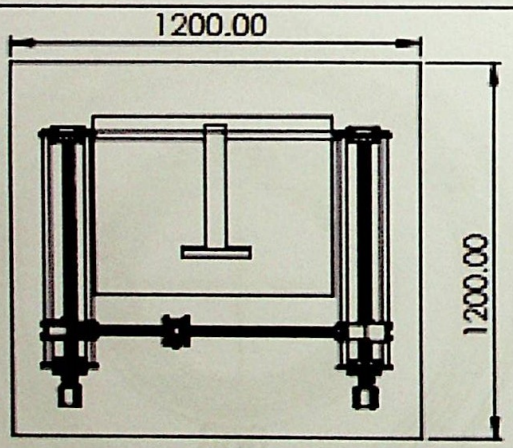


DETAIL T
SCALE 2 : 15

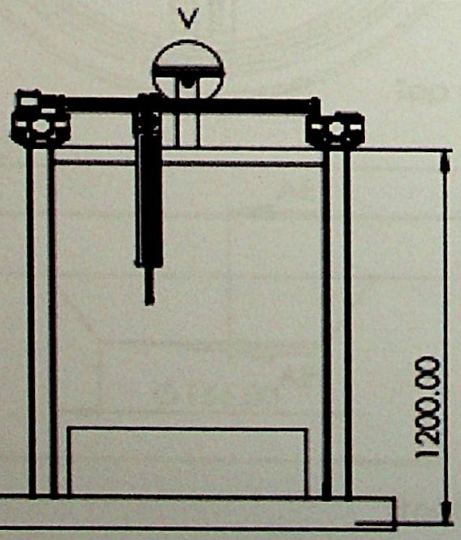
Item no	Part name	Description
09	Pan-holder shaft	stainless steel machined
08	Big pulley	Steel alloy pulley
07	Belt	Nylon rubber
06	Small pulley	Steel alloy pulley
05	Motor shaft	stainless steel
04	Pan holder	Machined holder
03	grooved pan	Black Rigid PVC
02	electric motor	18.5kW 4P 18M
01	washer stand	Fabricated

Scale1:10	Mechanized washer - sub assembly	
BIUST	AUTOMATED VISION BASED GOLD PAN	
	Drawn by: Blessing Chipfurwe Makoni	
	Checked by: Dr M. Namoshe	Checked by: Dr O. Matsebe
	Date 09/20	Sheet 2/7

Notes:
1. All dimensions are in mm unless stated
2. All permanent joints are welded unless stated
3. Finish is as machined unless stated



Top view



Front view



DETAIL AA
SCALE 1 : 10



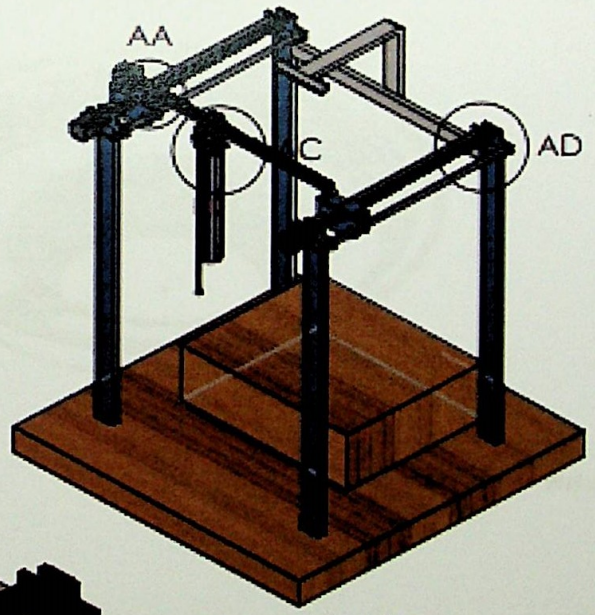
DETAIL AC
SCALE 1 : 10



DETAIL V
SCALE 1 : 10



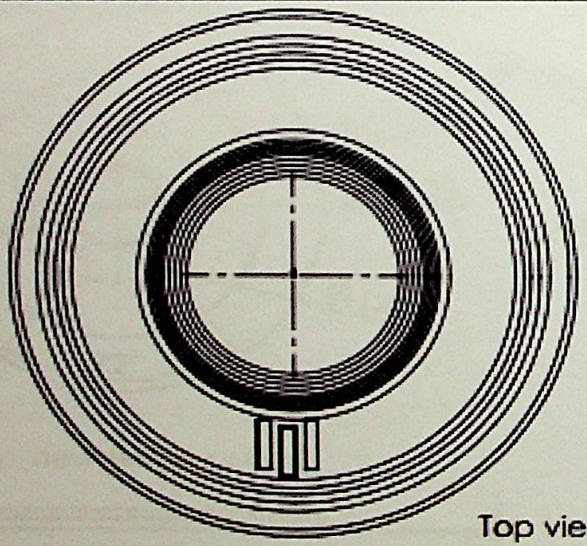
DETAIL AD
SCALE 1 : 10



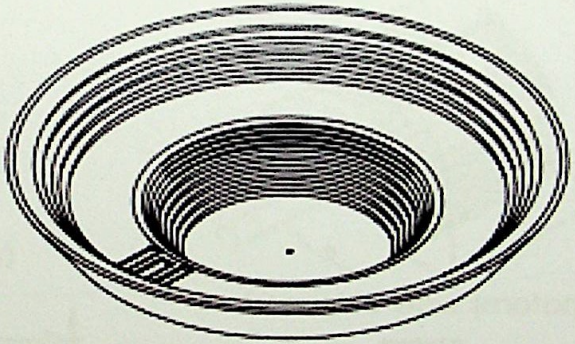
Isometric View

Notes:
1. All dimensions are in mm unless stated
2. All permanent joints are welded unless stated
3. Finish is as machined unless stated

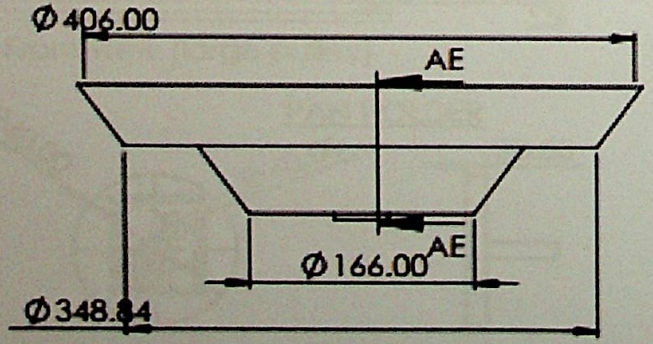
Scale1:15	Handling system -Sub-assembly	
BIUST	Automated vision based gold panning	
	Drawn by: Blessing Chipfurwe Makoni	
	Checked and approved by:	Dr M. Namoshe Dr O. Matsebe
	Date 09/20	Sheet 1/7



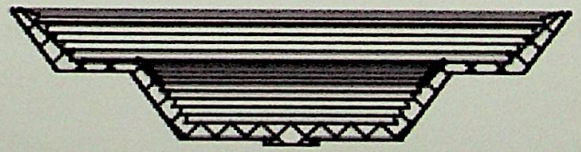
Top view



Isometric view



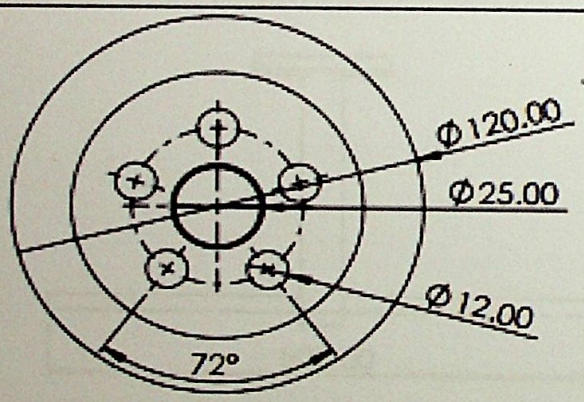
Front view



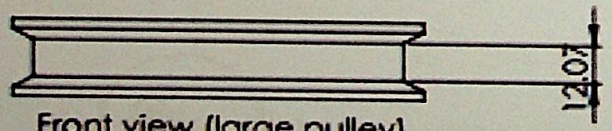
SECTION AE-AE Cross sectional view

Notes:
1. All dimensions are in mm unless stated
2. All permanent joints are welded unless stated
3. Finish is as machined unless stated

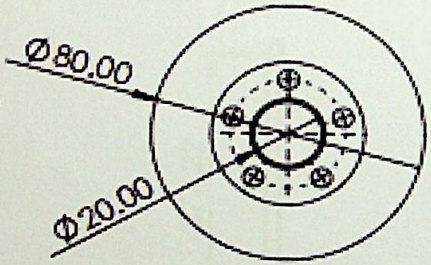
Scale1:15	Washing system - components (Pan)	
BIUST	Automated vision based gold panning	
	Drawn by: Blessing Chipfurwe Makoni	
	Checked and approved by:	Dr M. Namoshe Dr O. Matsebe
	Date 09/20	Sheet 1/7



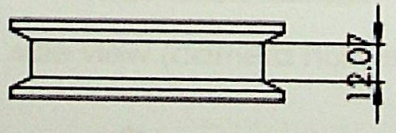
top view (large pulley)



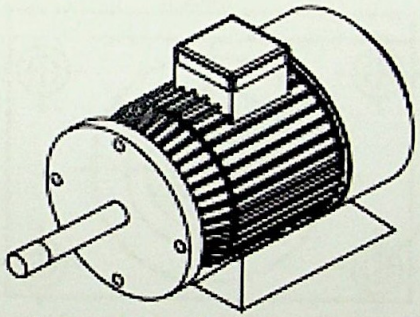
Front view (large pulley)



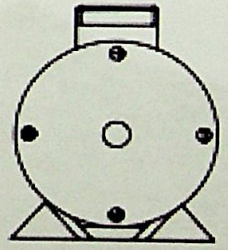
top view (small pulley)



Front view (small pulley)

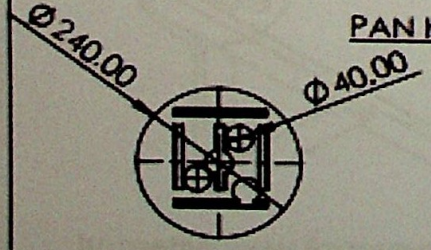


Isometric view (motor)

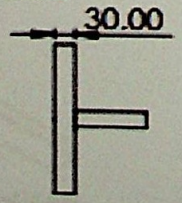


front view (motor)

PAN HOLDER



top view



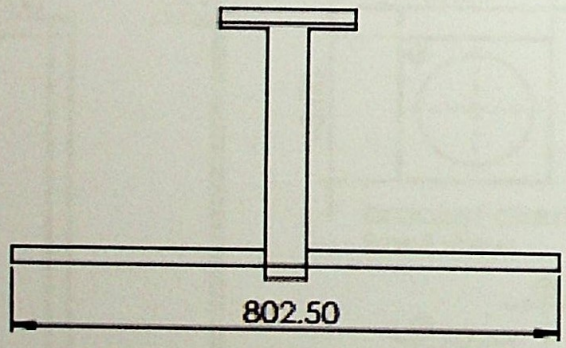
side view



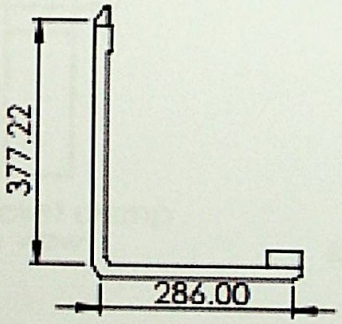
dimetric view

Notes:
1. All dimensions are in mm unless stated
2. All permanent joints are welded unless stated
3. Finish is as machined unless stated

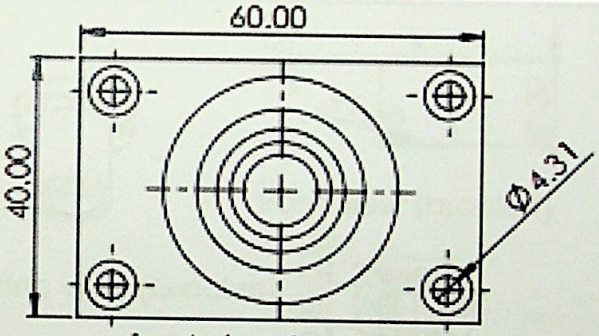
Scale1:15	Washing system - components	
BIUST	Automated vision based gold panning	
	Drawn by: Blessing Chipfurwe Makoni	
	Checked and approved by:	Dr M. Namoshe Dr O. Matsebe
	Date 09/20	Sheet 1/7



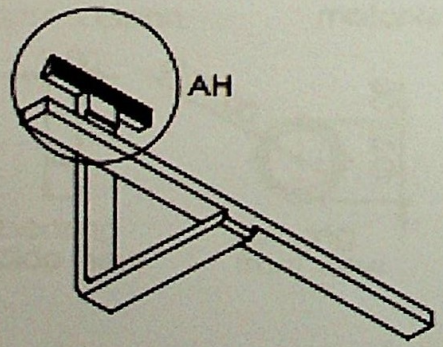
Top view (camera holder)



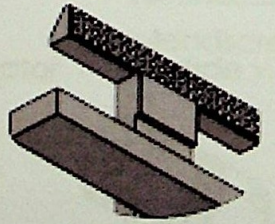
side view (camera holder)



front view (camera)

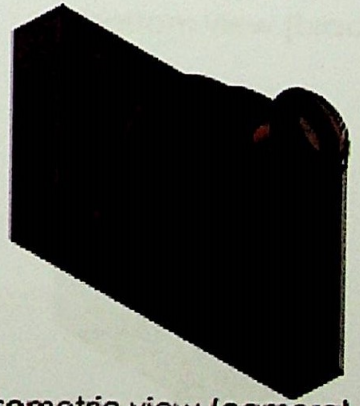


Isometric view (camera holder)



DETAIL AH
SCALE 1 : 5

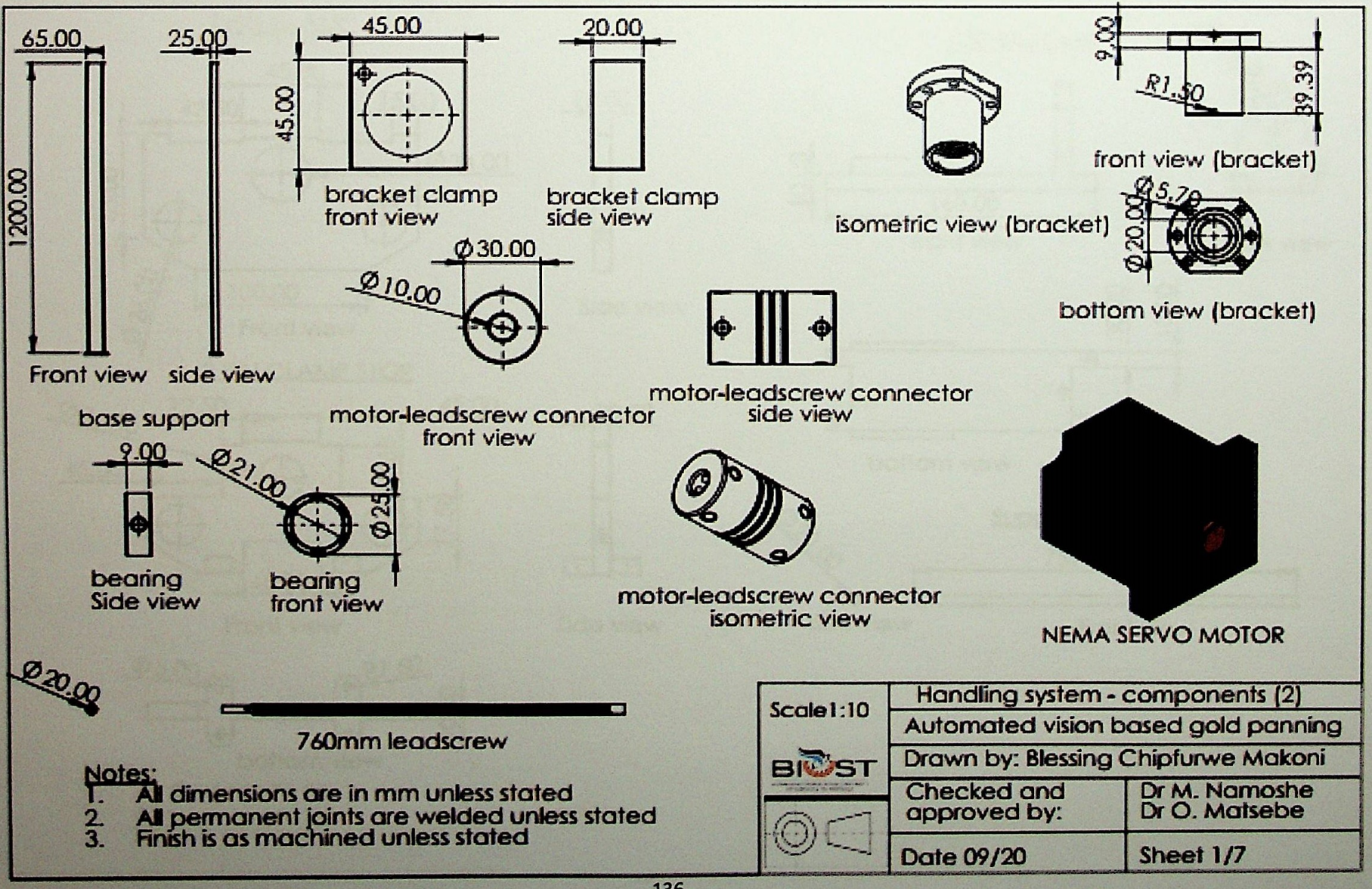
light emitting diodes (LEDs) strips



Isometric view (camera)

Notes:
1. All dimensions are in mm unless stated
2. All permanent joints are welded unless stated
3. Finish is as machined unless stated

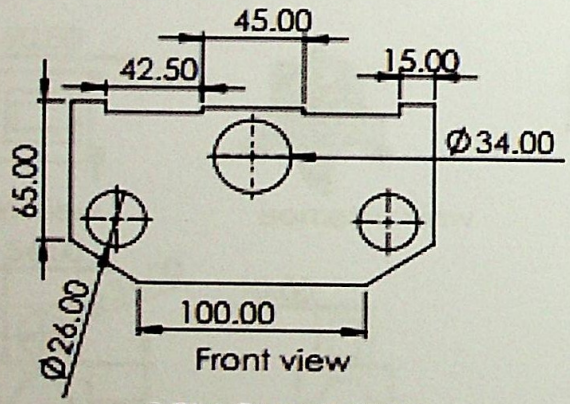
Scale1:10	Handling system - components (1)	
BIUST	Automated vision based gold panning	
	Drawn by: Blessing Chipfurwe Makoni	
	Checked and approved by:	Dr M. Namoshe Dr O. Matsebe
	Date 09/20	Sheet 1/7

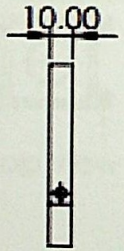


Notes:
1. All dimensions are in mm unless stated
2. All permanent joints are welded unless stated
3. Finish is as machined unless stated

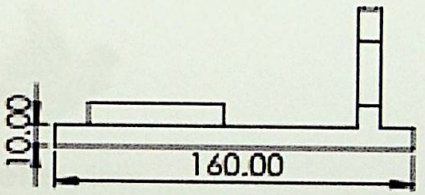
Scale1:10	Handling system - components (2)
BIUST	Automated vision based gold panning
	Drawn by: Blessing Chipfurwe Makoni
	Checked and approved by: Dr M. Namoshe, Dr O. Matsebe
	Date 09/20 — Sheet 1/7

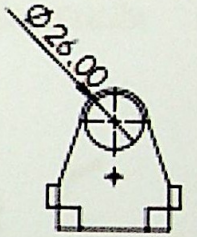
3 PIN CLAMP



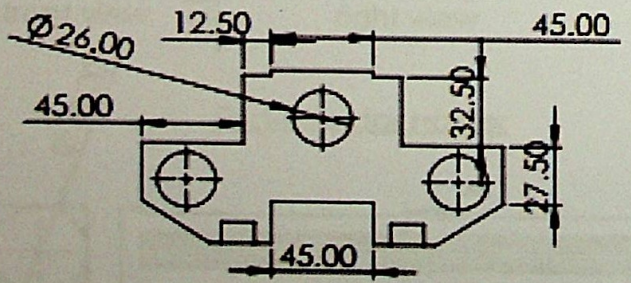


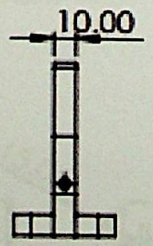
TOP BRACKET

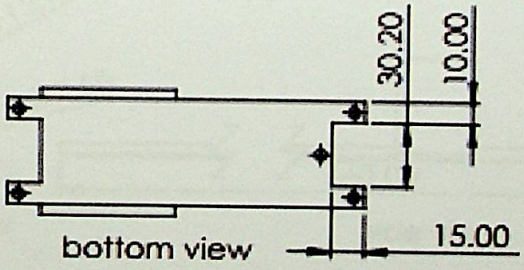




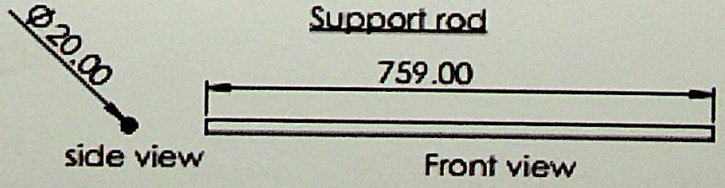
3 PIN CLAMP STOP

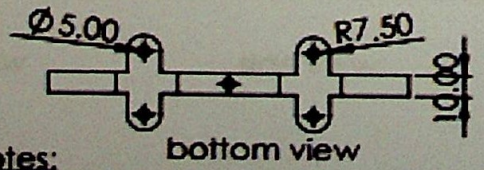






Support rod

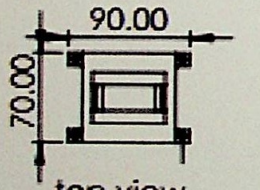




Notes:
1. All dimensions are in mm unless stated
2. All permanent joints are welded unless stated
3. Finish is as machined unless stated

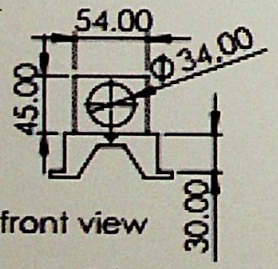
Scale 1:3	Handling system - components (3)	
BIUST	Automated vision based gold panning	
	Drawn by: Blessing Chipfurwe Makoni	
	Checked and approved by:	Dr M. Namoshe Dr O. Matsebe
	Date 09/20	Sheet 1/7

End-effector motor top support

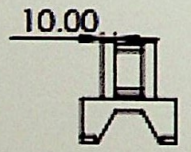


top view


isometric view

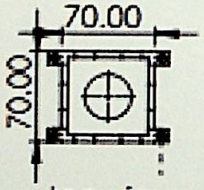


front view



right view

End-effector motor bottom support

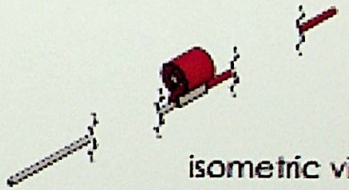


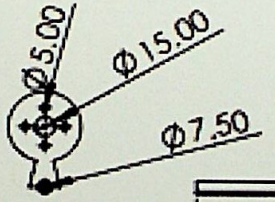
top view


isometric view

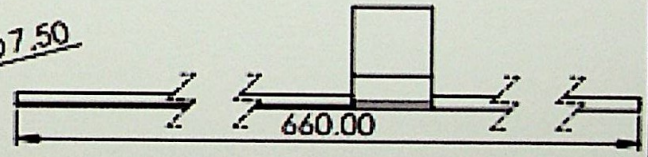

front view

End-effector suction nozzle


isometric view

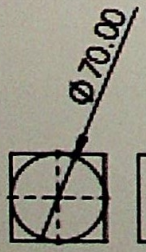


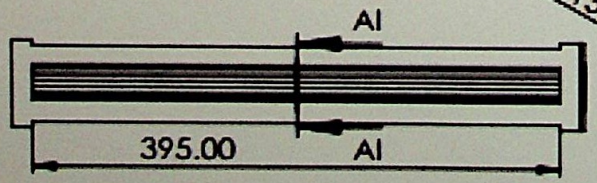
front view

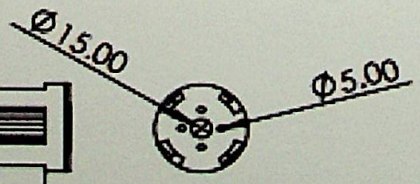


side view

End-effector holder







SECTION AI-AI
SCALE 1 : 5

front view

side view

Notes:
1. All dimensions are in mm unless stated
2. All permanent joints are welded unless stated
3. Finish is as machined unless stated

Scale1:5	Handling system - components (4)
BIUST	Automated vision based gold panning
	Drawn by: Blessing Chipfurwe Makoni
	Checked and approved by: Dr M. Namoshe, Dr O. Matsebe
	Date 09/20 — Sheet 1/7